



12th International Conference on Magnetic and Superconducting Materials

University of Duisburg-Essen,
Faculty of Physics
August 28 – September 2, 2022

BOOK OF ABSTRACTS

Supported by:

UNIVERSITÄT
DUISBURG
ESSEN

Offen im Denken



Contents

Plenary talks 4 - 13

Oral sessions 15 - 91

Monday, August 29

Tuesday, August 30

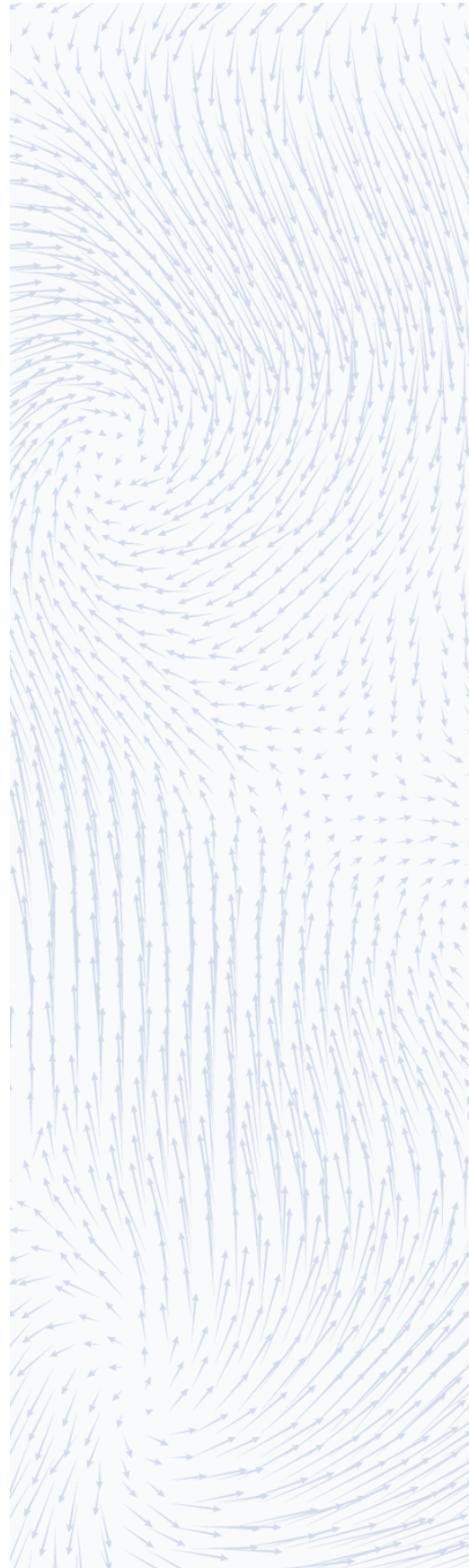
Wednesday, August 31

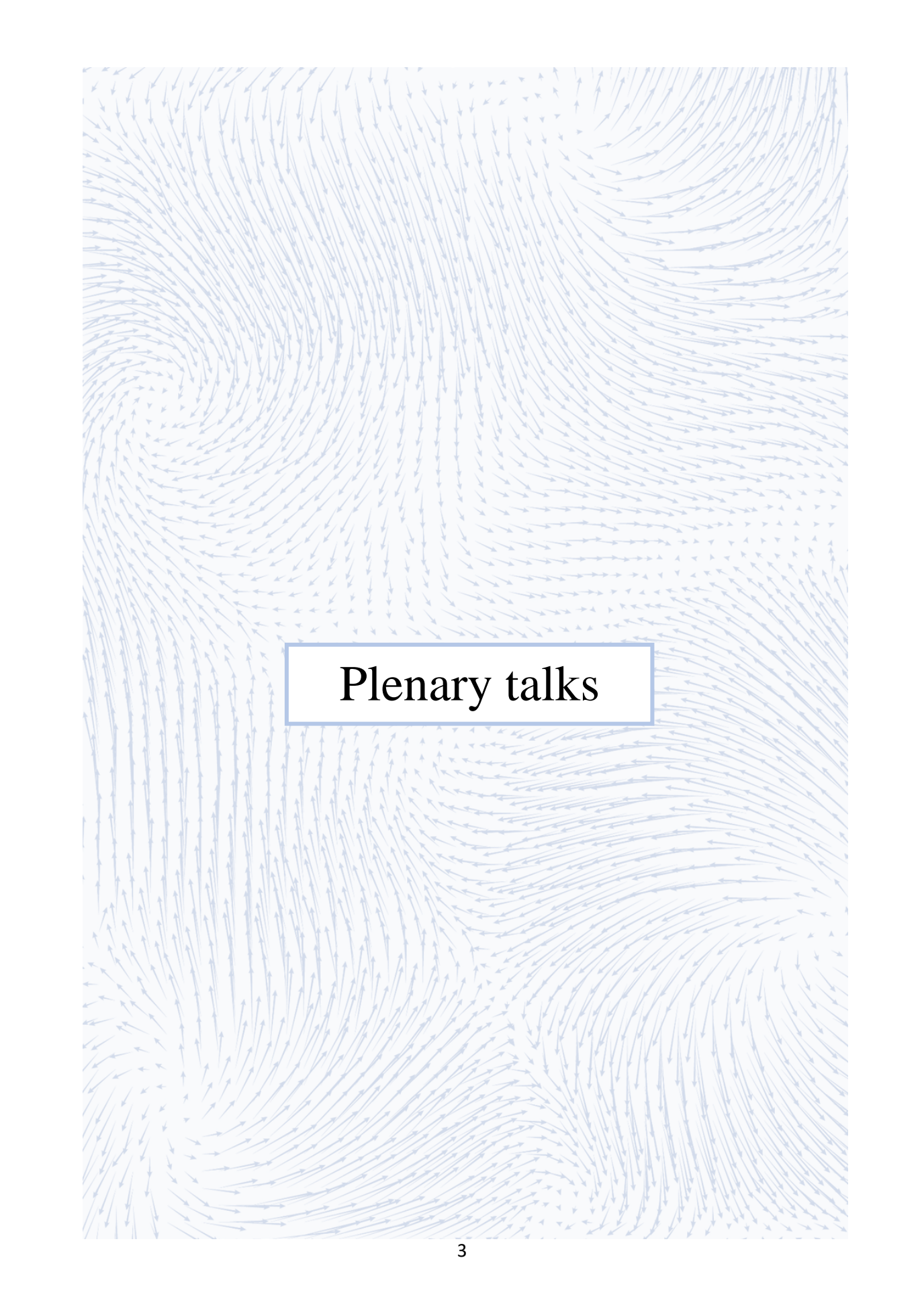
Thursday, September 1

Friday, September 2

Poster session 93 - 121

Monday, August 29



The background of the slide is a complex vector field pattern. It consists of numerous small, light blue arrows of varying lengths and directions, arranged in a way that creates a sense of fluid motion or a complex flow. The arrows generally curve and swirl, with some areas showing more pronounced vortices or eddies. The overall effect is a dense, textured field of directional lines.

Plenary talks

Monday, August 29 | Room MD162 | 08:40-09:30

Advanced magnetic materials for efficient energy, transport and cooling applications

Oliver Gutfleisch

TU Darmstadt, Material Science, Germany

oliver.gutfleisch@tu-darmstadt.de

High performance hard and soft magnets are key components of energy-related technologies, such as direct drive wind turbines and e-mobility. They are also important in robotics and automatization, sensors, actuators, and information technology. The magnetocaloric effect (MCE) is the key for new and disruptive solid state-based refrigeration. Magnetic hysteresis – and its inherent energy product - characterises the performance of all magnetic materials. Despite considerable progress in the modelling, characterisation and synthesis of magnetic materials, hysteresis is a long-studied phenomenon that is still far from being completely understood. Discrepancies between intrinsic and extrinsic magnetic properties remain an open challenge, the so-called Brown's paradox, and magnets do not operate yet at their physical limits. Basic material requirements, figure of merits, demand and supply, criticality of strategic elements are explained for both permanent magnets and magnetocalorics referring to the benchmark materials NdFeB and LaFeSi. New research avenues given by compositionally complex alloys (CCA), where the duality or unusual combinations of functional and mechanical properties can be explored, will be elucidated looking at soft magnetic materials. The search for perfect defects is driving the material design strategy.

- [1] O. Gutfleisch, M. A. Willard, E. Brück, C. H. Chen, S. G. Sankar, and J. P. Liu, Magnetic materials and devices for the 21st century: stronger, lighter, and more energy efficient. *Adv. Mater.* 23 (2011) 82.
- [2] K.P. Skokov and O. Gutfleisch, Heavy rare earth free, free rare earth and rare earth free magnets - vision and reality, *Scripta Materialia View Point Set*, 154 (2018) 289-294.
- [3] M. Duerrschabel, M. Yi, K. Uestuener, M. Liesegang, M. Katter, H.-J. Kleebe, B. Xu, O. Gutfleisch, L. Molina-Luna, Atomic structure and domain wall pinning in samarium -cobalt based permanent magnets, *Nature Communications* 8:54 (2017).
- [4] T. Gottschall, K.P. Skokov, M. Fries, A. Taubel, I. Radulov, F. Scheibel, D. Benke, S. Riegg, O. Gutfleisch, Making a cool choice: the materials library of magnetic refrigeration, *Progress Report in Advanced Energy Materials* 9 no. 34 (2019) 1901322.
- [5] T. Gottschall, A. Gracia-Condal, M. Fries, A. Taubel, L. Pfeuffer, L. Manosa, A. Planes, K.P. Skokov, O. Gutfleisch, A multicaloric cooling cycle that exploits thermal hysteresis, *Nature Materials* (2018).
- [6] O. Gutfleisch, T. Gottschall, M. Fries, D. Benke, I. Radulov, K. P. Skokov, H. Wende, M. Gruner, M. Acet, P. Entel and M. Farle, Mastering hysteresis in magnetocaloric materials, *Phil. Trans. R. Soc. A* 374 (2016) 20150308.
- [7] L. Han, Z. Rao, I.R. Souza Filho, F. Maccari, Y. Wei, G. Wu, A. Ahmadian, X. Zhou, O. Gutfleisch, D. Ponge, D. Raabe, Z. Li, Ultrastrong and ductile soft magnetic high-entropy alloys via coherent ordered nanoprecipitates, *Advanced Materials* 2102139 (2021).
- [8] L. Han, Z. Rao, I.R. Souza Filho, F. Maccari, Y. Wei, G. Wu, Al. Ahmadian, X. Zhou, O. Gutfleisch, D. Ponge, Z. Li, D. Raabe, Ultrastrong and ductile soft magnetic high-entropy alloys via coherent ordered nanoprecipitates, *Nature* 608 (2022) 310–316.

Monday, August 29 | Room MD162 | 14:00-15:00

Symmetry Breaking by Materials Engineering for Spin-Orbit-Torque Technology

2022 IEEE Magnetics Distinguished Lecture

Jingsheng Chen

Department of Materials Science and Engineering, National University of Singapore
msecj@nus.edu.sg

Electric manipulation of magnetization is essential for the integration of magnetic functionalities in integrated circuits. Spin-orbit torque (SOT), originating from the coupling of electron spin and orbital motion through spin-orbital interaction, is able to effectively manipulate magnetization. Symmetry breaking plays an important role in spintronics based on SOT. SOT requires inversion asymmetry in order to have a net effect on magnetic materials, which is commonly realized by spatial asymmetry: a thin magnetic layer sandwiched between two dissimilar layers. This kind of structure restricts the SOT by mirror and rotational symmetries to have a particular form: an “antidamping-like” component oriented in the film plane even upon reversal of the magnetization direction. Consequently, magnetization perpendicular to the film plane cannot be deterministically switched with pure electric current. To achieve all-electric switching of perpendicular magnetization, it is necessary to break the mirror and rotational symmetries of the sandwiched structure.

In this lecture, I will begin with a basic introduction of the physical origin of SOT, followed by the related symmetry analysis of a magnetic thin film in a sandwiched structure for the generation of a net SOT effect. Then I will introduce a new method — a composition gradient along the thin-film normal for breaking the inversion symmetry — to generate bulk-like SOT [1], which enables a thicker magnetic layer with high magnetic anisotropy. An overview of the methods commonly used to break mirror and rotational symmetries in order to realize all-electric switching of perpendicular magnetization will follow. I will give a detailed discussion on our methods for the realization of all-electric switching of perpendicular magnetization: the use of a spin source layer with low magnetic symmetry and low crystal symmetry, which generates an out-of-plane SOT [2] – [4]; interfacial 3m1 symmetry, which induces a new “3m” spin torque [5]; precise control of the tilting of magnetocrystalline anisotropy easy axis [6]; and a spin-current gradient along the current direction [7].

- [1] L. Liu et al., “Electrical switching of perpendicular magnetization in a single ferromagnetic layer,” *Phys. Rev. B*, vol. 101, 220402, June 2020.
- [2] J. Zhou et al., “Magnetic asymmetry induced anomalous spin-orbit torque in IrMn,” *Phys. Rev. B*, vol. 101, 184403, May 2020.
- [3] J. Zhou et al., “Large spin-orbit torque efficiency enhanced by magnetic structure of collinear antiferromagnet IrMn,” *Sci. Adv.*, vol. 5, eaau6696, May 2019.
- [4] Q. Xie et al., “Field-free magnetization switching induced by the unconventional spin-orbit torque from WTe₂,” *APL Mater.*, vol. 9, 051114, May 2021.
- [5] L. Liu et al., “Symmetry-dependent field-free switching of perpendicular magnetization,” *Nat. Nanotech.*, vol. 16, pp. 277-282, January 2021.
- [6] L. Liu et al., “Current-induced magnetization switching in all-oxide heterostructures,” *Nat. Nanotech.*, vol. 14, 939-944, September 2019.
- [7] S. Chen et al., “Free field electric switching of perpendicularly magnetized thin film by spin current gradient,” *ACS Appl. Mater. Interfaces*, vol. 11, pp. 30446-30452, July 2019.

Tuesday, August 30 | Room MD162 | 08:30-09:30

Spin Current in Superconductor/Ferromagnet Heterostructures

Sadamichi Maekawa

RIKEN Center for Emergent Matter Science (CEMS), Wako, 351-0198, Japan

Kavli ITS at University of Chinese Academy of Sciences, Beijing, China

Sadamichi.maekawa@riken.jp

Spin current is the flow of electron spins, which carries and manipulates energy and information, and is one of the key concepts in the recent spintronics [1]. Superconductivity in a conventional superconductor is carried by the Cooper-pair condensate in the spin-singlet state. In superconductor (SC)/ferromagnet (FM) heterostructures, the SC order parameter quickly decays due to the exchange field acting on the pairs in the FM. On the other hand, when the spin current enters into a SC, it stays there with long life time because the SC gap suppresses the relaxation of spin [2].

As a result, a variety of unique spin transport phenomena are expected in the SC/FM heterostructures. In a certain SC/FM/SC Josephson junction, the SC phase vs. Josephson current relation is reversed (π -Junctions) from that in the normal ones (0-Junction), and the half-integer Shapiro steps are observed in the I-V curve [3]. We examine the magnetization dynamics in the π -Junctions [4,5]. The Josephson current in π -Junctions is studied as well [6]. The π -junctions have a unique potential for qubits [7].

[1] “Spin Current” ed. S. Maekawa et al. (Oxford University Press, 2017).

[2] H. Yang et al., Nature Mater. 9, 586 (2010).

[3] Y. Yao et al., Phys. Rev. B104, Vol.10 (2021).

[4] C. Holmqvist et al., Phys. Rev. B83, 104521 (2011).

[5] S. Maekawa and Y. Tsutsumi, unpublished.

[6] M. Mori et al., Appl. Phys. Express 14, 103001 (2021).

[7] T. Yamashita et al., Phys. Rev. Lett., 95, 097001 (2005).

Tuesday, August 30 | Room MD162 | 14:00-15:00

Exploring the potentials of spin-orbitronics

2022 IEEE Magnetics Distinguished Lecture

Aurélien Manchon

Centre Interdisciplinaire de Nanoscience de Marseille (CINaM), Aix-Marseille University, France
aurelien.manchon@univ-amu.fr

The ever-increasing demand of information technology for power-efficient components has led to the search for alternative solutions to mainstream microelectronics. In this context, spintronics devices stand out as competitive candidates, especially for memory and logic applications. A promising route harvests unconventional transport properties arising from spin-orbit coupling in magnetic heterostructures lacking inversion symmetry.

In these systems, typically multilayers of transition-metal ferromagnets and heavy materials (e.g., W, Pt, Ta, Bi₂Se₃, WTe₂), interfacial spin-orbit coupling promotes a wealth of remarkable physical phenomena: the generation of spin-orbit torques, the interconversion between spin and charge currents, and the stabilization of topological magnetic skyrmions. These effects have gathered extraordinary interest and have led to remarkable experimental breakthroughs, including extremely fast magnetic reversal, terahertz emission, and current-driven skyrmion motion. The recent synthesis of novel classes of materials, including all-oxide heterostructures, noncollinear antiferromagnets, and van der Waals heterostructures, has profoundly enriched this vivid field of research by unlocking unforeseen forms of torques and magnetic interactions, thereby enhancing the functionalities of spin-orbitronic devices.

This lecture will provide a theoretical perspective of the advancement of the fascinating field of spin-orbitronics, focusing on two emblematic mechanisms: the spin-orbit torque and the Dzyaloshinskii-Moriya interaction. I will examine what theory and materials modeling can tell us about these two effects, and what future research directions they open. I will first introduce key concepts in spintronics, such as spin currents and spin-transfer torque, and show how spin-orbit coupling enables new physical effects of high interest for potential applications. I will present standard phenomenological descriptions of these two effects, spin-orbit torque and Dzyaloshinskii-Moriya interaction, determine the symmetry rules that govern them, and give a broad overview of the current state-of-the-art of the field from experimental and theoretical standpoints. Finally, I will explore how spin-orbitronics takes a completely new form in materials possessing low crystalline symmetries, such as Fe₃GeTe₂, CuPt/CoPt bilayers, and noncollinear antiferromagnets (e.g., Mn₃Sn).

I hope this seminar will not only encourage electrical engineers to engage in this beguiling field of research and explore the device implications of this new technology, but also reach out to scientists working in adjacent fields (terahertz science, for instance) who could bring inspiring new ideas to spintronics [1-5].

This work was supported by the King Abdullah University of Science and Technology (KAUST, Thuwal, Saudi Arabia) and by the Excellence Initiative of Aix-Marseille Université - A*Midex, a French "Investissements d'Avenir" program.

- [1] Manchon, Aurelien, et al. "Current-induced spin-orbit torques in ferromagnetic and antiferromagnetic systems." *Reviews of Modern Physics* 91.3 (2019): 035004.
- [2] A. Belabbes, G. Bihlmayer, F. Bechstedt, S. Blügel, and A. Manchon, "Hund's rule-driven Dzyaloshinskii-Moriya interaction at 3d-5d interfaces," *Phys. Rev. Lett.*, vol. 117, 247202, December 2016.
- [3] E. Jué, C. K. Safeer, M. Drouard, A. Lopez, P. Balint, L. Buda-Prejbeanu, O. Boulle, S. Auffret, A. Schuhl, A. Manchon, I. M. Miron, and G. Gaudin, "Chiral damping of magnetic domain walls," *Nature Mater.*, vol. 15, pp. 272-277, March 2016.
- [4] S. Laref, K.-W. Kim, and A. Manchon, "Elusive Dzyaloshinskii-Moriya interaction in monolayer Fe₃GeTe₂," *Phys. Rev. B*, vol. 102, 060402, August 2020.
- [5] L. Liu et al., "Symmetry-dependent field-free switching of perpendicular magnetization," *Nat. Nanotech.*, vol. 16, pp. 277-282, January 2021.

Tuesday, August 30 | Room MD162 | 16:50-17:50

Coherent magnonics for quantum information science

2022 IEEE Magnetics Distinguished Lecture

Michael E. Flatté

University of Iowa, United States of America

michael-flatte@uiowa.edu

The current revolution in quantum technologies relies on coherently linking quantum objects like quantum bits (“qubits”). Coherent magnonic excitations of low-loss magnetic materials can wire together these qubits for sensing, memory, and computing. Coherent magnonics may reduce the size of superconducting qubits (which otherwise struggle with the large scale of microwave excitations) and may increase the size of spin-based qubit networks (which otherwise contend with the very short distances of dipolar or exchange interactions). Compared to photonic devices, these magnonic devices require minimal energy and space. However, efforts to exploit coherent magnonic systems for quantum information science will require a new understanding of the linewidths of low-loss magnonic materials shaped into novel structures and operating at dilution-refrigerator temperatures.

This lecture will introduce the fundamental requirements for practically linking quantum objects into large-scale coherent quantum systems as well as the advantages of coherent magnonics for next-generation quantum coherent systems (i.e., spin-entangling quantum gates [1]). Other critical challenges for quantum information science then will motivate the development of coherent magnonics for quantum transduction from “stationary” spin systems to “flying” magnons and for quantum memory [2-4]. Finally, the advantages of all-magnon quantum information technologies that rely on manipulating and encoding quantum information in superpositions of fixed magnon number states will highlight the potential of new magnetic materials, devices, and systems.

- [1] M. Fukami, D. R. Candido, D. D. Awschalom, and M. E. Flatté, “Opportunities for long-range magnon-mediated entanglement of spin qubits via on and off-resonant coupling,” *PRX Quantum*, vol. 2, Oct. 2021, Art. no. 040314.
- [2] D. R. Candido, G. D. Fuchs, E. Johnston-Halperin, and M. E. Flatté, “Predicted strong coupling of solid-state spins via a single magnon mode,” *Mater. Quantum Technol.*, vol. 1, Dec. 2021, Art. no. 011001.
- [3] Ö. O. Soykal and M. E. Flatté, “Strong field interactions between a nanomagnet and a photonic cavity,” *Phys. Rev. Lett.*, vol. 104, Feb. 2010, Art. no. 077202.
- [4] T. Liu, X. Zhang, H. X. Tang, and M. E. Flatté, “Optomagnonics in magnetic solids,” *Phys. Rev. B, Condens. Matter*, vol. 94, Aug. 2016, Art. no. 060405(R).

Wednesday, August 31 | Room MD162 | 08:30-09:30

Magnetic skyrmionic textures in proximity to a superconductor: vortex-skyrmion interaction, Meissner currents, and charge/spin supercurrents

Samme Dahir, Anatoly F. Volkov,
and Ilya M. Eremin

Institut für theoretische Physik III, Ruhr-Universität Bochum, Bochum, Germany

Ilya.Eremin@ruhr-uni-bochum.de

Topological spin configurations in proximity to a superconductor have recently attracted great interest due to the potential application of the former in spintronics and as another platform for realizing nontrivial topological superconductors. Their application in these areas requires precise knowledge of the existing exchange fields and/or the stray fields, which are therefore essential for the study of these systems.

In this talk we will analyse theoretically a hybrid heterostructure with magnetic textures including skyrmions inside a chiral ferromagnet interfaced by a thin superconducting film via an insulating barrier. We find that Pearl vortices (PV) are generated spontaneously in the superconductor within the skyrmion radius, while anti-Pearl vortices (PV) compensating the magnetic moment of the Pearl vortices are generated outside of the Sk radius, forming an energetically stable topological hybrid structure. Finally, we analyze the interplay of skyrmion and vortex lattices and their mutual feedback on each other. In particular, we argue that the size of the skyrmions will be greatly affected by the presence of the vortices offering another prospect of manipulating the skyrmionic size by the proximity to a superconductor [1]. Furthermore, we calculated the magnetic stray field and Meissner current in a superconductors S created by various nonhomogeneous magnetic texture in a F film incorporated in an S/F/S system [2] We also discuss the implications of the recent experimental results realizing these skyrmions-vortex interaction [3].

We also theoretically the influence of the magnetic textures and domain walls (DWs) on the DC Josephson current in magnetic superconducting Sm/FI/F/FI/Sm junctions. The Josephson junction consists of two “magnetic” superconductors Sm (superconducting film covered by a thin ferromagnetic layer), spin filters FI, and a ferromagnetic layer F with or without DW(s). The spin filters FI allow electrons to pass with one specific spin orientation, such that the Josephson coupling is governed by a fully polarized long-range triplet component. Once a DW is introduced, it reduces the critical Josephson current I_c in the case of equal spin polarization and makes it finite in the case of opposite spin orientation. The critical current I_c is maximal when the DW is in the center of the F film. A deviation of the DW from the center generates a force that pushes the DW to the center of the F film [4].

- [1] S. Dahir, A.F. Volkov, and I. Eremin, Interaction of Skyrmions and Pearl Vortices in Superconductor-Chiral Ferromagnet Heterostructures, *Phys. Rev. Lett.* 122, 097001 (2019).
- [2] Samme M. Dahir, Anatoly F. Volkov, and Ilya M. Eremin, Meissner currents induced by topological magnetic textures in hybrid superconductor/ferromagnet structures, *Phys. Rev. B* 102, 014503 (2020)
- [3] A. P. Petrović, M. Raju, X. Y. Tee, A. Louat, I. Maggio-Aprile, R. M. Menezes, M. J. Wszyński, N. K. Duong, M. Reznikov, Ch. Renner, M. V. Milošević, and C. Panagopoulos, *Phys. Rev. Lett.* 126, 11720513 (2021).
- [4] Samme M. Dahir, Anatoly F. Volkov, and Ilya M. Eremin, Charge and spin supercurrents in magnetic Josephson junctions with spin filters and domain walls, *Phys. Rev. B* 105, 094517 (2022).

Navigating in the dark - studying the magnetic sense of mole-rats

E. Pascal Malkemper

Max Planck Research Group Neurobiology of Magnetoreception, Max Planck Institute for Neurobiology of Behavior – caesar, Ludwig-Erhard-Allee 2, Bonn, Germany
pascal.malkemper@mpinb.mpg.de

Magnetoreception, the ability to sense the Earth's magnetic field and use it for orientation, is widespread within the animal kingdom. Even though there is unequivocal behavioral evidence for a magnetic sense in birds, amphibians and mammals, the location and identity of the sensory organ remains a mystery [1]. Three main mechanisms for the transduction of magnetic signals into nerve impulses have been proposed: (1) a chemical mechanism based on radical pairs, (2) a mechanism based on electromagnetic induction, and (3) a mechanism based on biological magnetite nanoparticles (Figure 1). There is data supporting each of these mechanisms, so there might not be just one type of magnetoreceptor. Conclusive evidence, however, on the histological, cellular and molecular level is lacking and new results often challenge published key findings years later. Therefore, unravelling the magnetic sense is a highly exciting field of research.

Our research group focusses on the mechanisms by which mammals perceive the Earth's magnetic field and use it for orientation. As a model system, we employ subterranean African mole-rats of the genus *Fukomys*, which in the wild spent their entire life in the total darkness of underground tunnel systems. We know for more than 30 years that these hamster-sized rodents possess a magnetic compass that guides them in the total darkness of their tunnels [2]. To deepen our understanding of mole-rat magnetoreception, we follow a neuroethological approach that involves behavioral assays, measurements of neuronal activity and directed screens for magnetoreceptor cells. In a top-down manner, we aim to identify and characterize the brain structures encoding magnetic information in these mammals to learn more about the location of the primary magnetoreceptor cells [3]. In this talk, I will give an overview of this approach, focusing on some of the methods to identify the primary receptor cells, such as Synchrotron X-Ray fluorescence microscopy, MRI quantitative susceptibility mapping, and quantum magnetic imaging.

The financial funding from the European Research Council (ERC StG NeuroMagMa, 948728), the DFG (Project 490777637), and the Max Planck Society is gratefully acknowledged.

- [1] G.C. Nordmann et al., PLOS Biology 15(10), e2003234 (2017).
- [2] H. Burda et al., Experientia 46: 528–530 (1990).
- [3] E.P. Malkemper et al., J. Exp. Biol. 223, 21 (2020).

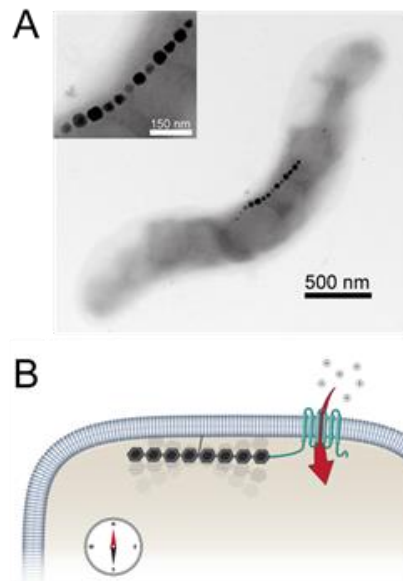


Figure 1. The magnetite hypothesis of magnetoreception. (A) TEM image of magnetotactic bacteria that produce a chain of single domain magnetite particles, which align them with the geomagnetic field lines. (B) A hypothetical magnetoreceptor based on single domain magnetite coupled to an ion channel in a vertebrate neuron. This neuron could fire depending on the chain's alignment in the geomagnetic field (not in scale, adapted from Ref 1). Magnetite is a likely mechanism for magnetoreception in many species including mole-rats.



Wednesday, August 31 | Parkhaus Hugel | 18:30

The changing landscape of science diplomacy

Laura H. Greene

The National MagLab and Florida State University

Since the invasion of Ukraine, CERN has published fewer scientific papers because German and Polish physicists have refused to publish with their Russian colleagues. Even historically neutral Switzerland has sanctioned Russia. Furthermore, to attend IUPAP sponsored meetings, Russian physicists are now required to claim IUPAP as their byline. The pursuit of science must remain a global endeavor to ensure broad access to large-scale facilities, diverse participation, and the continued ability to build constructive international partnerships. Science diplomacy has clearly changed since the mid 20th century. In addressing these new challenges, it is essential that we develop new policy to advise our leadership.

Thursday, September 1 | MD162 | 08:30-09:30

Superconductivity in infinite-layer nickelates

Harold Y. Hwang

Department of Applied Physics, Stanford University
Stanford Institute for Materials and Energy Sciences and Department of Photon Science, SLAC
National Accelerator Laboratory
hyhwang@stanford.edu

Finding unconventional superconductors in proximity to various strongly correlated electronic phases has been a recurring theme in materials as diverse as heavy fermion compounds, cuprates, pnictides, and twisted bilayer graphene. The recent discovery of superconductivity in layered nickelates [1] was motivated by looking for an analog of the cuprates. The synthesis of the nickelates is in and of itself interesting – it involves the removal of planes of oxygen from a 3D nickel oxide using soft chemistry techniques. We will introduce this new family of superconductors and our current understanding of their electronic and magnetic structure. Notable aspects are a doping-dependent superconducting dome [2], strong magnetic fluctuations [3], instabilities towards charge stripes [4], and a landscape of unusual normal state properties from which superconductivity emerges [5]. These features are strongly reminiscent of the cuprates, despite key differences in the electronic structure and the absence of a proximate correlated insulator.

This work was supported by the US Department of Energy, Office of Basic Energy Sciences, Division of Materials Sciences and Engineering grant DE-AC02-76SF00515; and the Gordon and Betty Moore Foundation's Emergent Phenomena in Quantum Systems Initiative grant GBMF9072.

- [1] D. F. Li et al., *Nature* 572, 624 (2019).
- [2] D. F. Li et al., *Phys. Rev. Lett.* 125, 027001 (2020).
- [3] H. Lu et al., *Science* 373, 213 (2021).
- [4] M. Rossi et al., arXiv: 2112.02484.
- [5] K. Lee et al., arXiv: 2203.02580.

Hard X-ray Magnetic Circular Dichroism: Where from? Where to?

Andrei Rogalev, Fabrice Wilhelm

ESRF, France

rogalev@esrf.fr

Discovery of X-ray magnetic circular dichroism (XMCD) 35 years ago [1] marks a major breakthrough in magnetism research reaching objectives that previously would have been unattainable. The XMCD is obtained as a difference in the X-ray absorption spectra of a magnetized sample recorded with left and right circularly polarized photons. In a way, it may be seen as the high-energy counterpart to the magneto-optical effects in the visible discovered by Faraday and Kerr. Unlike the latter, XMCD benefits of the unique advantage to be element specific and orbital selective since it originates from transitions of a core electron of an absorbing atom into its empty states picked out via the selection rules. Furthermore, derivation of magneto-optical sum rules [2,3] has greatly strengthened the XMCD, offering a unique capability of quantitative determination of the orbital and spin contributions to the total magnetic moment carried by the absorbing atom. Availability of high fluxes of circularly polarized X-rays at the 3rd generation synchrotron radiation facilities make this technique widely available. Sophisticated end stations have facilitated its use, offering a large variety of sample environments, including high magnetic field, ultralow temperature, high pressure, etc.

Two examples are selected to illustrate how XMCD helps to decipher a new quantum conundrum in condensed matter physics: coexistence of magnetism and superconductivity. The first example is Plutonium paramagnetism in the vortex phase of an exotic superconductor PuCoGa₅ [4]. The second one concerns the dual nature of Uranium 5f electrons in heavy fermion ferromagnetic superconductor UGe₂ [5].

Concomitant advances in X-ray instrumentation and theoretical approaches have metamorphosed XMCD from a scientific curiosity to a workhorse technique in modern magnetism research and have paved the way to further new applications of XMCD in chemistry, earth science, biology and other fields of science.

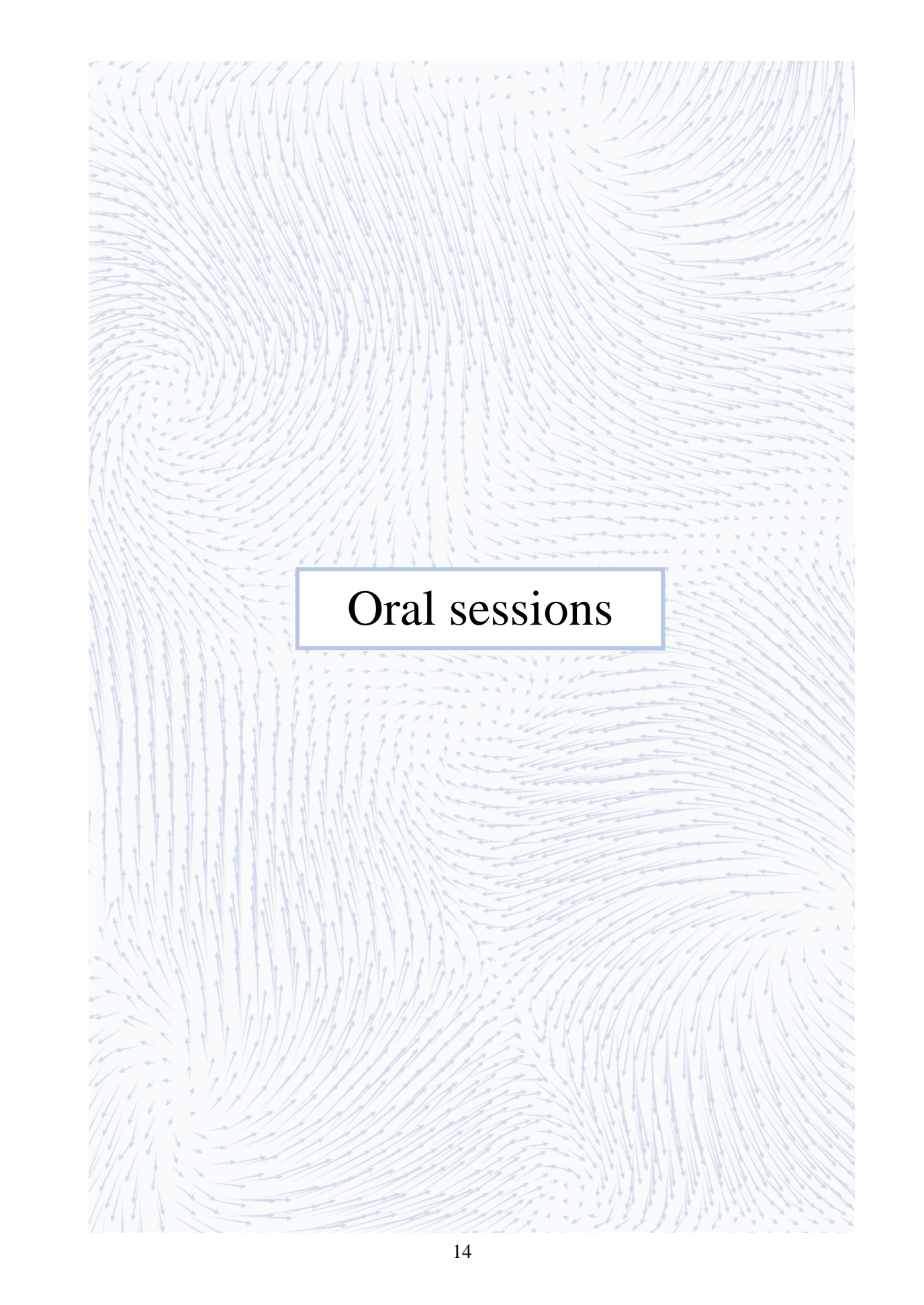
[1] G. Schütz et al., PRL 58, 737 (1987).

[2] B. T. Thole et al., PRL 68, 1943 (1992).

[3] P. Carra et al., PRL 70, 694 (1993).

[4] N. Magnani et al., PRL 119, 157204 (2017).

[5] F. Wilhelm et al., submitted (2022).



Oral sessions

Direct observation of tunable magnetic domains and walls in a noncentrosymmetric ferromagnetic Weyl semimetal

Ilya Sochnikov

University of Connecticut, Storrs, CT USA

ilya.sochnikov@uconn.edu

Textures and dynamics of domain walls (DW) in magnetic Dirac materials are predicted to have their electromagnetic behavior transformed by the emergent gauge or axial fields. The axial fields – a paradigm initially developed in the high-energy and particle physics – is yet to be confirmed in direct experiments in solid state materials. Therefore, knowing the detailed domain physics is important for the experimental detection of the axial effects. In this work, we imaged spontaneous magnetization and magnetic susceptibility of a non-centrosymmetric ferromagnetic (FM) Weyl semimetal: CeAlSi [1,2]. We utilized a scanning SQUID susceptometer microscopy, which can be considered a type of low-frequency and low-energy spectroscopic imaging technique [3,4]. We observed large ferromagnetic DWs and discovered the coexistence of stable and metastable phases, which likely arise due to magnetostriction effects and are potentially highly tunable with small strains. We found that the pattern of the FM domains is strongly correlated with both the magnitude and the orientation of an external in-plane magnetic field. Our results show how these domains, and the heterogeneous phases can be fine-tuned. Therefore, this work provides guidance for future studies of the fundamental interplay between magnetism and exotic electromagnetic fields in Dirac systems.

- [1] H.-Y. Yang et al., Phys. Rev. B, Editor's Choice Article, 103, 115143 (2021).
- [2] B. Xu et al., Adv. Quantum Technol., Cover Article, 2000101 (2021).
- [3] Z.-C. Wang et al., Advanced Materials, 2005755 (2021).
- [4] C. Herrera et al., Phys. Rev. B, Editor's Choice Article, 103, 024528 (2021).

Magnetic hedgehog structure in a magnetically frustrated Kondo-lattice CePtAl₄Ge₂

Soohyeon Shin^{1,*}, Jin-Hong Park², Romain Sibille³, Oksana Zaharko³, Harim Jang², Marisa Medarde¹, Ekaterina Pomjakushina¹, Michel Kenzelmann³, Tuson Park²

¹Laboratory for Multiscale Materials Experiments, Paul Scherrer Institut, CH-5232 Villigen PSI, Switzerland

²Center for Quantum Materials and Superconductivity (CQMS) and Department of Physics, Sungkyunkwan University, Suwon 16419, South Korea

³Laboratory for Neutron Scattering and Imaging, Paul Scherrer Institut, CH-5232, Villigen PSI, Switzerland

soohyeon.shin@psi.ch

CePtAl₄Ge₂ exhibits an antiferromagnetic state below 2.3 K in which the size of ordered moments modulates with an ordering wave vector $\mathbf{k} = (1.39, 0, 0.09)$ [1]. Single-crystal neutron diffraction experiments have been recently performed and revealed that the magnetic structure of CePtAl₄Ge₂ is of multi- \mathbf{k} structure in which symmetry-equivalent three arms of $\mathbf{k} = (1.39, 0, 0.09)$ are superposed. Theoretical calculation of the topological numbers on singular points in the multi- \mathbf{k} spin structure shows non-trivial hedgehog numbers, indicating that a three-dimensional topological spin texture is realized in this frustrated Kondo lattice. When subjected to a magnetic field applied along the [010] direction, the magnetic structure undergoes a phase transition at the critical field (H^* = 10 kOe) from the multi- \mathbf{k} to single- \mathbf{k} phase while the ordering wave vector \mathbf{k} remains the same. At H^* , the temperature-coefficient of electrical resistivity and magnetic entropy exhibit the maximum value, suggesting that the field-induced topological transition from the hedgehog state to a non-topological single- \mathbf{k} state is correlated with the quantum critical behavior. In this presentation, we will discuss the possible origin of the topological magnetic structure and the relationship between the topological transition and quantum criticality.

[1] S. Shin *et al.*, Physical Review B **101**, 224421 (2020).

Chern and Z_2 topological insulating phases in perovskite-derived oxide honeycomb lattices

Okan Koeksal, Rossitza Pentcheva

Department of Physics, University of Duisburg-Essen

okan.koeksal@uni-due.de

On the basis of density functional theory calculations plus the Hubbard U interaction, we explore the electronic and possibly topologically non-trivial phases in $(\text{LaXO}_3)_2/(\text{LaAlO}_3)_4$ (111) superlattices (SLs) with $X = 4d$ and $5d$ cations. Our results predict that the metastable ferromagnetic phases of LaTcO_3 and LaPtO_3 with preserved $P321$ symmetry turn out to be Chern insulators (CI) with $C = 2$ and 1 with band gaps of 43 and 38 meV at the in-plane lattice constant of LaAlO_3 ($a_{\text{LAO}} = 3.79 \text{ \AA}$), respectively. By applying lateral strain, the Chern insulating phase of $X = \text{Tc}$ is further stabilized, whereas a site disproportionation arises for $X = \text{Pd}$ and Pt when the lateral constant is increased from a_{LAO} to a_{LNO} . The candidate for a Chern insulator, i.e., $X = \text{Pt}$ shows a strong dependence on the Coulomb repulsion strength U with a sign reversal for higher values associated with the change of band gap opening mechanism. Moreover, non-magnetic systems such as $X = \text{Mo}$ and W emerge as potential candidates for Z_2 topological invariants at a_{LAO} with band gaps of 26 and 60 meV, respectively. The investigation of Berry curvatures, spin textures, edge states and Z_2 invariants provide additional insight into the nature of both the Chern and Z_2 topological insulating states.

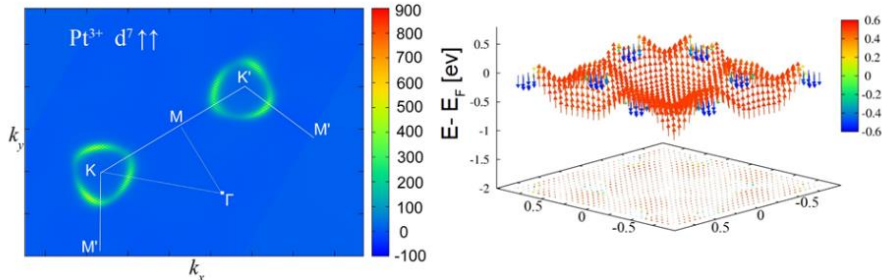


Figure 1. A SOC-induced band inversion leads to avoided band crossing around K visible as a ring-like structure in the Berry curvature $\Omega(\mathbf{k})$ (left) accompanied by a spin reversal in the spin texture (right)

The financial funding from DFG within CRC/TRR80 (Projektnummer 107745057), project G3 is gratefully acknowledged.

[1] O. Koeksal, Rossitza Pentcheva, Sci. Rep. 9, 1 (2019).

Ab initio study of spin-spin and spin-lattice couplings in two-dimensional Ising antiferromagnet FePS₃

Mohammad Amirabbasi, Peter Kratzer

Faculty of Physics and CENIDE, Universität Duisburg-Essen, 47057 Duisburg, Germany

mohammad.amirabbasi@uni-due.de

Understanding the magnetic properties of low-dimensional materials is one of the major challenges in the field of condensed matter physics. In particular, the availability of 2D magnetic semiconductors opens up numerous applications in spintronics and magneto-optics. In this context, two-dimensional transition metal phosphorus trisulfides MPS₃ (M=Fe, Ni and Mn) have gained special interest recently because they combine narrow band gaps with unusual magnetic behavior. In this contribution, we investigate the magnetic ordering in FePS₃, a two-dimensional Ising antiferromagnet FePS₃ with a Neel temperature of 120 K in bulk. Bulk FePS₃ is a layered material where Fe²⁺ (S=2) ions form a distorted honeycomb geometry, two bonds being longer than the other 4 bonds. This material has a strong out-of-plane easy axis, which renders stable magnetic order even in the monolayer limit. However, despite many experimental [1] and theoretical [2] investigations, the exact magnetic structure of the ground state is still under debate.

This motivated us to carry out a comprehensive computational study of the magnetic and vibrational properties employing the DFT+U approach (Density Functional Theory plus on-site electron-electron repulsion). We find that U=2.22 eV can produce the experimental band gap of 1.23 eV [3]. The Fe²⁺ ions have a fully occupied 3d shell in the majority spin channel, plus one minority-spin d-electron. Our obtained results show that the spin-orbit coupling is not quenched in this material, and our calculations indicate an orbital moment of Fe²⁺ of about 0.8 μ_B . The projected density-of-states and Lowdin analysis show that the minority-spin electron occupies a linear combination of the x^2-y^2 and yz 3d-orbitals, which gives rise to orbital ordering in the ground state. Thus, the phase transition to the paramagnetic state involves both the magnetic and the lattice degrees of freedom. Therefore, we introduce, within the DFT+U framework, a spin-lattice Hamiltonian governing the magnetic properties of this system at finite temperatures. The spin-lattice Hamiltonian includes isotropic and anisotropic terms, such Heisenberg, single-ion anisotropy, and Dzyaloshinskii-Moriya interactions. Interestingly, we find that the magnetic exchange interaction is ferromagnetic and antiferromagnetic along the long bonds and short bonds, respectively. This assignment turns out to be robust with respect to changes of the U parameter. We conclude that the magnetic ground state consists of ferromagnetic spin chains running along the long bonds which couple antiferromagnetically among each other. According to our findings, the atomic vibrations and the associated changes in bond lengths couple to the spin-spin interaction. Approaching the Neel temperature from below, the excitations of the system are combined magnonic and phononic excitations, in accord with the observation of temperature-dependent shifts of Raman-active modes [4].

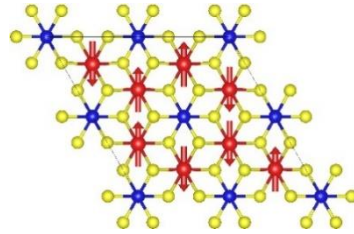


Figure 1. Ground state spin structure as obtained from our DFT+U calculations. The red, blue and yellow spheres denote Fe, P and S atoms, respectively.

[1] D. Lancon et al., Phys. Rev. B **94**, 214407 (2016).

[2] T. Olsen, J. Phys. D: Appl. Phys. **54**, 314001 (2021).

[3] M. Ramos et al., npj 2D Materials and Applications **5**, 1 (2021).

[4] X. Wang et al., 2D Materials **3**, 031009 (2016).

Comparative study of magnetic properties of Mn³⁺ magnetic clusters in GaN using classical and quantum mechanical approach

Y.K. Edathumkandy and D. Sztenkiel

Institute of Physics, Polish Academy of Sciences, Warszawa, Poland

[sztienkiel@ifpan.edu.pl](mailto:sztenkiel@ifpan.edu.pl)

Currently, simulations of many-body quantum systems are known to be computationally too demanding to be solved on classical computers. The main problem is that the computation time (number of elementary operations) and memory necessary for performing the calculations usually grow exponentially with the number of particles. An efficient approach to simulate many-body quantum systems is the use of classical approximation. Such an approach can reduce the overall computational complexity, but it usually face difficulties in proper reproduction of temperature-dependent properties of the system due to neglect of spin quantization [1]. It is important then to somehow assess the validity of this classical approximation. For practical reasons the quantum simulations of interacting Mn³⁺ ions in GaN, coupled by ferromagnetic super-exchange interaction $JS_i \cdot S_j$, are restricted up to small magnetic clusters. Therefore in this work [2], we compare the results of numerical calculations of magnetic clusters (singlet, pairs, triplets and quartets) in (Ga,Mn)N where the Mn spins are treated classically with those where they are treated quantum-mechanically (crystal field model) [3,4]. In the first case, we solve the LLG equation, that describe the precessional dynamics of spins represented by classical vectors. On the other hand, in crystal field model, the Mn³⁺ state (d^4 configuration, with $S=2$, $L=2$) is characterized by the set of orbital and spin quantum numbers $|m_S, m_L\rangle$. The relevant energy level structure of singlet, pair, triplet and quartet of Mn ions are found by the numerical diagonalization of full (25×25) , $(25^2 \times 25^2)$, $(25^3 \times 25^3)$ and $(25^4 \times 25^4)$ Hamiltonian matrix respectively. Particular attention is paid to use numerical parameters that ensure the same single ion magnetic anisotropy in classical and quantum approximation. Finally, a detailed comparative study of magnetization $M(H, T)$ as a function of magnetic field H , temperature T , number of ions in given cluster N and the strength of super-exchange interaction J , obtained from both approaches will be presented.

The work is supported by the National Science Centre, Poland, through projects DEC-2018/31/B/ST3/03438 and by the Interdisciplinary Centre for Mathematical and Computational Modelling at the University of Warsaw through the access to the computing facilities.

- [1] R. F. L. Evans *et al.*, *J. Phys.: Condens. Matter.* **26**, 103202 (2014).
- [2] Y. K. Edathumkandy and D. Sztenkiel, *arXiv* :2108.01474.
- [3] J. Gosk, *et al.*, *Phys.Rev. B.* **71**, 094432 (2005).
- [4] D. Sztenkiel *et al.*, *Nature Comm.* **7**, 13232 (2016)

Thermally induced spin transport and magnon propagation length in garnet heterostructures

Hari Srikanth

University of South Florida, Tampa, FL

sharihar@usf.edu

Thermal spin transport is a topical area of interest for the spintronics community. The origin of Spin Seebeck effect (SSE) and its relationship with magnetic anisotropy as well as magnon propagation across magnetic insulator/heavy metal interfaces have remained challenging issues. We have pioneered the technique of RF transverse susceptibility to probe the effective magnetic anisotropy in magnetic materials and heterostructures. Combining these experiments with SSE and anomalous Nernst effect (ANE) measurements, a distinct correlation between bulk and surface anisotropy with the field and temperature dependence of SSE in yttrium iron garnet (YIG)/Pt heterostructures and other compensated ferrimagnets have been obtained [1,2]. We have also demonstrated, for the first time, universal scaling of longitudinal SSE in gadolinium iron garnet (GdIG) films with different thickness and on different substrates across the compensation temperature [3]. Our current work on thulium iron garnet (TmIG) heterostructures with varying film thickness reveals the clear role of anisotropy and damping on the SSE. From RF susceptibility, SSE and FMR spin pumping experiments, quantitative analysis of the magnon propagation length has been done. Overall, this talk would present new results in the thermal spin transport of garnet heterostructures which are of fundamental importance in next generation spin caloritronic devices.

- [1] “Giant spin Seebeck effect through an interface organic semiconductor” - V. Kalappattil, R. Geng, R. Das, M. Pham, H. Luong, T. Nguyen, A. Popescu, L.M. Woods, M. Klauel, H. Srikanth and M.H. Phan, *Materials Horizons* 7, 1413 (2020)
- [2] “Tunable competing magnetic anisotropies and spin reconfigurations in ferrimagnetic Fe_{100-x}Gdx alloy films” -A. Chanda, J. E. Shoup, N. Schulz, D. A. Arena and H. Srikanth, *Physical Review B* 104, 094404 (2021)
- [3] “Scaling of the thermally induced sign inversion of longitudinal spin Seebeck effect in a compensated ferrimagnet: role of magnetic anisotropy” -A. Chanda, C. Holzmann, N. Schulz, J. Seyd, M. Albrecht, M.H. Phan and H. Srikanth, *Advanced Functional Materials* 32, 2109170 (2022)

Recent progress in ultrafast magneto-acoustics

Vasily Temnov

LSI, Ecole Polytechnique, CEA/DRF/IRAMIS, CNRS, IP Paris, F-91128, Palaiseau, France

vasily.temnov@cnrs.fr

Here I review some of our recent experimental and theoretical results in ultrafast magneto-acoustics in magnetostrictive materials and nanostructures [1] in the GHz-to-THz frequency range. Ultrafast magneto-acoustics investigates the coupling between magnetization and elementary excitations of magnetic order with lattice vibrations in the highest experimentally accessible frequency range.

The first example discusses magneto-elastic excitations of ferromagnetic resonance (FMR) with quasi-monochromatic GHz-frequency Surface Acoustic Waves (SAWs) optically excited in nickel thin films on glass using the transient grating geometry [2]. The underlying theoretical modeling, starting from the analysis of phenomenological Landau-Lifshitz-Gilbert (LLG) equations, results in a simple equation of an externally and parametrically driven FMR-oscillator. The letter captures the most essential experimental observations such as the resonant enhancement of FMR amplitude, the linear parametric sum- and difference frequency mixing and generation of fractional parametric frequencies [3]. The peculiarities of time-resolved experiments with GHz-frequency excited on permanent gratings will be illustrated using recent magneto-elastic experiments with permanent grating on glass and silicon substrates.

The second example discusses how perpendicular standing spin wave modes in ferromagnetic thin films in ~100 GHz frequency range, i.e. exchange magnons, can be excited by ultrashort pulses of longitudinal acoustic phonons propagating across the film. The dominant role of the acoustic bandwidth in this process is revealed [4].

The outlook discusses some recent theoretical results about resonantly enhanced interactions between acoustic and magnonic cavity modes in suspended hybrid metal-ferromagnetic multilayer structures [5].

The financial funding from ANR-21-CE15-0048-01 MRSEI "IRON-MAG" is gratefully acknowledged.

[1] W.G. Yang and H. Schmidt, *Appl. Phys. Rev.* 8, 021304 (2021).

[2] J. Janusonis et al., *Phys. Rev. B* 94, 024415 (2016).

[3] C.L. Chang et al., *Phys. Rev. B* 95, 060409 (2017).

[4] V. Besse et al., *J. Magn. Magn. Mat.* 502, 166320 (2020).

[5] U. Vernik et al., <https://arxiv.org/abs/2205.09805> (2022).

Inverse magneto-plasmonics for laser-induced spin dynamics

Ilya Razdolski, Andrzej Stupakiewicz

Faculty of Physics, University of Białystok, 15-245 Białystok, Poland

i.razdolskiy@uwb.edu.pl

Optical technologies for magnetic recording require nanoscale spatial resolution, thus highlighting the importance of nanophotonics for localizing light-spin interaction. Surface plasmons are known for their ability to confine light in subwavelength volumes and strongly increase the optical energy density which is key for numerous applications. Plasmon-based excitation mechanisms of spin dynamics enjoy high potential for taking the all-optical magnetization switching onto the nanoscale and approaching the fundamental thermodynamical energy limit for switching magnetic bits.

In this work, we present a novel perspective of plasmonics beyond the conventional enhancement of the electromagnetic fields. We demonstrate our approach in the framework of nanophotonic control of inverse magneto-optical (opto-magnetic) Faraday effect (IFE) and photo-magnetism (PM). Taking the free energy approach and following [1], after the separation of symmetric (γ) and antisymmetric (α) parts of the susceptibility tensor for the effective light-induced magnetic field we get:

$$H_i(0) = \alpha_{ijk} E_j E_k^* + \gamma_{ijkl} E_j E_k^* M_l(0) + c. c. + \dots$$

Here E is the electric field of light, and $M(0)$ is the static magnetization of the medium. The first and the second terms are responsible for the IFE and PM together with the inverse Cotton-Mouton effect, respectively. We discuss a model surface plasmon-polariton excitation at an interface between a metal and magnetic dielectric. In these systems, Eq. (1) can be rewritten in terms of a total optical intensity $\propto |E|^2$ and a phase shift between the electric field components. We argue that the key role of nanophotonic excitations consists in effectively modifying this phase while simultaneously enhancing and, notably, confining the excitation at the nanoscale. We experimentally and numerically demonstrate its efficiency and flexibility at setting the magnetization into motion via ultrafast plasmonic excitation of the spin system in the dielectric. An exchange precession mode in Yb,Gd-doped BIG [2] and a Kittel mode in Co-doped YIG [3,4] is excited with about one order enhancement of the specific efficiency, as shown by the quantitative analysis.

Our results emphasize the potential of hybrid magneto-plasmonic structures featuring noble (plasmonic) metals and transparent magnetic dielectrics. We further discuss future development of this novel approach and outline a promising class of nanophotonic systems demonstrating inverse magneto-plasmonic effects.

The funding from National Science Center Poland (Grant No. DEC-2019/35/B/ST3/00853) is gratefully acknowledged.

[1] A.V. Kimel and A. K. Zvezdin, *Low Temp. Phys.* 41, 682–688 (2015).

[2] A.L. Chekhov, A. I. Stognij, T. Satoh, T. V. Murzina, I. Razdolski and A. Stupakiewicz, *Nano Lett.* 18, 2970 (2018).

[3] A. Kazlou, A.L. Chekhov, A. I. Stognij, I. Razdolski, and A. Stupakiewicz, *ACS Photon.* 8, 2197–2202 (2021).

[4] T. Kaihara, I. Razdolski, and A. Stupakiewicz, *Opt. Mater. Express* 12 (2), 788–797 (2022).

Spin-wave driven bidirectional domain wall motion in kagome antiferromagnets

K. M. D. Hals¹, A. Salimath¹, D. R. Rodrigues², K. Everschor-Sitte²

¹Department of Engineering Sciences, University of Agder, 4879 Grimstad, Norway
kjetil.hals@uia.no

²Institute of Physics, Johannes Gutenberg University, 55128 Mainz, Germany

Insulator-based spintronics is a promising new pathway for developing the next-generation low-power technologies [1-3]. In contrast to metallic spin electronics, in which the magnetic bits are controlled via the itinerant charge carriers, the spin information in insulators is manipulated by the collective spin-wave excitations of the magnetic material, i.e., the magnons. In this work [4], we predict a new mechanism to controllably manipulate domain walls in kagome antiferromagnets via a single linearly polarized spin-wave source. We show by means of atomistic spin dynamics simulations of antiferromagnets with kagome structure

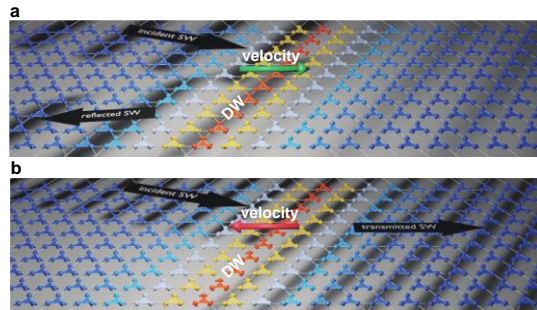


Fig. 1: Frequency controlled spin wave-induced domain wall motion. For a low (b high) frequencies, linearly polarized spin waves move the domain wall away from (towards) the spin-wave source. The figure is taken from Ref. [4].

that the speed and direction of the domain wall motion can be regulated by only tuning the frequency of the spin waves (Fig. 1). Starting from microscopics, we establish an effective action and derive the corresponding equations of motion for the spin-wave-driven domain wall. Our analytical calculations reveal that the coupling of two spin-wave modes inside the domain wall explains the frequency-dependent velocity of the spin texture. The findings imply that the placement of the domain walls can be manipulated via a single linearly polarized spin-wave source and thus provides a route toward significantly simplifying the bits' control mechanism in racetrack memories. We expect our predictions to be valid for a large class of materials ranging from iron jarosites to Weyl semimetals.

The work received funding from the Research Council of Norway via Grant No. 286889 and the DFG via the Emmy Noether project 320163632 and TRR 173 – 268565370 (project B12). A. Salimath acknowledges A. Abbout for the assistance during the development of the atomistic spin dynamics code. D.R. Rodrigues and K. Everschor-Sitte acknowledge H. Gomonay for discussions on noncollinear antiferromagnets.

- [1] Y. Kajiwara, K. Harii, S. Takahashi, J. Ohe, K. Uchida, M. Mizuguchi, H. Umezawa, H. Kawai, K. Ando, K. Takanashi, S. Maekawa, and E. Saitoh, *Nature*, **464**, 262 (2010).
- [2] L. J. Cornelissen, J. Liu, R. A. Duine, J. B. Youssef, and B. J. van Wees, *Nat. Phys.*, **11**, 1022 (2015).
- [3] R. Lebrun, A. Ross, S. A. Bender, A. Qaiumzadeh, L. Baldrati, J. Cramer, A. Brataas, R. A. Duine, and M. Kläui, *Nature*, **561**, 222 (2018).
- [4] D. R. Rodrigues, A. Salimath, K. Everschor-Sitte, K. M. D. Hals, *Phys. Rev. Lett.* **127**, 157203 (2021).

Spin pumping in noncollinear antiferromagnets

Mike A. Lund, Akshaykumar Salimath, Kjetil M. D. Hals

Department of Engineering Sciences, University of Agder, 4879 Grimstad, Norway

mikeal@uia.no

The spin pumping [1, 2] and spin-transfer torque [3, 4] mechanisms in antiferromagnets (AFMs) have been theoretically investigated in several works, and sub-THz spin pumping has recently been experimentally observed [5, 6]. Most of these works have concentrated on collinear AFMs, which are characterized by a single order parameter vector (the staggered field). However, several AFMs require two or even three orthogonal staggered fields to describe the spin order correctly. These systems are referred to as noncollinear antiferromagnets (NCAAFMs), whose order parameter is an $SO(3)$ rotation matrix defining the orientation of the reference frame spanned by the orthogonal staggered fields. To date, little knowledge exists on how spin currents couple to the $SO(3)$ -valued antiferromagnetic order parameter of NCAAFMs. Apart from a few works on spin transfer torque [7 - 9], there has been no thorough investigation of the spin pumping process in these nontrivial spin systems.

In this work [10] we theoretically investigate the ac spin pumping of NCAAFMs. Starting from an effective action description of the spin system, we derive the Onsager coefficients connecting the spin pumping and spin-transfer torque associated with the dynamics of the $SO(3)$ -valued antiferromagnetic order parameter. Our theory is applied to a kagome AFM resonantly driven by a uniform external magnetic field. We demonstrate that the reactive (dissipative) spin-transfer torque parameter can be extracted from the pumped ac spin-current in phase (in quadrature) with the driving field. Furthermore, we find that the three spin-wave bands of the kagome AFM generate spin currents with mutually orthogonal polarization directions (Fig. 1). This offers a unique way of controlling the spin orientation of the pumped spin current by exciting different spin-wave modes.

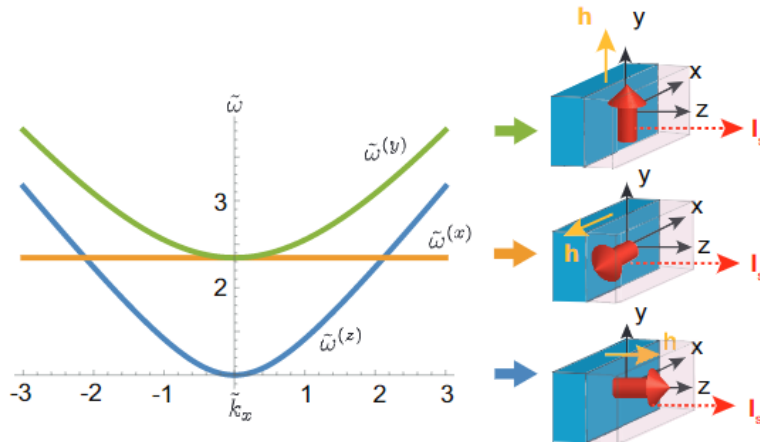


Figure 1. The spin wave dispersion relation of the kagome AFM (left) and the spin current (right) pumped from the NCAAFM (blue) into an adjacent normal metal (transparent pink), when driven at resonance by the field h (yellow arrow). The three spin wave bands pump a spin current with mutually orthogonal spin polarization directions (red arrows)

The financial funding from RCN (Young Research Talents Grant No. 286889) is gratefully acknowledged.

- [1] R. Cheng, J. Xiao, Q. Niu, and A. Brataas, Physical Review Letters **113**, 057601 (2014).
- [2] R. E. Troncoso, M. A. Lund, A. Brataas, A. Kamra, Phys. Rev. B **103**, 144422 (2021).
- [3] K.M.D. Hals, Y. Tserkovnyak, and A. Brataas, Phys. Rev. Lett. **106**, 107206 (2011).
- [4] For a review see T. Jungwirth et al., Nat. Phys. **14**, 200 (2018).



- [5] P. Vaidya et al., *Science* **368**, 160 (2020).
- [6] J. Li et al., *Nature* **578**, 70 (2020).
- [7] H. V. Gomonay, R. V. Kunitsyn, and V. M. Loktev, *Phys.Rev. B* **85**, 134446 (2012).
- [8] Y. Tserkovnyak and H. Ochoa, *Phys. Rev. B* **96**, 100402(R) (2017).
- [9] B. Li and A. A. Kovalev, *Phys. Rev. B* **103**, L060406 (2021).
- [10] M. A. Lund, A. Salimath, and K. M. D. Hals, *Phys. Rev. B* **104**, 174424 (2021)

Ferromagnetic resonance study of spin pumping in epitaxial Fe/Rh bilayers

Jonas Wiemeler, Ali Can Aktas, Michael Farle, Anna Semisalova

Faculty of Physics and CENIDE, University of Duisburg-Essen, 47057 Duisburg, Germany

jonas.wiemeler@uni-due.de

The alloy FeRh of various Fe composition has been studied extensively for structural, electrical, and magnetic properties. A nearly equiatomic composition represents a special interest since it undergoes a first order magnetic phase transition from antiferromagnetism to ferromagnetism, driven by temperature, strain or external magnetic fields, which makes a bulk FeRh system suitable for magnetocaloric applications. High prices and limited worldwide supply of Rh make a bulk application economically inefficient. Therefore, investigation focuses on FeRh thin films. In equiatomic FeRh thin film, the (111) interface would represent Fe and Rh multilayers of monolayer thicknesses [1].

Fe/Rh thin film bilayer systems with Fe and Rh layer thicknesses greater than the monolayer limit were not studied in detail yet. In this work, 5 nm Fe films capped with Rh of thicknesses (0, 1, 2, 3, 5, 10, 15) nm were grown on GaAs(100) substrates using molecular beam epitaxy (MBE). The growth characteristics of Rh on a 5 nm Fe layer have been investigated using Low Energy Electron Diffraction (LEED) and Auger electron spectroscopy (AES) during the Rh growth. The AES intensities of 703 eV Fe and 302 eV Rh peaks are compared in Figure 1. It was found, that Rh grows epitaxially on Fe in a deviated layer-by-layer manner [2], as supported by literature [3, 4].

Ferromagnetic resonance (FMR) experiments at room temperature, combining both angular X-Band and frequency (1-40 GHz) dependence, were used to characterise magnetic anisotropy and magnetic damping α . The thickness dependence of α , measured in-plane, shows an exponential behaviour which was analysed in terms of a spin pumping effect using a model developed by Tserkovnyak [5], that can be seen in Figure 2. We found that Rh spin mixing conductance compares to that of platinum [6], while the spin-diffusion-length compares to that of palladium [7] making Fe/Rh a promising combination for further spintronics studies.

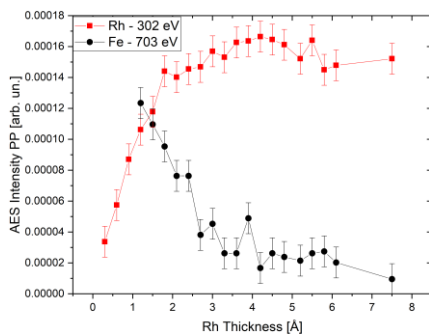


Figure 1. AES intensity of Fe and Rh peaks during submonolayer growth of Rh on Fe.

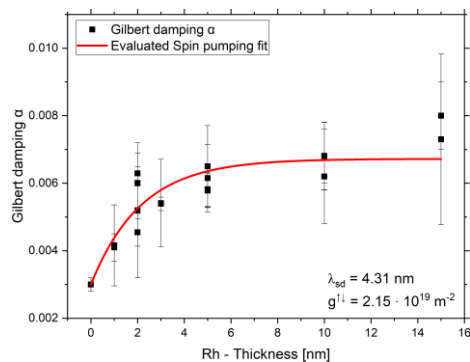


Figure 2. The precession damping of 5 nm Fe/GaAs(100) capped with Rh of varied thickness.

Funding by DFG Project No. 392402498 (SE 2853/1-1 — AL 618/37-1) and helpful discussion with R. Meckenstock and T. Strusch are acknowledged.



- [1] I. Suzuki et al., APL 105, 17, 172401 (2014)
- [2] K. Bryant et al., JAP 97, 024904 (2004)
- [3] R. Pfandzelter et al., Surf. Rev. Lett. 10, 117–120 (2003)
- [4] T. Kachel et al., PRB 46, 19, 12888–12891 (1992)
- [5] Y. Tserkovnyak et al., PRB 66, 224403 (2002)
- [6] Y. Huo et al., AIP Advances 7, 056024 (2017)
- [7] A. Kumar et al., PRB 95, 6, 064406 (2017)

Quantum spins and hybridization in artificially-constructed chains of magnetic adatoms on superconducting 2H-NbSe₂

Eva Liebhaber¹, Lisa Rütten¹, Gaël Reecht¹, Jacob F. Steiner², Harald Schmid², Sebastian Rohlf³, Kai Rossnagel³, Felix von Oppen², Katharina J. Franke^{1,*}

¹Fachbereich Physik, Freie Universität Berlin, 14195 Berlin, Germany

²Dahlem Center for Complex Quantum Systems and Fachbereich Physik, Freie Universität Berlin, 14195 Berlin, Germany

³Institut für Experimentelle und Angewandte Physik, Christian-Albrechts-Universität zu Kiel, 24118 Kiel, Germany

franke@physik.fu-berlin.de

Exchange coupled magnetic adatoms on superconductors are prime examples to study the competition of magnetism and superconducting pairing. A fingerprint of the interaction can be found as Yu-Shiba-Rusinov (YSR) states inside the superconducting energy gap of the substrate. These states can be detected in scanning tunneling spectroscopy at the single-atom scale.

Here, we explore the quasi-two-dimensional superconductor 2H-NbSe₂ as a substrate for magnetic adatom structures. Fe adatoms induce four pairs of YSR states, associated to the singly-occupied crystal-field-split d orbitals. The energy of the YSR states scales with the modulated charge density across the surface, highlighting the spatial variation of the competition of exchange coupling and superconducting pairing.

In a second step, we place magnetic adatoms in close proximity and investigate the interaction of their YSR states. We observe a shift and splitting of the YSR states, including a quantum phase transition from a screened-spin state to a free-spin state. The transition is driven by substrate mediated magnetic interactions (RKKY interactions) becoming possible in the free-spin state [2, 3].

We then deliberately increase the chain length by adding individual Fe atoms with the STM tip, up to a length of 51 atoms. In each step we track the evolution of the YSR states. We find signatures of YSR band formation consistent with ferromagnetic coupling of quantum spins [2,4].

[1] E. Liebhaber et al., Nano Lett. 20, 339 (2020).

[2] E. Liebhaber, et al., Nature Commun. 13, 2160 (2022).

[3] H. Schmid, et al, Phys. Rev. B 105, 235406 (2022).

[4] J. F. Steiner, et al., Phys. Rev. Lett. 128, 036801 (2022).

Yu-Shiba-Rusinov states of Fe dimers on $2H\text{-NbSe}_2$

Lisa M. Rütten¹, Eva Liebhaber¹, Gaël Reecht¹, Kai Rossnagel^{2,3}, Felix von Oppen¹,
Katharina J. Franke

¹Fachbereich Physik, Freie Universität Berlin, 14195 Berlin, Germany

l.ruetten@fu-berlin.de

²Institut für Experimentelle und Angewandte Physik, Christian-Albrechts-Universität zu Kiel, 24118
Kiel, Germany

³Ruprecht Haensel Laboratory, Deutsches Elektronen-Synchrotron DESY, 22607 Hamburg,
Germany

⁴Dahlem Center for Complex Quantum Systems and Fachbereich Physik, Freie Universität Berlin,
14195 Berlin, Germany

Unpaired adatom spins on superconductors interact with the Cooper pairs of the substrate and induce Yu-Shiba-Rusinov (YSR) states inside the superconducting gap [1-3]. These can be probed by scanning tunneling spectroscopy at the single-atom scale. $2H\text{-NbSe}_2$ is a superconducting, layered van der Waals material, where the YSR wave functions of magnetic impurities extend over several nanometers [4]. This provides a wide range of adatom spacings over which their interaction is sufficiently strong to be potentially observed as a splitting in the tunneling spectra.

In addition to superconductivity, $2H\text{-NbSe}_2$ hosts an incommensurate charge-density wave (CDW). The imposed variation of the local density of states leads to shifts in the energy of the YSR states and alters the spatial symmetry of YSR wave functions [5]. Here, we arrange Fe atoms on $2H\text{-NbSe}_2$ using the tip of a scanning tunneling microscope and realize dimers with different spacings and symmetries. We investigate the influence of spacing and position of the atoms with respect to the CDW on the interaction between the YSR states.

[1] L. Yu, Acta Phys. Sin. 21.1 (1965).

[2] H. Shiba, "Classical spins in superconductors." Prog. Theor. Phys. 40.3 (1968).

[3] A. Rusinov, JETP Lett. (USSR)(Engl. Transl.); (United States) 9 (1969).

[4] G. Ménard, et al., Nature Physics 11.12 (2015).

[5] E. Liebhaber, et al., Nano letters 20.1 (2019).

Non-symmorphic band sticking in a topological superconductor

Warren Pickett, Yundi Quan, Matthew Staab, Inna Vishik, Valentin Taufour
 Department of Physics and Astronomy, University of California Davis, Davis California
wepickett@ucdavis.edu

Unconventional superconductors continue to challenge our understanding of condensed matter systems. These condensates have Cooper pairs with lower symmetries than in conventional superconductors. In most unconventional superconductors, the additional symmetry breaking occurs in relation to typical ingredients such as strongly correlated Fermi liquid phases, magnetic fluctuations, or strong spin-orbit coupling in non-centrosymmetric structures.

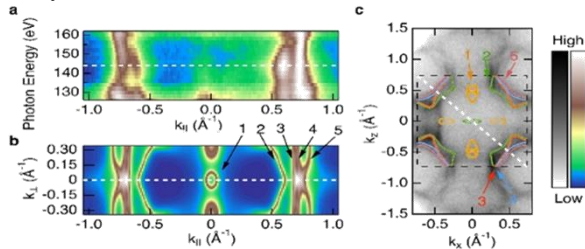


Figure 1: Photon energy dependence of ARPES intensity and overlaid ARPES data of the $k_y = 0$ plane. **a** Photon energy dependence of ARPES intensity along the Γ -A diagonal, k_{\parallel} , through the BZ. **b** DFT calculation of spectral weight $A(k, \omega)$ along the same plane as **a**. Comparing the structure of **a** and **b** indicates that the $k_y = 0$ plane of the BZ can be accessed with a photon energy of 144 eV. **c** ARPES measured Fermi surface along the $k_y = 0$ plane overlaid with DFT calculated Fermi surface contours. White dashed line indicates same location in all panels.

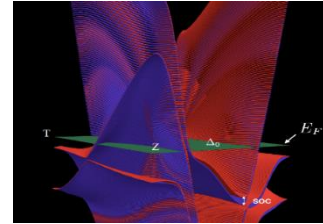


Figure 2: Energy surface plot for $Cmc1$ LaNiGa_2 on the $k_z = \pi/c$ plane, with the Z - T line indicated. The intersection of various bands with the Fermi energy E_F can be seen. The Dirac band touching point is identified by the small vertical arrow. The small SOC splitting is visible between nearby bands in several places. Along the T - Z - T line, SOC splitting vanishes, leaving the Dirac points as the only true degeneracies. Also evident from the figure is the combination of bands near the nodal point with very small, moderate, and large velocities—a highly anisotropic electronic structure.

In this presentation, I will show that the \square SR observed time-reversal symmetry breaking in the unconventional superconductor LaNiGa_2 is enabled by its previously unknown topological electronic band structure. Our single crystal diffraction experiments indicate a nonsymmorphic crystal structure [1], in contrast to the previously reported symmmorphic structure. The nonsymmorphic symmetries transform the plane of the Brillouin zone boundary into a nodal-surface.

Through band-structure calculations we reveal that distinct Fermi surfaces become degenerate on the nodal-surface and form Dirac lines and a Dirac loop at the Fermi level. Within the Dirac loop are two symmetry related Dirac points which remain degenerate under spin-orbit coupling.[2] ARPES measurements confirm the calculations and provide evidence for the Fermi surface degeneracies on the nodal-surface.[1] These unique topological features enable an unconventional superconducting gap in which time-reversal symmetry can be broken in the absence of other typical ingredients.

LaNiGa_2 provides the first example of a topological crystalline superconductor that breaks time-reversal symmetry without any overlapping magnetic ordering or fluctuations. Our findings will enable future discoveries of additional topological superconductors.

Financial support from AFOSR, DOE, and NSF is gratefully acknowledged.

[1] J. R. Badger et al., *Commun. Phys.* 5, 22 (2022).

[2] Y. Quan, W. E. Pickett, et. al., *Phys. Rev. B* 105, 064517 (2022).

The Conductivity Parameters of $\text{YBa}_2\text{Cu}_3\text{O}_{6.5+\delta}$ Superconductor Compound

Emad K. Al-Shakarchi and Ali Mohsin

Al-Nahrain University, College of Science, Physics Department, Baghdad, Iraq
eks2000@hotmail.com

The high-temperature superconductor like $\text{YBa}_2\text{Cu}_3\text{O}_{6.5+\delta}$ was prepared by solid-state reaction method at calcination temperatures (900 °C). The crystal structure was confirmed using X-ray diffraction, and it was found that $\text{YBa}_2\text{Cu}_3\text{O}_{6.5+\delta}$ showed an orthorhombic phase with lattice parameters ($a=3.82030$, $b=3.88548$, and $c = 11.6835 \text{ \AA}$) with space group (Pmmm). The sample was sintered at sintering temperatures (900 °C) for (24 hr). The oxygen excess (δ) was nearly (0.36), which was effective in the appearing superconducting properties. The sample $\text{YBa}_2\text{Cu}_3\text{O}_{6.86}$ had a critical temperature of about (92 K). The simulation of the XRD pattern was necessary to predicate the shape of the unit cell and the position of atoms in the unit cell. The last is very important to find some theoretical data, which are beneficial in the prediction of the conductivity parameters through the sequences unit cells, which are useful in the conductivity mechanism. This mechanism is depending on the concept of interlayer coupling, so the number of the layers including the unit cell is an effective parameter in the conductivity mechanism through the normal resistivity created.

Effect of uniaxial and hydrostatic pressure on competing phases in iron-based superconductors

Elena Gati

Max-Planck-Institute for Chemical Physics of Solids, Noethnitzer Str. 40, 01187 Dresden, Germany

elena.gati@cpfs.mpg.de

Iron-based superconductors represent an exceptional playground to explore the competition of correlated electronic phases by tuning the crystal lattice via pressure [1]. Pressure is such an excellent tool to explore this competition since the different components of the stress tensor can couple to certain order parameters directly, thus providing an effective mean to study competition of different ordered phases. In addition, the different components of the stress sensor can nowadays be controlled experimentally with very high precision.

In this talk, I will illustrate the impact of different types of pressures on the phase diagram of archetypical iron-based superconductors. First, I will introduce how non-symmetry breaking hydrostatic pressure impacts the phase diagram of FeSe and discuss how specific heat measurements under hydrostatic pressure reveal interesting manifestations of the competition of magnetic and superconducting phases [2,3]. Second, I will discuss how symmetry-breaking uniaxial pressure affects the phase diagram of materials from the CaKFe₄As₄ family [4]. Last, I will introduce a novel technique, that allows to combine hydrostatic with uniaxial pressure, show proof-of-principle results on BaFe₂As₂ [5] and outline how this technique might be of relevance for studies of the wider class of quantum materials.

Work is performed in collaboration with Sergey L. Bud'ko and Paul C. Canfield (Ames Laboratory/Iowa State University). Part of the work was carried out at Iowa State University and supported by Ames Laboratory, US DOE, under Contract No. DE-AC02-07CH11358.

- [1] E. Gati et al., Ann. Phys. 532, 2000248 (2020).
- [2] E. Gati et al., Phys. Rev. Lett. 123, 167002 (2019).
- [3] E. Gati et al., Rev. Sci. Instrum. 90, 023911 (2019).
- [4] M. Xu et al., arXiv:2204.10925 (2022).
- [3] E. Gati et al., Rev. Sci. Instrum. 91, 023904 (2020)

Disorder in FeSe_{1-x}S_x (0 ≤ x ≤ 1) superconducting crystals

Cedomir Petrovic

Brookhaven National Laboratory

Petrovic@bnl.gov

Connections among crystal chemistry, disorder and critical temperature T_c have been at the forefront of superconductivity, one of the most widely studied phenomena in physics, chemistry and materials science alike. In Fe-based superconductors T_c correlates with the average anion height above the Fe plane, i.e. with the geometry of the FeAs₄ or FeCh₄ (Ch = Te, Se, S) tetrahedron. By synthesizing FeSe_{1-x}S_x (0 ≤ x ≤ 1) single crystal alloys with atomic defects we find that their T_c is not correlated with the anion height of other Fe superconductors. Instead, changes in $T_c(x)$ and tetragonal-to-orthorombic (nematic) transition $T_s(x)$ on cooling are correlated with Bragg plane and Fe vibrations disorder in direction orthogonal to Fe planes and thereby induced scattering rates $(1/\tau)(x)$ [1,2]. The disorder stems from deformed Fe(Se,S)₄ tetrahedra with different Fe-Se and Fe-S bond distances. Moreover, high-temperature metallic resistivity in the region of strong disorder exceeds Mott limit and provides an example of the strong violation of Matthiessen's rule and Mooij law which is known to be a dominant when adding moderate disorder past the Drude/Matthiassen's regime in all materials [2]. Scattering mechanism of Mott limit-exceeding resistivity is unrelated to phonons and arises for strong Se/S atom disorder in tetrahedral surrounding of Fe. Our findings shed light on the intricate connection between nanostructure details and unconventional scattering mechanism, possibly related to charginematic or magnetic spin fluctuations.

[1] Aifeng Wang et al., Inorganic Chemistry (in press 2022).

[2] Aifeng Wang et al., under review (2022).

Hydrogen in metal/metal oxide hydrides

M.R. Mohammadzadeh¹, Hamed Arab¹, S. Vahid Hosseini¹, M. Abbasnejad², M. Sedighei¹,
Z. Alizadeh¹

¹Superconductivity Research Laboratory (SRL), Department of Physics, University of Tehran, North
Kargar Ave., P. O. Box 14395-547, Tehran, Iran.

²Faculty of Physics, Shahid Bahonar University of Kerman, Kerman, Iran

Hydrogen is a very important element in new high pressure metal hydrides. We have studied the influence of H in some metal and metal oxides. For example, new compositions of palladium hydride at pressure 50 GPa have been investigated using USPEX genetic algorithm. At this pressure, compounds such as PdH, Pd₂H and Pd₄H were proposed. The phonon calculations show that these compounds do not show any imaginary frequency in the phonon dispersion curve, so they have mechanical stability. However, superconductivity calculations based on BCS theory showed that the electron-phonon interaction in these compounds is very low and the superconducting transition temperature was less than 1 K.

Two distinct possibilities of realizing room-temperature superconductivity in high- T_c cuprates and high pressure hydrides

S. Dzhumanov

Institute of Nuclear Physics, Uzbek Academy of Sciences, 100214, Ulugbek, Tashkent, Uzbekistan
dzhumanov@inp.uz

The theory of three-dimensional (3D) and two-dimensional (2D) Bose-liquid superconductivities in high- T_c cuprates and other materials is developed. The high- T_c cuprates and related high pressure hydrides with strong electron-phonon coupling are believed to be in the limit of bosonic superconductors [1]. According to the theory of a superfluid Bose-liquid of Cooper pairs, the superconducting transition temperature T_c is much lower in the bulk of high- T_c cuprates than at planes in them and the 3D superconductivity in these systems above the bulk T_c is destroyed, after which 2D superconductivity persists only at grain boundaries, interfaces and planes in the laminated blocks in the temperature range $T_c < T < T_c^{2D}$. The possibility of realizing room-temperature superconductivity in some families high- T_c cuprate superconductors (with $T_c > 100$ K) containing grain boundaries, interfaces and laminated blocks is discussed. The crossover from bulk to surface Bose-liquid superconductivity in these high- T_c materials can serve as a starting point in the theoretical and experimental search for room-temperature superconductivity. In particular, the crossover from 3D to 2D Bose-liquid superconductivity in alternating 3D/2D sandwich layers might be possible route to room-temperature superconductivity in promising *Bi*-based cuprate materials. Since the crossover from 3D to 2D Bose-liquid superconductivity at grain boundaries, interfaces and planes in the laminated blocks in such high- T_c cuprates can lead to an increase in T_c to room temperature. The possibility of increasing T_c up to room temperature in 2D superconductors depends on several parameters (i.e. on the effective mass m_B^* of bosonic carriers (tightly-bound Cooper pairs), the density of superfluid bosons ρ_s , the interboson coupling constant γ_B and the energy of optical phonons $\hbar\omega_0$). The theory of 3D superfluid Bose-liquid of Cooper pairs predicts an alternative route to room-temperature superconductivity in recently discovered high- T_c hydrides, which should not be considered as the conventional superconductors described by the BCS-like and Migdal-Eliashberg theories. In these new superconducting materials, Cooper pairs might be in the bosonic limit and the 3D Bose-liquid superconductivity can occur at room temperature under high pressures. Since the coupling constant γ_B and the density of superfluid bosonic carriers ρ_s in high- T_c hydrides under high pressures may increase significantly and their superconducting transition temperature T_c can reach up to room temperature [1].

Various experiments on some families of high- T_c cuprates [2,3,4,5] lend support to the theory of Bose-liquid superconductivity and the signatures of the superconducting transitions at temperatures far above the bulk T_c and sometimes close to room temperature. Apparently, other experiments [6] on high- T_c hydrides also support for predictions of this theory concerning the possibility of room-temperature superconductivity in high pressure hydrides.

The financial funding from Project F-FA-2021-433 is gratefully acknowledged.

- [1] S. Dzhumanov, Arxiv. 1912.12407.
- [2] A. Ulug et al., Physica C 235-240, 879 (1994).
- [3] J.L. Tholence et al., Physica C 235-240, 1545 (1994).
- [4] I. Bozovic et al., Quantum Stud.: Math. Found, DOI 10.1007/5 40509-017-012-X.
- [5] D.D. Gulamova, Private Communication.
- [6] E. Snider et al., Nature 586, 373 (2020).

Elemental substitution at Tl-site of $Tl_{1-x}X_x(Ba,Sr)CaCu_2O_7$ superconductor with $X = Cr, Bi, Pb, Se$ and Te

J. Nur-Akasyah¹, R. Abd-Shukor²

¹School of Mechanical Engineering, Universiti Sains Malaysia, 14300 Nibong Tebal, Penang, Malaysia
jnurakasyah@gmail.com

²Department of Applied Physics, Universiti Kebangsaan Malaysia, 43600 Bangi, Selangor, Malaysia

The Sr and Ba bearing Tl-1212 phase, $Tl(Ba,Sr)CaCu_2O_7$ is an interesting superconductor. The Sr only bearing $TlSr_2CaCu_2O_7$ is not easily prepared in the superconducting form. The Ba only bearing $TlBa_2CaCu_2O_7$ on the other hand does not show improvement in the transition temperature with elemental substitution. In this work, the effect of elemental substitutions at the Tl-site of $Tl_{1-x}X_x(Ba,Sr)CaCu_2O_7$ ($X = Cr, Bi, Pb, Se$ or Te) superconductors for $x = 0$ and 0.4 was studied.

The aim of this study was to determine the element that enhance and suppress the superconducting transition temperature of $Tl_{1-x}X_x(Ba,Sr)CaCu_2O_7$ (Tl-1212) phase. The selected elements were from transition metal (Cr), post-transition metal (Bi and Pb), non-metal (Se) and metalloid (Te) categories.

The samples were prepared by the solid-state reaction method. XRD patterns showed single Tl-1212 phase was formed in pure samples. The pure sample ($x = 0$) also showed plate-like structure with larger voids. Substitution of Pb showed similar morphology with the pure sample. The highest superconducting transition temperatures ($T_{c\ onset}$, $T_{c\ zero}$ and T_p) were achieved by Cr-substituted samples (Table 1). However, substitution of Te suppressed the superconductivity of Tl-1212 phase (Fig. 1). $J_{c\ inter}(T_p)$ for all samples were calculated to be in the range of 12-17 A/cm².

This work showed that the transition temperature decreased linearly with the ionic radius except for Cr and Se which showed high T_c although its ionic radius is smaller. The roles of ionic radius of the substituted elements on the superconductivity of $Tl(Ba,Sr)CaCu_2O_7$ are discussed in this paper.

Table 1. $T_{c\ onset}$, $T_{c\ zero}$, ΔT_c , $T_{c\ zero}^*$, T_p , $J_{c\ inter}(T_p)$, lattice parameters, unit volume cell and volume fraction of Tl-1212 phase for $Tl_{1-x}X_x(Ba,Sr)CaCu_2O_7$ with $X = Cr, Bi, Pb, Se$ or Te .

$Tl_{1-x}X_x(Ba,Sr)CaCu_2O_7$	$T_{c\ onset}/K$	$T_{c\ zero}/K$	$\Delta T_c/K$	$T_{c\ zero}^*/K$	T_p/K	$J_{c\ inter}(T_p)/A/cm^2$	$a/\text{\AA}$	$c/\text{\AA}$	$V/\text{\AA}^3$	Tl-1212 phase / %
$x = 0$	96	81	15	95	74	17	3.8220	12.370	180.70	100
X = Cr ($x = 0.15$)	106	77	29	107	75	12	3.8320	12.304	180.67	99
X = Cr ($x = 0.4$)	113	85	28	111	76	14	3.8270	12.289	179.98	83
X = Bi ($x = 0.4$)	95	87	8	92	75	15	3.8170	12.282	178.94	68
X = Pb ($x = 0.4$)	82	70	8	83	67	12	3.8250	12.327	180.35	95
X = Se ($x = 0.4$)	100	85	15	100	51	17	3.8190	12.314	179.99	78
X = Te ($x = 0.4$)	77	60	17	62	48	16	3.8240	12.394	181.21	51

The financial funding from Ministry of Higher Education of Malaysia under grant no. FRGS/1/2020/STG07/UKM/01/1 is gratefully acknowledged.

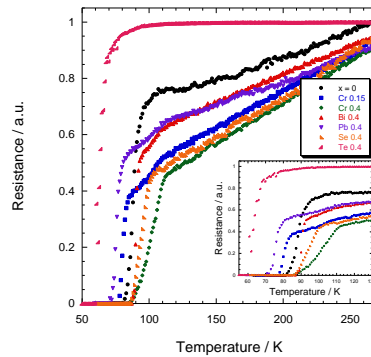


Figure 1. Electrical resistance versus temperature curves of $Tl_{1-x}X_x(Ba,Sr)CaCu_2O_7$ ($X = Cr, Bi, Pb, Se$ or Te) for $x = 0$ and 0.4 .

Competition of crystal structure motives in Heusler alloys Fe_2NiZ ($Z = \text{Al}, \text{Ga}, \text{In}, \text{Sn}$) and its influence on phase stability and ground state properties

Vladimir Sokolovskiy¹, Olga Miroshkina², Vasilii Buchelnikov¹, and Markus Gruner²

¹Chelyabinsk State University, Chelyabinsk, Russia
vsokolovsky84@mail.ru

²University of Duisburg-Essen, Duisburg, Germany

The Heusler alloys have attracted great attention from experimental and fundamental points of view due to their remarkable magnetic, mechanical, and thermodynamic properties. Many of them exhibit a martensitic transformation from high-symmetry cubic austenite to lower symmetry martensite with tetragonal or orthorhombic structure. A lowering in a crystal symmetry induces a large magnetocrystalline anisotropy energy (MAE) [1]. As a consequence, the low cost Heusler alloys possessing a high MAE, Curie temperature and saturation magnetization would be useful in the field of rare-earth free permanent-magnet technology.

In the present work we focus on Heusler alloy family $\text{Fe}_2\text{Ni}_{1+x}\text{Z}_{1-x}$ ($Z = \text{Al}, \text{Ga}, \text{In}, \text{Sn}$) with the framework of ab initio calculations and the projector augmented wave method as implemented in VASP code [2]. We considered regular ($L2_1$) and inverse (XA) Heusler structures together with three types of layered atomic ordering. Three new types of atomic ordering based on the inverse structure - tetragonal symmetry structures T^p , T^c , $T^{\#}$ - are obtained by rearrangement of atom pairs. All these structures are modeled using the 16-atom supercells. The full description of each structure can be found in [3].

For all compositions under study, the total energy and magnetic moments as a function of lattice parameters and tetragonal ratio are calculated. The possibility of martensitic transition for off-stoichiometric compounds is determined. Fig. 1 displays the total energies as a function of tetragonal distortion (c/a) for Fe_2NiGa and Fe_2NiIn alloys with different crystal structures considered. It can be seen that the preferable structure is the proposed layered T^p structure although the XA and T^c structures are very close in the energy as compared to the $L2_1$ structure. Similar trends are also found for other compounds. Besides, the MAE (out-of-plane direction) which twice larger than that for the tetragonal $L1_0$ FeNi is predicted for Fe_2NiZ with favorable T^p crystalline structure.

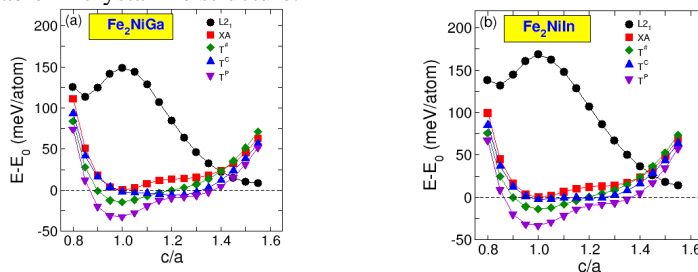


Figure 1. Total energy as a function of tetragonal ratio for Fe_2NiGa and Fe_2NiIn with different crystal structures. The energy difference is plotted with respect to the energy of XA structure.

The financial funding from Ministry of Science and Higher Education of the RF within the framework of the Russian State Assignment under Contract No. 075-01391-22-00 is gratefully acknowledged.

- [1] Y. Matsushita et al., J. Phys. D 50, 095002 (2017).
- [2] G. Kresse and J. Furthmüller, Phys. Rev. B 54, 11169 (1996).
- [3] V.V. Sokolovskiy et al., Phys. Rev. Mat. 6, 025402 (2022).

Ab initio study of the 4d Heusler alloy Rh₂FeZ

Danil Baigutlin¹, Vladimir Sokolovskiy¹, Vasilij Buchelnikov¹, Olga Miroshkina²

¹Chelyabinsk State University, 454001, Chelyabinsk, Russian Federation

d0nik1996@mail.ru

²University of Duisburg-Essen, 47057, Duisburg, Germany

Half-metallic ferromagnets are a class of materials with 100 % spin polarization on the Fermi level. They have attracted a lot of interest due to their possible applications in the spintronics area [1]. One of the most common methods is spin injection from a ferromagnetic material, in particular, half-metallic Heusler alloys [1]. The half metall full Heusler alloys are based on the 3d transition metals quite well investigated [1]. On the contrary, there is much less information about half metallic ferromagnets containing 4d transition elements. The goal of this work is investigation of structural, electronic and magnetic properties of Heusler alloys based on the Rh₂FeZ (Z = Al, Si, Ga, Ge, In, Sn) family.

The calculation was performed within the framework of the Density Functional Theory using the plane augmented waves approach implemented in the VASP code [2]. Since the alloy contains strongly correlated 3d and 4d elements, the meta-GGA SCAN approximation was used to approximate the exchange-correlation functional [3].

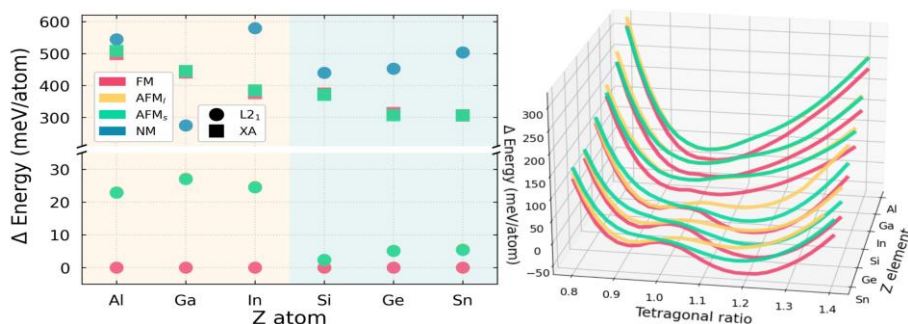


Figure 1. The total energy difference (ΔE) as a function of the lattice parameter of Rh₂FeZ (Z = Al, Si, Ga, Ge, In, Sn) for L2₁ and X_A lattice. The ΔE is plotted with respect to the L2₁ lattice with ferromagnetic alignment.

The regular L2₁ structure is energetically advantaged for all Z elements and functional. The FM ordering is preferable, however the energy distance between FM and AFM orders is lower in the case of fourth main group elements, which shows the possibility of a meta-magnetic transition for such alloys. At the same time, the antiferromagnetic ordering competes with each other. To establish the possibility of a martensitic transformation, the dependencies of the total energy on the tetragonal ratio are plotted in Fig. 1. In the case of the Z element from the third group the two almost degenerate martensite minimums with small c/a distortion ≈ 0.98 and 1.02 are observed. For FM ordering. When passing to the elements of the fourth group, these minima become clearly distinguishable. The tetragonal distortion ratios 0.92 and 1.2, respectively, whereby a martensitic structure with c/a > 1 is favorable.

The research was supported by the RSF - Russian Science Foundation project No. 22-12-20032.

[1] C. Felser et al., Angew. Chem. Int. Ed 46(5), 668-699 (2007)

[2] G. Kresse, D. Joubert, Phys. Rev. B. 59, (1999) 1758.

[3] J. Sun, A. Ruzsinszky, J. P. Perdew, Phys. Rev. Lett. 115, (2015) 036402.

Tuning of the effective magnetic decoupling in Ni-Mn-(In,Sn) Heusler alloys

Olga N. Miroshkina¹, Francesco Cugini^{2,3}, Simone Chicco², Fabio Orlandi⁴, Giuseppe Allodi², Pietro Bonfà², Vincenzo Vezzoni², Greta Cavazzini^{2,3}, Franca Albertini³, Roberto De Renzi², Massimo Solzi^{2,3}, and Markus E. Gruner¹

¹Department of Physics and CENIDE, University of Duisburg-Essen, Duisburg, Germany

olga.miroshkina@uni-due.de

²University of Parma, Parma, Italy

³National Research Council (IMEM-CNR), Parma, Italy

⁴Rutherford Appleton Laboratory, Chilton, United Kingdom

The magnetocaloric effect at first-order phase transitions is considered as an efficient and ecologically friendly alternative to conventional compressor cooling [1]. A promising class of materials for magnetic cooling devices are multifunctional Heusler materials [2,3]. We explore the complex magnetic ordering mechanisms in magnetocaloric Ni-Mn-(In,Sn) Heusler alloys by means of density functional theory, which provides an accurate and efficient characterization of the relation between structure, magnetism, and electronic properties in these materials. The calculations accompany extensive experimental investigations, which reveal a non-monotonic trend in the Curie temperature and an effective magnetic decoupling of *4a* and *4b* sublattices exhibiting different temperature dependence of their magnetization [4], see Fig. 1.

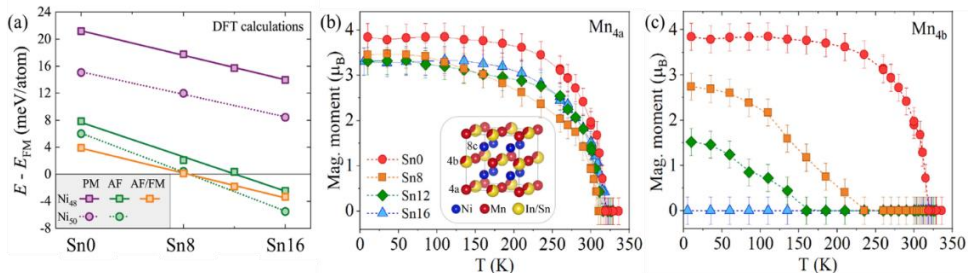


Figure 1. (a) Total energies of different magnetic arrangements (AF, AF/FM, paramagnetic) relative to the FM state of the Ni-Mn-In-Sn alloys as a function of the Sn content. (b,c) Mn magnetic moment in the (b) *4a* and (c) *4b* sublattices as a function of temperature, obtained from the refinement of neutron powder diffraction data.

Our first-principles reveal a composition-dependent competition of the effective ferromagnetic (FM) and antiferromagnetic (AFM) coupling between the sublattices, which can be directly controlled by electron doping in terms of In/Sn substitution. This result shows the possibility of fine-tuning of Heusler materials via exchanging the main-group element increasing the range of their potential applications.

The financial funding from DFG (CRC/TRR 270, Project-ID 405553726) is gratefully acknowledged.

[1] A. Kitanovski et al., *Magnetocaloric Energy Conversion: From Theory to Applications* (Springer, Cham, 2016).

[2] O. Gutfleisch et al., *Philos. Trans. R. Soc. A* 374, 20150308 (2016).

[3] F. Scheibel et al., *Energy Technol.* 6 (8), 1397–1428 (2018).

[4] F. Cugini et al., arXiv:2203.12498 [cond-mat.mtrl-sci] (2022).

Metamagnetism and magnetocaloric effect: case study of Au₂Mn

Elvina Dilmieva¹, Andrei Rogalev¹, Fabrice Wilhelm¹, Jean-Paul Jacques Kappler²,
Alex Aubert³, Konstantin P. Skokov³

¹European Synchrotron Radiation Facility, 38043 Grenoble, France

elvina.dilmieva@esrf.fr

²Synchrotron Soleil L'Orme des Merisiers, 91190 Saint-Aubin, France

³Institute of Materials Science, Technical University of Darmstadt, Darmstadt 64287, Germany

The magnetocaloric materials remain at the forefront of research motivated by a possibility of using them in eco-friendly refrigeration over a wide temperature interval or in gas liquefaction at low temperatures. Structural, magnetic and electronic subsystems contribute differently to the magnetocaloric effect (MCE) and definite answer to the question of the driving force is still to be found [1].

Au₂Mn compound is remarkable system that allows one to elucidate roles of different subsystems to the MCE. It exhibits the 1st order metamagnetic (field induced) transition from a spin-spiral state [2, 3] to a ferromagnetic one, which is not accompanied by the structural changes [4]. In this work we present the results of thorough study of magnetic properties of Au₂Mn across the metamagnetic transition. X-ray magnetic circular dichroism (XMCD) measurements have been performed at the *L*_{2,3}-edges of *Au* and at the *K*-edge of *Mn* under a magnetic field up to 17 T. The XMCD results showed the presence of a finite magnetic moment on *Au* atoms, induced *via* hybridization of the 5*d* states with 3*d* orbitals of *Mn* atoms. The magnetic moments of *Au* atoms orders in their own spiral despite the weakness of the moment (~0.01 μ_B) (see Fig.1). It should be noted that the spin-to-orbital moment ratio is the same for the spin-spiral and the ferromagnetic states. In the region of the metamagnetic transition, the inverse MCE has been studied by both indirect and direct methods up to 14 T. The extremely low value ($\Delta S \sim 0.04$ J/(kgK) at $\mu_0 H = 2$ T) of the MCE is unambiguously detected. Since both the structural and electronic subsystems do not contribute to the MCE in Au₂Mn, we can conclude that the observed small contribution is due to the magnetic subsystem only. The obtained results are discussed from a more general point of view of influence of metamagnetic transitions on magnetocaloric properties.

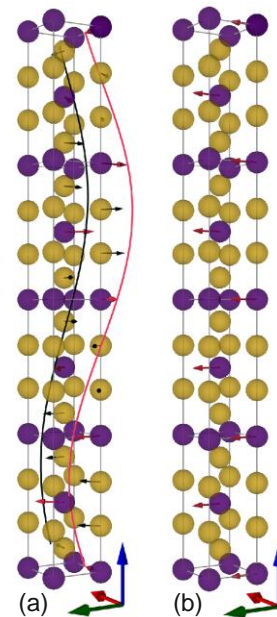


Figure 1. Spin-spiral (a) and field induced (b) magnetic structures of Au₂Mn. Arrows indicate the direction of *Mn* (red) and *Au* (black) magnetic moments.

[1] A.S. Komlev et al., JAC 898, 163092 (2022).

[2] L. Liu et al., PRB 96 (18), 184429 (2017).

[3] J. Glasbrenner et al., PRB 90 (14), 144421 (2014).

[4] D. P. Morris and R.P. Preston Proc. Phys. Soc. B 69, 849 (1956).

The study of electronic structure and magnetic properties of selected U-based intermetallics from the first-principles

Mane Sahakyan^{1,*}, Manuel Richter², Vinh Hung Tran¹

¹Institute of Low Temperature and Structure Research, Polish Academy of Sciences, P. O. Box 1410,
50-422 Wrocław, Poland

²Leibniz IFW Dresden, Helmholtzstraße 20, 01069 Dresden, Germany
m.sahakyan@intibs.pl

Due to the localized or itinerant nature of the $5f$ electrons, actinide compounds displaying various intriguing phenomena, such as the Kondo effect, heavy fermion behavior and etc., have been continuously studied in recent decades. Moreover, it can be noticed that in uranium intermetallic compounds the magnetic properties strongly correlate with the features of both the electronic and the crystal structure, since any small change can lead to large changes in magnetism.

In this report we present the theoretical investigation of the electronic structure and magnetic properties study of two intermetallic U_2PdGa_3 and U_2PtGa_3 compounds crystallizing in an orthorhombic $CeCu_2$ -type structure (space group $Imma$). Based on the electrical resistivity, magnetization, magnetic susceptibility data, compounds ordering antiferromagnetically [1, 2]. Moreover, the magnitude of ordered uranium magnetic moments obtained by neutron-diffraction patterns is evaluated to $0.32(5) \mu_B/U$ and $0.38(5) \mu_B/U$ for U_2PdGa_3 and U_2PtGa_3 , respectively, which are strongly reduced in comparison of moments of free uranium ions (U^{3+} ($3.6 \mu_B/U$) and U^{4+} ($3.58 \mu_B/U$)). This fact and the number of other features proves the assumption that Kondo effect is operative in an antiferromagnetically ordered state. Employing Density functional theory methods we observe significant changes in the magnetic moments and electronic properties of these compounds. Using Full-Potential Linearized Augmented Plane-Wave (FP-LAPW) method [3], the electronic structure properties are discussed in terms of effects brought by the Coulomb interaction (U) and the Hund coupling (J). Moreover, taking into account the importance of orbital magnetism in uranium compounds the Orbital Polarization Correction (OPC) was used to model the magnetic properties in the Full-potential local-orbital method [4].

This work was supported by the National Science Centre (Poland) under the Scientific activity No. 2020/04/X/ST300094. We gratefully acknowledge computational center of IFW Dresden for giving opportunity to perform calculations in the high-performance computing environment.

[1] Tran V. H., J. Phys.: Condens. Matter 8, 6267 (1996).

[2] Tran V. H., Steglich F., and Andre G., Phys. Rev. B 65, 134401 (2002).

[3] Wimmer, E.; Krakauer, H.; Weinert, M.; Freeman, A. J 1103/PhysRevB..1981, 24, 864 –875.

[4] K. Koepemik and H Eschrig, Phys. Rev. B 59, 1743 (1999). <https://www.fpllo.de/>.

Non-collinear spin reorientation in FeRh from first principles: Ultrafast laser-quenching vs. coherent rotation of Fe moments

Mike J. Bruckhoff, Markus E. Gruner, Rossitza Pentcheva

Faculty of Physics and Center for Nanointegration (CENIDE) Duisburg - Essen,
 University of Duisburg - Essen, Lotharstr. 1, 47057 Duisburg, Germany
mike.bruckhoff@uni-due.de

The binary alloy FeRh exhibits a large magnetocaloric effect (MCE) around room temperature at the isostructural, metamagnetic first-order phase transition from antiferromagnetic (AFM) to ferromagnetic (FM) order, which can be driven by an external magnetic field or laser excitation [1].

Here, we present a comprehensive non-collinear DFT study where we investigate the multidimensional energy landscape $E(M,V)$, by constraining the total spin moment in the whole unit cell in order to compare different kinds of spin reorientation pathways. The absence of significant energy barriers suggests that the coherent in-plane rotation of the Fe moments is a likely scenario for the magnetic phase transition (Fig. 1) in an external magnetic field. The response of FeRh to a laser pulse is calculated by means of real-time time-dependent DFT (RT-TDDFT). Here, we observe an ultrafast demagnetization of the Fe magnetic moments and a net Rh-to-Fe charge transfer [1] in both phases (Fig. 2). The magnitude of the response depends strongly on the magnetic phase, the photon energy and the laser fluence of the incident laser pulse. We conclude that laser excitation and applied magnetic fields initiate distinct transition pathways, which may be exploited to avoid hysteresis losses.

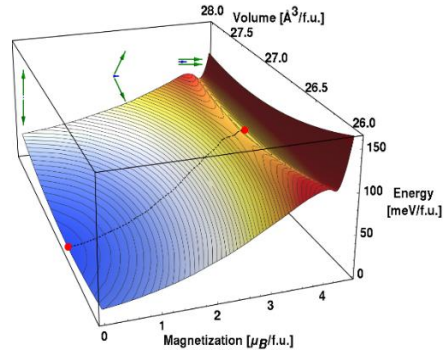


Figure 1. Energy landscape $E(M,V)$ for a coherent rotation of the Fe magnetic moments within the y - z plane. Path of steepest descent from AFM global minimum to FM local minimum (black dashed).

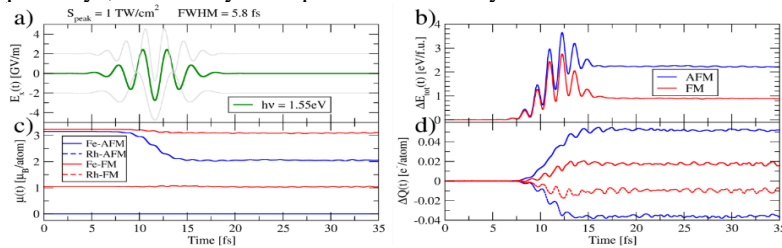


Figure 2. Ultrafast response to a) an optical laser pulse of b) the total energy change, c) magnetic atomic moments and d) change of atomic charges in dependence on the magnetic phase (AFM blue line, FM red line)

We gratefully acknowledge funding by the DFG within TRR/CRC270 as well as within CRC1242. Calculations were carried out on the MagnitUDE supercomputer system at the University of Duisburg-Essen.

[1] Pressacco, F., Sangalli, D., Uhlř, V. *et al. Nat Commun* **12**, 5088 (2021)

The influence of exchange correlation functional on the properties of Mn₂V(Al,Si) Heusler alloys

V.D. Buchelnikov¹, D.R. Baigutlin¹, V.V. Sokolovskiy¹ and O.N. Miroshkina^{1,2}

¹Chelyabinsk State University, Chelyabinsk, Russia

buche@csu.ru

²University of Duisburg-Essen, Duisburg, Germany

Half-metallic (HM) magnetics attract interest due to their potential spintronics applications involving novel thermoelectrics, spin filters, data storage, and other spin-based devices [1]. Recently, we reported that the implementation of electron correlation effects using the strongly constrained and appropriately normed (SCAN) meta-GGA functional yields nearly degenerate HM and metallic phases in Mn₂ScSi and Mn₂VGe [2,3]. It has been suggested that switching between these two phases could be achieved by applying volume change within the cubic phase, by the application of an external magnetic field or doping of alloy by fourth element. The aim of this work is to provide a theoretical description of Mn-V-Al-Si Heusler alloy, which is shown to demonstrate a switchable low (LMS) to high magnetic state (HMS) behavior. These alloys are more cost effective and stable to segregation. Calculations were performed using the DFT scheme with the PAW method as implemented in the VASP package [4]. We show that such a switching mechanism can be treated via the exchange-correlation effects described within the SCAN functional. Stoichiometric Mn₂VAl and Mn₂VSi are found to display an energy difference between the LMS and HMS phases, which is too large to allow easy switching between these two phases. For this reason, we explore the effects of Si or Al doping, which drives the LMS and HMS phases into near degeneracy. It is shown that the effect of doping significantly decreases the energy between the LMS and HMS phases (Figure 1).

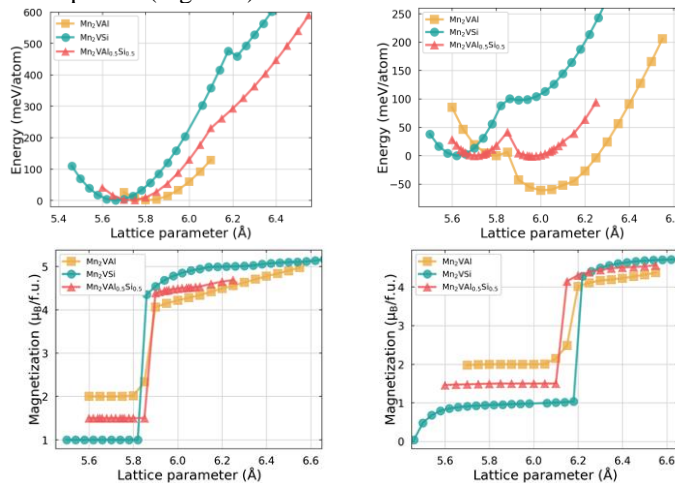


Figure 1. The dependence of energy and magnetization from lattice parameter for Mn₂VAl, Mn₂VSi and Mn₂VAl_{0.5}Si_{0.5} for PBE (left panel) and SCAN (right panel) functional.

The financial funding from RSF # 22-12-20032 is gratefully acknowledged.

- [1] B. Dieny, et al, Nat. Electron. 3, 446 (2020).
- [2] V. D. Buchelnikov et al, Phys. Rev. B 103, 054414 (2021).
- [3] V. D. Buchelnikov et al, Adv. Theory and Simul. 4, 2100311 (2021).
- [4] G. Kresse, J. Furthmüller, Phys. Rev. B 54, 11169 (1996).

Geometrical effects in three-dimensional magnetic and superconductor circuits

Amalio Fernández-Pacheco

Institute of Nanoscience & Materials of Aragón, CSIC-University of Zaragoza, Spain

amaliofp@unizar.es

The expansion of magnetism and superconductivity to three dimensions provides exciting opportunities to explore new physical phenomena and opens great prospects to create 3D novel devices for green computing technologies [1,2].

In this talk, I will present some of our recent works dedicated to the investigation of three-dimensional artificial circuits with complex-shaped geometries (see Figure 1). The talk will give an overview of the new methods we have developed to fabricate and characterize magnetic [3] and superconducting [4] nanomaterials, and some of the new functionalities obtained [5, 6]. This includes the creation of localized spin textures, topological defects and stray fields exploiting geometrical effects [7,8], the automotive 3D motion of information in magnetic circuits [9] and the strong magnonic contribution to the magnetoelectrical signals of the devices under investigation [10].

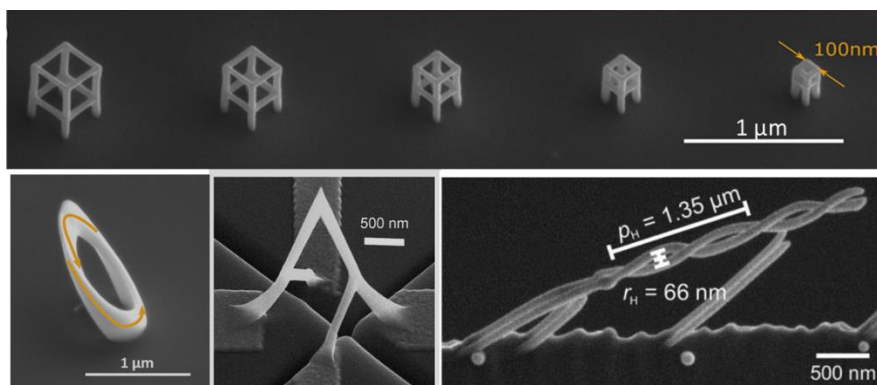


Figure 1. Selection of three-dimensional nanomaterials where geometrical effects have been investigated.

Financial support from an EPSRC Early Career Fellowship EP/M008517/1, the EPSRC Cambridge NanoDTC EP/L015978/1, the Winton Program for the Physics of Sustainability, the project CALIPSOplus under Grant Agreement 730872 from the EU Framework Programme for Research and Innovation HORIZON 2020, and by the European Community under the Horizon 2020 Program, Contract no. 101001290, 3DNANOMAG. is gratefully acknowledged.

- [1] A. Fernández-Pacheco et al, Nature Comm. 8, 1 (2017).
- [2] D. Makarov et al, Adv. Mater. 34, 2101758 (2022).
- [3] A. Fernández-Pacheco et al, Materials 13, 3774 (2020).
- [4] I. Guillamón et al, Nature Physics 5, 651 (2009).
- [5] L. Skoric, Nano Letters 20, 184 (2020).
- [6] D. Sanz-Hernández et al, ACS Nano 11, 11066 (2017).
- [7] D. Sanz-Hernández et al, ACS Nano 14, 8084 (2020).
- [8] C. Donnelly et al, Nature Nanotechnol. 17, 136 (2022).
- [9] L. Skoric et al, arXiv:2110.04636.
- [10] F. Meng et al, ACS Nano 15, 6765 (2021).

Topological magnetic structures and their dynamics

Karin Everschor-Sitte

Faculty of Physics and Center for Nanointegration Duisburg-Essen (CENIDE), University of Duisburg-Essen

karin.everschor-sitte@uni-due.de

The current-induced dynamics of magnetic structures is quite complex. For example, magnetic skyrmions allow for ‘banana kicks’ in magnetism, i.e., not only a motion of the skyrmions along but also transverse to the current direction. This effect, which has become known as the skyrmion Hall effect [1,2,3], is often disruptive for device applications. In this talk, we will present possibilities of how to eliminate the skyrmion Hall effect [4,5]. As a particular example, we discuss helical phases which provide confined one-dimensional channels for high-speed skyrmion motion. We discuss how skyrmions can be generated in such helical backgrounds and analyze their stability [6].

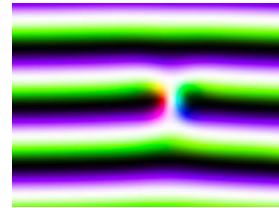


Figure 3: Skyrmion in a helical background [6].

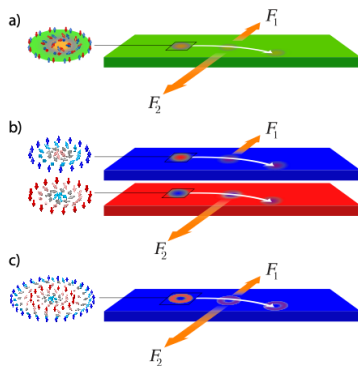


Figure 2: Net Skyrmion Hall effect in topologically neutral skyrmionics structures [7].

Moreover, we will address the role played by topology in the physics of the skyrmion Hall effect. For example, it is widely believed that the skyrmion Hall effect, vanishes for overall topologically neutral structures such as (synthetic) antiferromagnetic skyrmions and skyrmioniums due to a compensation of Magnus forces. While this is true for spin-transfer torque-driven skyrmions, we show that this simple picture is generally false for spin-orbit torque-driven objects [7]. We find that the skyrmion Hall angle for spin-orbit torque-driven skyrmions is directly related to their helicity, which imposes an unexpected roadblock for developing faster and lower input racetrack memories based on spin-orbit torques.

The financial funding from DFG (Projects 320163632, 403233384, 268565370 (B12)) and the Emergent AI Center funded by the Carl-Zeiss-Stiftung is gratefully acknowledged.

- [1] T. Schulz, et al., Nat. Phys. 8, 301 (2012)
- [2] K. Litzius, et al., Nat. Phys. 13, 170 (2017)
- [3] W. Jiang, et al., Nat. Phys. 13, 162 (2017)
- [4] R. Zarzuela, et al., Phys. Rev. B 101, 054405 (2020)
- [5] K.-W. Kim, et al., Phys. Rev. B 97, 224427 (2018)
- [6] R. Knapman, et al., J. Phys. D: Appl Phys. 54, 404003 (2021)
- [7] R. Msiska, et al., arXiv:2110.07063 (accepted at Phys. Rev. Appl.)

Magnetic skyrmion braids and antiskyrmions in cubic chiral magnets

N. S. Kiselev¹, F. Zheng^{2,3}, F. N. Rybakov^{4,5}, V. M. Kuchkin¹, D. Song², A. Kovács², H. Du⁶,
L. Yang², S. Blügel¹ and R. E. Dunin-Borkowski²

¹Peter Grünberg Institute and Institute for Advanced Simulation, Forschungszentrum Jülich and JARA, 52425 Jülich, Germany

n.kiselev@fz-juelich.de

²Ernst Ruska-Centre for Microscopy and Spectroscopy with Electrons and Peter Grünberg Institute, 52425 Jülich, Germany

³Spin-X Institute, School of Physics and Optoelectronics, State Key Laboratory of Luminescent Materials and Devices, Guangdong-Hong Kong-Macao Joint Laboratory of Optoelectronic and Magnetic Functional Materials, South China University of Technology, Guangzhou 511442, China

⁴Department of Physics and Astronomy, Uppsala University, SE-75120 Uppsala, Sweden

⁵Department of Physics, KTH-Royal Institute of Technology, SE-10691 Stockholm, Sweden

⁶The Anhui Key Laboratory of Condensed Matter Physics at Extreme Conditions, High Magnetic Field Laboratory, Chinese Academy of Science (CAS), Hefei, Anhui Province 230031, China

We report the most recent findings [1,2] on magnetic skyrmions in B20 type FeGe obtained by transmission electron microscopy (TEM). In these crystals, the skyrmions represent vortex-like spin textures that form strings. In buck crystals and relatively thick plates of cubic chiral magnets, we found that the skyrmions can form braids — the superstructures of skyrmion strings that wind around one another. Experimental observations of skyrmion braids are supported by comprehensive theoretical analysis, which explains the mechanism of their stability, dependencies on the external field, and plate thickness. A reliable approach for the creation of skyrmion braids composed of an arbitrary number of skyrmion strings is provided.

Besides the skyrmion braids in this talk, we also report on the stability of antiskyrmions — skyrmion antiparticle. Earlier it was assumed that the coexistence of statically stable skyrmions and antiskyrmions is impossible in isotropic chiral magnets. The experimental observation of the skyrmion-antiskyrmion pairs in FeGe plates is consistent with the earlier theoretical findings in two-dimensional (2D) systems [3] but has some essential peculiarities connected with the additional twist of magnetization across the thickness of the plate. For instance, contrary to 2D systems, skyrmion antiskyrmion pairs in FeGe can appear as statically stable configurations. We present a reliable approach for nucleation of antiskyrmions in plates of isotropic chiral magnets. We estimate the antiskyrmion stability range and show the effect of skyrmion-antiskyrmion pair annihilation.

The authors acknowledge financial funding from the European Research Council under the European Union's Horizon 2020 Research and Innovation Programme (Grant 856538 - project “3D MAGiC”) and the Deutsche Forschungsgemeinschaft through SPP 2137 “Skyrmionics” Grants KI 2078/1-1 and BL 444/16.

[1] F. Zheng et al., Nature Commun. 12, 5316 (2021).

[2] F. Zheng et al., Nature Phys. (2022) accepted.

[3] V. M. Kuchkin and N. S. Kiselev Phys. Rev. B 101, 064408 (2020).

Spin-wave resonance modes in 3D skyrmion lattice

Andrii S. Savchenko^{1,2}, Vladyslav M. Kuchkin¹, Filipp N. Rybakov^{3,4}, Stefan Blügel¹ and Nikolai S. Kiselev¹

¹Peter Grünberg Institut and Institute for Advanced Simulation, Forschungszentrum Jülich, Jülich, Germany

a.savchenko@fz-juelich.de

²Donetsk Institute for Physics and Engineering, National Academy of Sciences of Ukraine, Ukraine

³Uppsala University, SE-75120 Uppsala, Sweden

⁴KTH Royal Institute of Technology, SE-10691 Stockholm, Sweden

The resonance excitations of the three-dimensional (3D) skyrmion lattice (SkL) in the plate of an isotropic chiral magnet were studied using spin dynamics simulations. We calculated the dependencies of the impedance part of dynamic magnetic susceptibility $\text{Im } \chi(\omega)$ on plate thickness L to illustrate the features of the eigenmodes. The plate was in a constant magnetic field \mathbf{B}_{DC} directed along normal. The eigenmodes were excited by an alternating magnetic field \mathbf{B}_{AC} that oriented $\mathbf{B}_{AC} \perp \mathbf{B}_{DC}$ or $\mathbf{B}_{AC} \parallel \mathbf{B}_{DC}$. The dependencies of $\text{Im } \chi_{xx}(\omega)$ on L are characterized by a set of low-frequency and high-frequency modes appearing in pairs for the case of $\mathbf{B}_{AC} \perp \mathbf{B}_{DC}$ (see Fig.1(a)). In this case, the maxima of the spin-wave excitations are localized in the inter-skyrmion area or in the skyrmion core, where magnetization is normal to the film plane. These resonance modes correspond to chiral standing spin waves (SSW). Contrary to standard SSW in ferromagnets without Dzyaloshinskii-Moriya interaction (DMI), the profiles of dynamic magnetization of chiral SSW are characterized by helical modulation with the pitch determined by the competition between DMI and Heisenberg exchange. An important consequence of such modulation of dynamic magnetization is the periodic fading of the absorption spectra intensity with the variation of the plate thickness. This effect takes place not only in the 3D SkL but also in the case of the field saturated state and the conical phase. For the case of $\mathbf{B}_{AC} \parallel \mathbf{B}_{DC}$ the dependencies of $\text{Im } \chi_{zz}(\omega)$ on L (Fig.1(b)) also demonstrates the appearance of SSW, which are localized in the skyrmion shell where spins lie in the plane of the plate. The helical modulations of the dynamic magnetization profile are not present in this case. Thus, SSW for $\mathbf{B}_{AC} \parallel \mathbf{B}_{DC}$ have more in common with standard SSW in pure ferromagnets. The effect of the chiral surface twist plays an essential role in this case.

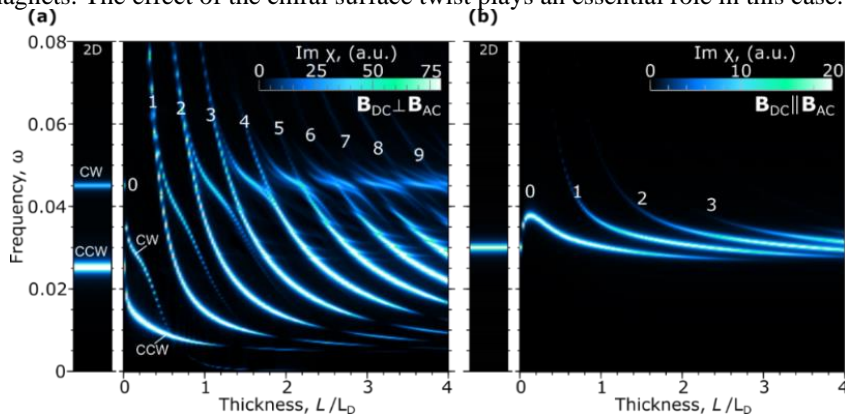


Figure 1. (a) Absorption spectra $\text{Im } \chi_{xx}(\omega)$ of 2D (left) and 3D SkL (right) as a function of film thickness, L for $\mathbf{B}_{AC} \perp \mathbf{B}_{DC}$; L_D is the period of the helical spin spiral at zero field; $\mathbf{B}_{DC} = 0.5\mathbf{B}_D$; \mathbf{B}_D is the saturation field required for transition into ferromagnetic state; CW and CCW modes correspond to clockwise and counterclockwise precession; white digits indicate the number of nodes of SSW. (b) The thickness dependent spectra of $\text{Im } \chi_{zz}(\omega)$ for $\mathbf{B}_{AC} \parallel \mathbf{B}_{DC}$.



The authors acknowledge funding from the European Research Council (ERC) under the European Union's Horizon 2020 research and innovation program (Grant No. 856538, project "3D MAGiC"). F.N.R. acknowledges support from the Swedish Research Council.

Steering Majorana braiding via skyrmion-vortex pairs: a scalable platform

Jonas Nothhelfer¹, Sebastián A. Díaz¹, Stephan Kessler², Tobias Meng³, Matteo Rizzi^{4,5}, Kjetil M.D. Hals⁶, Karin Everschor-Sitte^{1,7}

¹Faculty of Physics, University of Duisburg-Essen, 47057 Duisburg, Germany

sebastian.diaz@uni-due.de

²Institute of Physics, Johannes Gutenberg University Mainz, 55128 Mainz, Germany

³Institute of Theoretical Physics, Technische Universität Dresden, 01062 Dresden, Germany

⁴Forschungszentrum Jülich, Institute of Quantum Control, Peter Grünberg Institut (PGI-8), 52425 Jülich, Germany

⁵Institute for Theoretical Physics, University of Cologne, 50937 Cologne, Germany

⁶Department of Engineering Sciences, University of Agder, 4879 Grimstad, Norway

⁷Center for Nanointegration Duisburg-Essen (CENIDE), University of Duisburg-Essen, 47057 Duisburg, Germany

Majorana zero modes are quasiparticles that hold promise as building blocks for topological quantum computing. However, the litmus test for their detection, the observation of exotic non-abelian statistics revealed by braiding, has so far eluded experimental efforts. Here we take advantage of the fact that skyrmion-vortex pairs in superconductor-ferromagnet heterostructures harboring Majorana zero modes can be easily manipulated in two spatial dimensions. We adiabatically braid the hybrid topological structures and explicitly confirm the non-abelian statistics of the Majorana zero modes numerically using a self-consistent calculation of the superconducting order parameter. Our proposal of controlling skyrmion-vortex pairs provides the necessary leeway toward a scalable topological quantum computing platform.

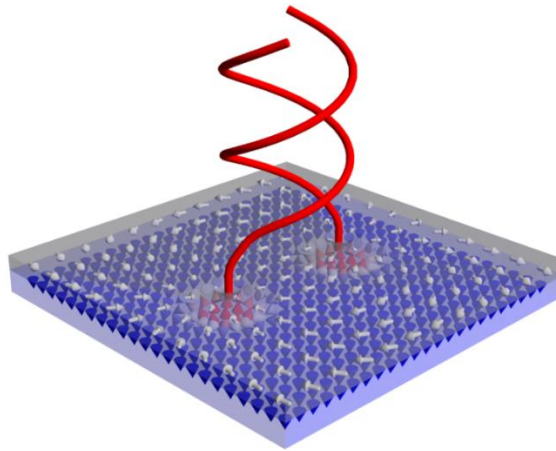


Figure 1. Braiding of two skyrmion-vortex pairs in a superconductor-ferromagnet heterostructure.

[1] J. Nothhelfer, S. A. Díaz, S. Kessler, T. Meng, M. Rizzi, K. M. D. Hals, K. Everschor-Sitte, arXiv:2110.13983.

[2] J. Nothhelfer, K. M. D. Hals, K. Everschor-Sitte, M. Rizzi, International Patent Application WO2020EP66120.

Stability of antiferromagnetic skyrmions

David Ramos-Salamanca¹, Pierre Pujol², Luis A. Núñez¹

¹Escuela de Física, Universidad Industrial de Santander

david2208450@correo.uis.edu.co

²Laboratoire de Physique Theorique, CNRS and Université de Toulouse, UPS, Toulouse, France

Magnetic skyrmions are particle-like spin textures that form in chiral magnets. The non-trivial topology of skyrmions grants them great stability and makes them promising candidates to be the base of new information storage and logic devices. Magnetic skyrmions have been observed in many ferromagnetic materials [1, 2] and they have been predicted to exist in antiferromagnets [3] but they have not been observed yet. Recently, there has been great interest in antiferromagnetic skyrmions as they have been found more suitable for applications in data storage [4]. This has resulted in an effort to determine the conditions under which antiferromagnetic skyrmions can form.

In this study, we explored the zero-temperature phase space of square-lattice chiral antiferromagnets with easy-axis anisotropy in the presence of a magnetic field. By numerically solving the Euler-Lagrange equations associated to the energy functional of the material, we found a region of phase space where skyrmion solutions have a non-vanishing size and a lower energy than the antiferromagnetic phase. Furthermore, using Monte Carlo simulations, we show that in said region of phase space, antiferromagnetic skyrmions (or antiskyrmions) are stable configurations at finite temperatures even in the absence of a magnetic field. These results can help identify antiferromagnetic materials where skyrmions can form and in what range of temperatures they can be stable.

[1] S. Muhlbauer et al., *Science* 323, 5196 (2009).

[2] X. Z. Yu et al., *Nature* 465, 7300 (2021).

[3] A. N. Bogdanov et al., *PRB* 66, 214410 (2002).

[4] B. Göbel et al., *Phys. Rep.* 895 (2021).

Nematic *d*-wave superconductivity in magic-angle twisted bilayer graphene from atomistic modeling

Tomas Löthman, Johann Schmidt, Fariborz Parhizgar, and Annica Black-Schaffer*

Department of Physics and Astronomy, Uppsala University, Uppsala Sweden

annica.black-schaffer@physics.uu.se

Bilayer graphene at specific small twist angles develops large-scale moiré patterns with flat energy bands hosting correlated insulating states and superconductivity. The large system size and intricate band structure have however hampered investigations into the properties of the superconducting state. By using full-scale atomistic modeling with local electronic interactions, mimicking closely those of the high-temperature cuprate superconductors, and solving fully self-consistently for the superconducting order, we find a highly inhomogeneous superconducting state with nematic ordering on both the atomic and moiré length scales, see Fig. 1. Specifically, we obtain locally anisotropic real-valued *d*-wave pairing with a nematic vector winding throughout the moiré pattern and a three-fold degenerate ground state. Despite the *d*-wave nature, the superconducting state has a full energy gap, which we show is tied to a *p*-phase interlayer coupling. We further show that the superconducting nematicity is easily detected through signatures in the local density of states. These results show both that atomistic modeling is essential for superconductivity in twisted bilayer graphene and that the superconducting state is distinctly different from that of the cuprate superconductors.

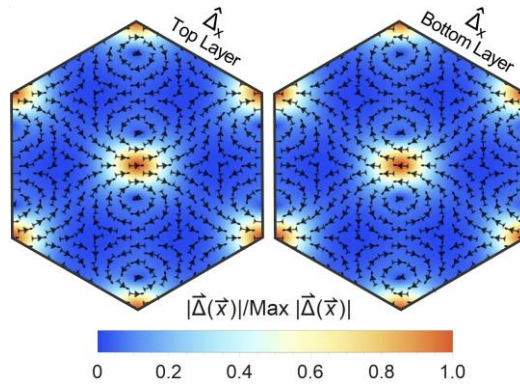


Figure 1. Order parameter in moiré cell in the top (left) and bottom (right) graphene layer. Underlying color intensity plot shows the amplitude, clearly depicting a global, moiré-scale, nematicity. Streamlines show of the local nematic vector field, illustrating the intricate atomic-scale nematicity in the local *d*-wave bond order parameters, as well as the superconducting π -phase-shift between the two layers. From Ref. [1].

Financial funding from the Swedish Research Council (Vetenskapsrådet Grant No. 2018-03488) and the Knut and Alice Wallenberg Foundation through the Wallenberg Academy Fellows program. The numerical work was enabled by resources provided by the Swedish National Infrastructure for Computing (SNIC) at the Uppsala Multidisciplinary Center for Advanced Computational Science (UPPMAX) partially funded by the Swedish Research Council through Grant No. 2018-05973.

[1] T. Löthman, J. Schmidt, F. Parhizgar, and A. M. Black-Schaffer, *Commun. Phys.* 5, 92 (2022)

Nematicity in unusual iron-based superconductors

Anna Böhmer

Ruhr-Universität Bochum

boehmer@physik.rub.de

I will discuss nematic fluctuations in iron-based superconductors that do not show the stripe-type magnetic order that is typically associated with this kind of structural distortion. In the most studied and cited model systems, the onset of stripe-type magnetic order coincides with or is only narrowly preceded by a tetragonal-to-orthorhombic (“nematic”) transition. $\text{CaK}(\text{Fe}_{1-x}\text{Ni}_x)_4\text{As}_4$ resembles the archetypal 122-type iron-based materials but hosts one of the few examples of the so-called spin-vortex crystal magnetic order, a non-collinear magnetic configuration that preserves tetragonal symmetry, in contrast to the stripe-type magnetic configuration common to the 122-type systems. The evolution of nematic fluctuations in such an unusual case is studied via elastoresistance and elastic modulus measurements combined with phenomenological modeling and density functional theory. Despite the absence of a finite nematic order parameter, we find clear experimental signatures of considerable nematic fluctuations. We address the effect of the specific crystal symmetry of the 1144-type structure in determining its magnetic ground state and on the nematic fluctuations.

The strongly-hole doped iron-based superconductors AFe_2As_2 ($A=\text{K},\text{Rb},\text{Cs}$) exhibit no magnetic order but stand out because of their strong electronic correlations. The symmetry channel and strength of nematic fluctuations, as well as possible nematic order, in these compounds remains obscure. We address these questions using transport measurements under elastic strain and elucidate the evolution of the elastoresistance across the hole-doping series from optimal to the fully overdoped end-members. Our technical development takes into consideration the extreme thermal expansion of some of these compounds. By decomposing the strain response into the appropriate symmetry channels, we demonstrate the emergence of a giant in-plane symmetric contribution, associated with the growth of both strong electronic correlations and their strain-sensitivity, whereas nematic fluctuations are continuously weakened.

We acknowledge support by the Helmholtz Association under Contract No. VH-NG-1242 and the German Research Foundation (DFG) under CRC/TRR 288 (Project A02).

- [1] Anna E. Böhmer, Fei Chen, William R. Meier, Mingyu Xu, Gil Drachuck, Michael Merz, Paul W. Wiecki, Sergey L. Bud'ko, Vladislav Borisov, Roser Valentí, Morten H. Christensen, Rafael M. Fernandes, Christoph Meingast, Paul C. Canfield, arXiv:2011.13207 (2020).
- [2] P. Wiecki, M. Frachet, A. -A. Haghighirad, T. Wolf, C. Meingast, R. Heid and A. E. Böhmer, PRL **125**, 187001 (2020).
- [3] P. Wiecki, A.-A. Haghighirad, F. Weber, M. Merz, R. Heid, and A. E. Böhmer, Nat. Commun. **12**, 4824 (2021).

Non-reciprocity in current-biased Josephson junctions in the presence of Yu-Shiba-Rusinov bound states

M. Trahms¹, B. Mahendru¹, I. Tamir¹, L. Melischek¹, J. F. Steiner¹,
N. Bogdanoff¹, O. Peters¹, G. Reecht¹, C. B. Winkelmann²,
F. von Oppen¹ and K. J. Franke¹

¹Freie Universität Berlin, Berlin, Germany

martina.trahms@fu-berlin.de

²Univ. Grenoble Alpes, Institute Néel, Grenoble, France

Magnetic impurities on a superconducting surface are known to locally disturb Cooper pairs and form Yu-Shiba-Rusinov-states, thereby influencing the superconducting ground-state. We employ current-biased Josephson spectroscopy in a scanning tunnelling microscope to study the phase dynamics of Josephson junctions in the presence of Yu-Shiba-Rusinov-states of single atoms. For that purpose magnetic Mn and Cr adatoms are evaporated on a superconducting Pb(111) surface and investigated with a superconducting Pb tip. We observe switching currents that are significantly larger than the retrapping currents, identifying the junction as underdamped. In the presence of magnetic atoms, a local reduction of switching currents is observed. Additionally, we find a non-reciprocal behavior of the retrapping currents with respect to the current-sweep direction, i.e., the absolute value of the retrapping current depends on whether the current sweep starts at positive or negative bias values. In our experiment both species of magnetic atoms lead to a non-reciprocal retrapping-current behavior, albeit with a different directionality. We suggest a correlation between the damping of the Josephson junction and the electron-hole asymmetry of the Yu-Shiba-Rusinov-states.

Superconductor-Insulator transition in Lead-Graphene Hybrid system

Suraina Gupta, Santu Prasad Jana, Rukshana Pervin, Anjan Kumar Gupta

Department of Physics, Indian Institute of Technology Kanpur, Kanpur 208016, India

suraina@iitk.ac.in

Superconductor-Insulator transition has been observed in a range of systems such as homogeneously disordered thin films, granular superconductors, high T_c -superconductors and arrays of Josephson junctions [1]. The two-dimensional nature of graphene with high mobility and inertness with exposure to the environment has opened up prospects for the fabrication of graphene hybrid systems [2]. We have observed that lead (Pb) deposition at different temperatures and thickness, on exfoliated single-layer graphene, leads to formation of lead nano-islands of different sizes with varying separation between these islands as shown in Fig. 1. Optimizing these parameters for the fabrication of our lead-graphene hybrid system, we have observed that the lead nano-islands become superconducting below its transition temperature. These superconducting islands are coupled to each other through graphene and are characterised as granular superconductors. Superconductor-insulator transition is observed with change in carrier-density of graphene, by varying back-gate voltages applied to it. For gate voltages applied such that the fermi level of graphene is close to its Dirac point, resistance measurements with lowering temperature show “re-entrant” behavior. At low temperatures, the system becomes insulator. Away from the Dirac point, the system shows a transition in resistance at the T_c of Pb, see Fig. 2, indicating superconducting behavior. However, the resistance remains finite at low temperatures possibly due to phase fluctuations, which destroy phase coherence of the system.

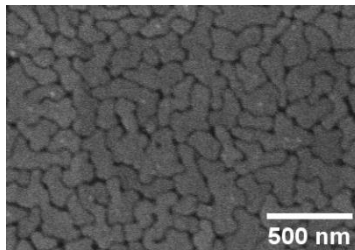


Figure 1. SEM image of lead-graphene hybrid system showing lead nano-islands formed on graphene.

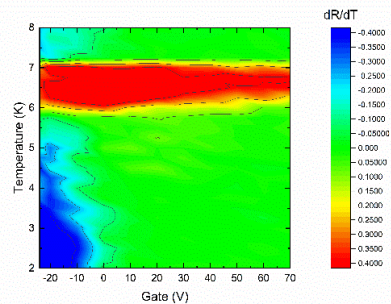


Figure 2. Phase diagram of the SIT transition. dR/dT versus gate voltage (V) and temperature (T). Red region: superconducting transition at T_c of lead; Blue region: insulating behavior; Green region: metallic behavior

We have also conducted magnetoresistance measurements with varying gate voltages and temperatures and have noticed negative magnetoresistance for gate voltages close to the Dirac point at low temperatures. This system can be useful to understand the concept of charge-phase duality behind superconductor-insulator transition.

The financial funding from SERB-DST is gratefully acknowledged.

[1] Gantmakher, V. F. & Dolgoplov, V. T. *Phys. Usp.* **53**, 1-49 (2010).

[2] Allain, A., Han, Z. & Bouchiat, V. *Nature Mater.* **11**, 590-594 (2012).

Correlated normal state fermiology and topological superconductivity in UTe_2

Hong-Chul Choi^{1,2}, Seung-Hun Lee^{1,2,3}, Bohm-Jung Yang^{1,2,3,*}

¹Department of Physics and Astronomy, Seoul National University, Seoul, South Korea

²Center for Correlated Electron Systems, Institute for Basic Science, Seoul, South Korea

³Center for Theoretical Physics (CTP), Seoul National University, Seoul, South Korea

bjyang@snu.ac.kr

UTe_2 is a promising candidate of spin-triplet superconductors where a paramagnetic normal state becomes superconducting due to spin fluctuations. The subsequent discovery of various unconventional superconducting properties, including gaplessness, Kondo effect, and time-reversal symmetry breaking, etc., has promoted UTe_2 as an exciting playground to study unconventional superconductivity, while fathoming the normal state fermiology still requires further investigation. Here, we theoretically show that electron correlation induces a dramatic change of the normal state fermiology with an emergent correlated Fermi surface (FS) driven by Kondo resonance at low temperature [Ref. 1] (See Figure 1). This emergent correlated FS can account for various unconventional superconducting properties in a unified way. Especially, the geometry of the correlated FS can naturally host topological superconductivity in the presence of odd-parity pairings which become leading instability due to strong ferromagnetic spin fluctuations. Moreover, two pairs of odd-parity channels appear as accidentally degenerate solutions, which can naturally explain the multi-component superconductivity with broken time-reversal symmetry. Interestingly, the resulting time-reversal breaking superconducting state turns out to be a Weyl superconductor in which Weyl points migrate along the correlated FS as the relative magnitude of nearly degenerate pairing solutions varies. We believe that the correlated normal state fermiology we discovered provides a unified platform to describe the unconventional superconductivity in UTe_2 .

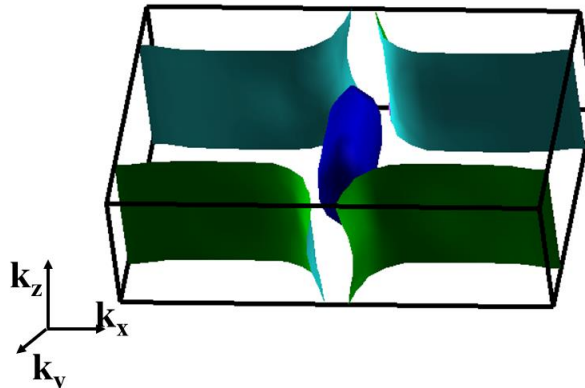


Figure 1. Emergent correlated Fermi surface from Kondo resonance in UTe_2

The financial funding from the Institute for Basic Science in Korea (Grant No. IBS-R009-D1), Samsung Science and Technology Foundation under Project Number SSTF-BA2002-06, the National Research Foundation of Korea (NRF) grant funded by the Korea government (MSIT) (No.2021R1A2C4A002773, and No. NRF-2021R1A5A1032996) is gratefully acknowledged.

[1] Hong-Chul Choi, Seung-Hun Lee, and Bohm-Jung Yang, “Correlated normal state fermiology and topological superconductivity in UTe_2 ” (submitted).

Superfluid and non-superfluid properties of emergent Bose liquid: Exotic transport and optical properties resembling unconventional superconductors

Wei Ku

Tsung-Dao Lee Institute, Shanghai Jiao Tong University, China

weiku@sjtu.edu.cn

Unconventional superconductors often exhibit exotic non-Fermi liquid behavior that are qualitatively distinct from those in textbooks. These include prototypical properties not only in their low-temperature superconducting phase, but more importantly also in their high-temperature non-superconducting phase. Examples include unorthodox transport properties known as the “strange metal”, “bad metal”, “weak insulating behavior”, strongly temperature dependent Hall coefficient. Other examples include puzzling optical properties such as “Fermi arc”, “pseudogap”, or non-Fermi liquid quasi-particle scattering rate. This talk will survey the recent studies on various basic transport, optical, and superfluid properties of an emergent Bose liquid, including the first homogeneous Bose metal phase. These generic behaviors of an emergent Bose liquid naturally display all the above-mentioned exotic behaviors found in materials with just a single model and a single set of parameters, thus leading to a strong suggestion that many of the puzzling strongly correlated materials, particularly unconventional superconductors, can be intuitively understood as emergent Bose liquid.

- [1] A. Hegg, J Hou, and Wei Ku, PNAS 118 (46) e2100545118 (2021)
- [2] T Zeng, A Hegg, L Zou, S Jiang, and Wei Ku, arXiv:2112.05747
- [3] X Yue, A Hegg, X Li, and Wei Ku, arXiv:2104.07583
- [4] Zi-Jian Lang, Fan Yang, and Wei Ku, arXiv:1902.11206
- [5] Shengtao Jiang, Long Zou, and Wei Ku, PRB 99, 104507 (2019)
- [6] Y. Yildirim and Wei Ku, PRB 92, 180501(R) (2015)
- [7] Y. Yildirim and Wei Ku, PRX 1, 011011 (2011)

Audio Recognition with Skyrmion Mixture Reservoirs

Robin Msiska¹, Jake Love¹, Jonathan Leliaert², Jeroen Mulkers², George Bourianoff³,
Karin Everschor-Sitte¹

¹University of Duisburg-Essen, Duisburg, Germany

robin.msiska@uni-due.de

²Ghent University, Ghent, Belgium

³Senior Principle Engineer, Intel Corp. (Retired)

Physical reservoir computing is an information processing scheme that enables energy efficient temporal pattern recognition to be performed directly in physical matter [1]. Previously, random topological magnetic textures have been shown to have the characteristics necessary for efficient reservoir computing [2] and allowed for simple pattern recognition with two input channels [3].

We propose a skyrmion mixture reservoir that implements the reservoir computing model multi-dimensional inputs. Through micro-magnetic simulations, we show that our implementation can solve audio classification tasks at the nanosecond timescale to a high degree of accuracy. Due to the quality of the results shown and the low power properties of magnetic texture reservoirs, we argue that skyrmion magnetic textures are a competitive substrate for reservoir computing.

The financial funding from the Emergent AI Centre (Carl-Zeiss-Stiftung), DFG (320163632), FWO-Vlaanderen and computer resources by VSC (Flemish Supercomputer Center) are gratefully acknowledged.

[1] G. Tanaka et al., *Neural Networks* 115, 100 (2019).

[2] D. Prychynenko et al., *Physical Review Applied* 9, 014034 (2018)

[3] D. Pinna et al., *Phys. Rev. Applied* 14, 054020 (2020)

Magnetic domains in [Pt/Co/Ta]₁₀ multilayers

Liz Montañez¹, Valentin Ahrens², Markus Becherer², Sabine Pütter¹

¹Forschungszentrum Jülich GmbH, Jülich Centre for Neutron Science at MLZ, Lichtenbergstrasse 1, 85748, Garching, Germany

²Chair of Nano and Quantum Sensors, Department of Electrical and Computer Engineering, Technical University of Munich, Munich, Germany
l.montanez.huaman@fz-juelich.de

Multilayers composed of heavy metals and ferromagnets with strong perpendicular anisotropy are potential candidates for magnetic memory applications [1,2]. In particular, magnetic skyrmions may enable ultra-dense storage devices due to the extremely low spin currents needed to move/manipulated them [2]. Pt/Co-based multilayers generally exhibit worm domains, which can nucleate into skyrmions through breaking/nucleation processes [3,4]. Recent studies have demonstrated the nucleation of skyrmions by varying external magnetic field, temperature, and current in sputtered Pt/Co/Ta multilayers [4,5].

In this work, [Pt/Co/Ta]₁₀ multilayers with cobalt layer thickness between 5 Å to 21 Å were grown by molecular beam epitaxy. The uniformity and quality of the multilayers are demonstrated by pronounced Bragg peaks and Kissig fringes observed in the X-Ray reflectivity (XRR) patterns. We study the dependence of the domain structure in [Pt/Co/Ta]₁₀ multilayers on the thickness of the Co layer, and the application of external oop magnetic fields, by means of magnetic force microscopy (MFM) at room temperature. The multilayers exhibit worm domains over the entire film (Figure 1a). Furthermore, we observed skyrmions under a magnetic field of ~38 mT (Figure 1b).

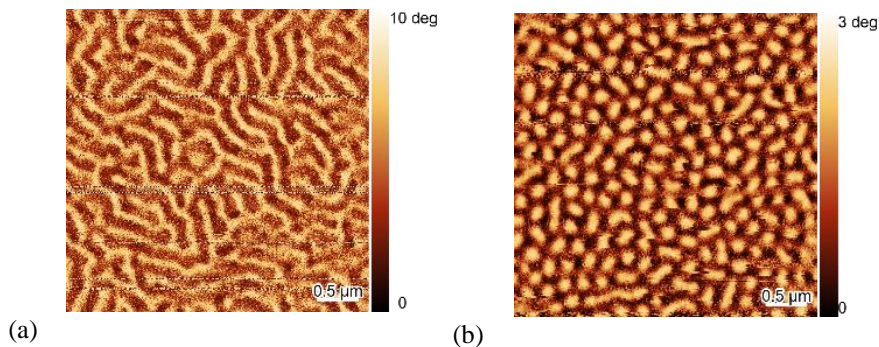


Figure 1. Magnetic force microscopy (MFM) images for [Pt/Co/Ta]₁₀ multilayer with 17 Å Co. The measurements were performed without external field (a) and under an external oop magnetic field of ~38 mT (b).

- [1] A. Fert and V. Sampaï, Nat. Nanotechnol. 8 (2013) 152–156
- [2] C. Wang et al., J. Phys. D: Appl. Phys. 46 (2013) 285001
- [3] M. Ma et al., J. Appl. Phys. 127 (2020) 223901
- [4] J. Brandao et al., Appl. Nano Mater. 2 (2019) 7532–7539
- [5] S. Zhang et al., Appl. Phys. Lett. 112 (2018) 132405

Element-specific, spatially and time resolved observation of different phasic magnetic resonances of Fe₃O₄ nanoparticle ensembles in a bacterium *Magnetospirillum Magnetotacticum*

Thomas Feggeler¹, Johanna Lill², Damian Günzing², Ralf Meckenstock², Detlef Spoddig², Mariia Efremova^{3,4,5}, Sebastian Wintz^{6,7}, Markus Weigand⁷, Benjamin W. Zingsem^{2,8}, Michael Farle², Heiko Wende², Katharina J. Ollefs² and Hendrik Ohldag^{1,9,10}

¹Advanced Light Source, Lawrence Berkeley National Laboratory, Berkeley CA 94720, United States

²Faculty of Physics and CENIDE, University of Duisburg-Essen, 47048 Duisburg, Germany

³Department of Chemistry & TUM School of Medicine, Technical University of Munich, Germany

⁴Institute for Synthetic Biomedicine, Helmholtz Zentrum München, 85764 Neuherberg, Germany

⁵Department of Applied Physics, Eindhoven University of Technology, Netherlands

⁶Max Planck Institute for Intelligent Systems, 70569 Stuttgart, Germany

⁷Helmholtz Center Berlin, 12489 Berlin, Germany

⁸Ernst Ruska Centre for Microscopy and Spectroscopy with Electrons and Peter Grünberg Institute, Forschungszentrum Jülich GmbH, 52425 Jülich, Germany

⁹Department of Material Sciences and Engineering, Stanford University, United States

¹⁰Department of Physics, University of California Santa Cruz, Santa Cruz CA 95064, United States

tfeggeler@lbl.gov

Nanoscaled magnetic particle ensembles are promising candidates for future magnon based binary logic concepts [1, 2]. Element-specific real-space spatial sampling of magnetic resonance modes in the GHz regime allows the experimental verification of future complex magnonic devices. Here we use the element-specific technique of Time-Resolved Scanning Transmission X-ray Microscopy (TR-STXM) [3, 4] to monitor different phasic magnetic resonance modes within a chain of magnetically dipolarly coupled (Figure 1) Fe₃O₄ nanoparticles (40-50 nm edge length) grown by biomineralization inside a single cell of a magnetotactic bacterium *Magnetospirillum Magnetotacticum*. The magnetization dynamics is probed at the Fe L₃ X-ray absorption edge with 25 nm spatial resolution in response to a microwave excitation of 4.07 GHz. A multitude of resonant responses for resonances fields between 0.03 to 0.116 T within multiple particle segments oscillating in- and out-of-phase could be observed.

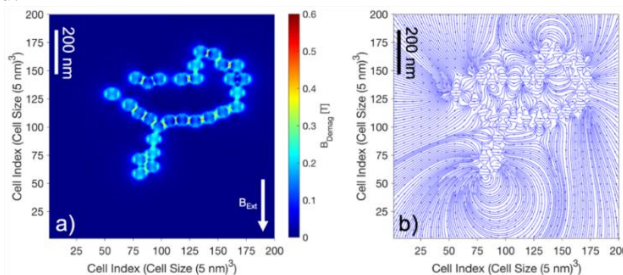


Figure 1: a) Demagnetization and stray field intensity summarized in the quantity B_{Demag} for the investigated Fe₃O₄ nanoparticle chain. b) The respective demagnetization and stray field distribution.

Lawrence Berkeley National Laboratory is acknowledged for funding through LDRD Award: Development of a Continuous Photon Counting Scheme for Time Resolved Studies. We thank the Deutsche Forschungsgemeinschaft (DFG, German Research Foundation) – Project No. OL513/1-1, 321560838 and Project-ID 405553726 TRR 270 for financial funding.

[1] A. Barman, G. Gubbiotti, et al. J Phys Condens Matter, 2021.

[2] B. Zingsem, T. Feggeler, et al. Nature Communications, 2019. **10**: p. 4345.

[3] S. Bonetti, R. Kukreja, et al. Review of Scientific Instruments, 2015. **86**(9): p. 093703-1-093703-9.

[4] T. Feggeler, R. Meckenstock, et al. Physical Review Research, 2021. **3**(3).

Indirect Spin-Readout of Rare-Earth-Based Single-Molecule Magnet with Scanning Tunneling Microscopy

H. Chen^{1,*}, T. Frauhammer¹, T. Balashov², G. Derenbach^{1,3}, S. Klyatskaya⁴,
E. Moreno-Pineda⁵, M. Ruben^{3,4,6}, and W. Wulfhekel^{1,3}

¹Physikalisches Institut, Karlsruhe Institute of Technology (KIT), 76131 Karlsruhe, Germany

²Physikalisches Institut, RWTH Aachen, 52074 Aachen, Germany

³Institute for Quantum Materials and Technologies, Karlsruhe Institute of Technology (KIT), 76021 Karlsruhe, Germany

⁴Institute of Nanotechnology, Karlsruhe Institute of Technology (KIT), 76021 Karlsruhe, Germany

⁵Departamento de Química-Física, Escuela de Química, Facultad de Ciencias Naturales, Exactas y Tecnología, Universidad de Panamá 0824, Panama

⁶Centre Européen de Sciences Quantiques (CESQ) in the Institut de Science et d'Ingénierie Supramoléculaires (ISIS), 8 allée Gaspard Monge BP 70028, 67083 Strasbourg Cedex, France

hongyan.chen@kit.edu

Rare-earth based single-molecule magnets are promising candidates for magnetic information storage including qubits as their large magnetic moments are carried by localized 4f electrons. However, this in turn hampers a direct readout of the moment. Here, we present the indirect readout of the Dy moment in Bis(phthalocyaninato)dysprosium (DyPc₂) molecules on Au(111) using milli-Kelvin scanning tunneling microscopy. Because of an unpaired electron on the exposed Pc ligand, the molecules show a Kondo resonance that is, however, split by the ferromagnetic exchange interaction between the unpaired electron and the Dy angular momentum. Using spin-polarized scanning tunneling spectroscopy, we read out the Dy magnetic moment as a function of the applied magnetic field, exploiting the spin polarization of the exchange-split Kondo state [1].

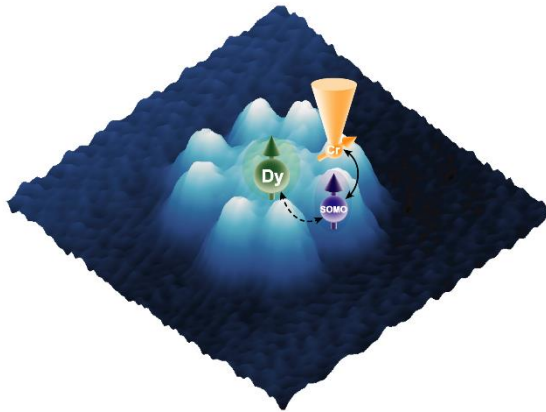


Figure 1. Basic idea to access the Dy magnetic moment

[1] T. Frauhammer, H. Chen, T. Balashov, G. Derenbach, S. Klyatskaya, E. Moreno-Pineda, M. Ruben, and W. Wulfhekel, Phys. Rev. Lett. 127, 123201 (2021).

Inducing and Controlling Molecular Magnetism through Supramolecular Manipulation

Manuel Gruber¹, Jan Homberg², Alexander Weismann², and Richard Berndt²

¹Faculty of Physics and CENIDE, University of Duisburg-Essen, 47057 Duisburg, Germany

manuel-gruber@uni-due.de

john.author@correspondence.email.com

²Institut für Experimentelle und Angewandte Physik, Christian-Albrechts-Universität, 24098 Kiel, Germany

Magnetic molecules on surfaces have attracted considerable interest, in particular, in view of tuning spin-dependent electron transport through molecular junctions. The interaction between a molecule and a substrate can significantly alter the molecular spin through charge transfer, extreme cases being the creation or quenching of spin magnetic moment. The charge transfer can be modified by charges close to the molecule [1]. The interaction between a localized spin and Cooper pairs of a superconductor leads to the emergence of Yu-Shiba-Rusinov (YSR) states. In low-temperature scanning tunneling spectroscopy (STS), YSR resonances are observed as pair(s) of peaks, symmetrically located around the Fermi energy E_F within the gap of the superconductor. Here, we show the emergence of a spin moment in initially diamagnetic H₂ phthalocyanine molecules within a self-assembled monolayer on Pb(100) using YSR resonances for spin detection. The spin moments are found to significantly vary from molecule to molecule. The magnitude of the induced moment is determined by the electrostatic field that results from polar bonds in the surrounding Pc molecules. Each molecule generates an approximate quadrupole field, which can be inverted by repositioning the hydrogen atoms of the inner macrocycle of the molecule. We fabricated supramolecular arrays and selectively swapped hydrogen atoms to tune the magnetic moment with a precision of ~ 0.01 Bohr magneton [2].

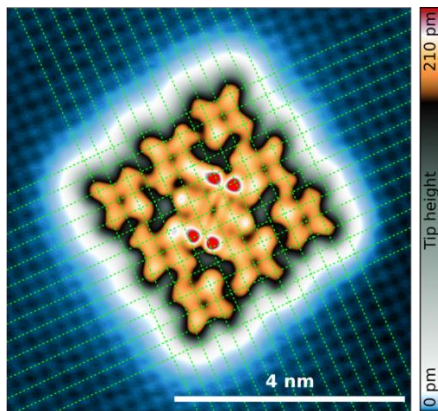


Figure 2. Scanning tunneling microscopy image of H₂ phthalocyanine enneamer on a Pb(100) surface. Dashed green lines are overlaid over atomic rows of the substrate.

The financial funding from European Union's Horizon 2020 program (grant No. 766726) and the Deutsche Forschungsgemeinschaft (SFB 677) is acknowledge.

[1] A. Mugarza et al., Nat. Commun. 2, 490 (2011).

[2] J. Homberg et al., ACS Nano 14, 17387 (2020).

Magnetolectric effect of Ni – PZT – Ni layered structures obtained by nickel electrochemical deposition in an external magnetic field

Natallia Poddubnaya, Vladimir Laletin

Institute of Technical Acoustics of the National Academy of Sciences of Belarus, Vitebsk, Belarus

poddubnaya.n@rambler.ru

The paper presents studies of the influence of external electric and magnetic fields on the magnetolectric (ME) properties in layered structures metal - piezoelectric metal on the ME effect.

Structures zirconate - lead titanate are made with a thickness of 400 microns by chemical deposition of nickel 0.5 microns and electrochemical deposition of nickel 50 microns on each side. Electrochemical deposition was carried out on non-polarized (P/EI) and polarized (EI/P) ceramics. Some of the samples were obtained by electrochemical deposition in a magnetic field on non-polarized (EI+H/P) and polarized (P/EI+H) ceramics. A magnetic field of 14 kA/m was applied in all cases in the direction of structure polarization (Fig. 1). The structures had the shape of a square 4 mm wide.

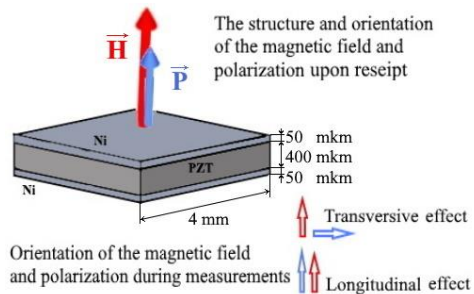


Figure 1. The sample structure and orientation of the magnetic field and polarization upon receipt.

The results of the study of the ME coefficient for the longitudinal and transverse orientation of the external magnetic field to the polarization of the structure are shown in Fig. 2.

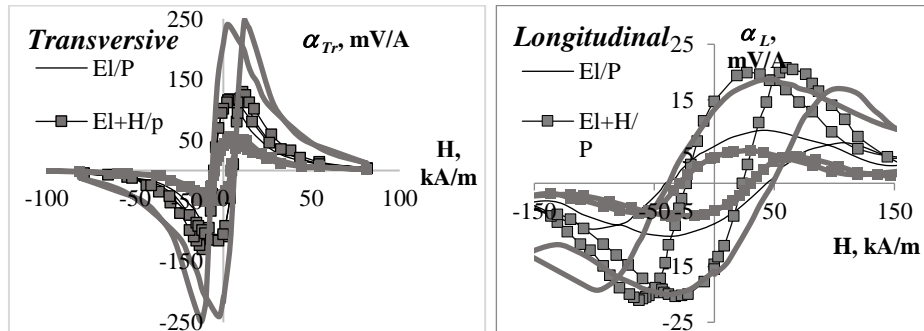


Figure 2. ME coefficient for the longitudinal and transverse orientation of the external magnetic field to the polarization of the structure.

The graphs show that the value of the transverse ME coefficient is higher for prepolarized structures. The imposition of a magnetic field during the deposition of nickel coatings leads to a significant decrease in the transverse ME coefficient. In the case of the longitudinal effect, the value of the ME coefficient is higher for pre-polarized structures obtained without exposure to a magnetic field, and lower for polarized preforms metallized in a magnetic field. The use of a magnetic field in the preparation of structures made it possible to halve the magnetolectric hysteresis in the case of the longitudinal effect.

Is lead really a prototypical type I superconductor? New results on the phase diagram at ultra-low temperatures

Wulf Wulfhchel^{1,2}, Thomas Gozliniski¹, Qili Li¹, Rolf Heid², Jörg Schmalian²

¹Physikalisches Institut, KIT, Germany

²Institute for Quantum Materials and Technologies, KIT, Germany

wulf.wulfhchel@kit.edu

Superconductors are classified by their behavior in a magnetic field into type I, which transitions from a superconducting Meissner to a normal metallic state at the critical field [1] and type II, which have an additional Shubnikov phase of an Abrikosov lattice consisting of magnetic vortices with one magnetic flux quantum, each [2]. For type I superconductors of finite lateral dimensions, the transition to the normal state is, however, known to occur locally in form of domains in the so-called intermediate Landau state [3]. Basis for this classification are thermodynamic considerations near the critical temperature and a single band description of superconductivity.

Although bulk lead (Pb) is classified as a prototypical type I superconductor, we surprisingly observe single and multi-flux quanta vortices in the intermediate state at temperatures far below the critical temperature using a 25 mK scanning tunneling microscope hand in hand with a complex superconducting behaviour of the two distinct Fermi surfaces of Pb. The vortices have a diameter of at least 100 nm, growing in size with the number of confined flux quanta. By probing the quasiparticle local density of states (LDOS) inside the vortices and comparison with quasi-classical simulations based on DFT band-structure calculations, we identify the Caroli-de-Gennes-Matricon states [4] of the two superconducting bands of Pb and are consequently able to determine their winding number.

Finally, we investigate how stacking fault pyramids near the Pb surface selectively act as confining boxes for Cooper pairs on the two Fermi surfaces.

This study shines a light at the complexity of multiband superconductors forcing to rethink established models of seemingly simple type I superconductors.

The financial funding from DFG (Project Wu 349/14-1) is gratefully acknowledged.

[1] V. L. Ginzburg, L. D. Landau, Zh. Eksp. Teor. Fiz. 20, 1064 (1950).

[2] A. A. Abrikosov, Sov. Phys. JETP 5, 1174 (1957).

[3] L. D. Landau, Zh. Eksp. Teor. Fiz. 7, 371 (1937).

[4] C. Caroli, P. G. De Gennes, J. Matricon, Phys. Lett. 9, 307 (1964).

Tailored High T_c Superconductor Materials for Power and Magnet Applications

Bernhard Holzapfel

Institute for Technical Physics, Karlsruhe Institute of Technology, Karlsruhe, Germany

bernhard.holzapfel@kit.edu

High field magnet applications like MRI, NMR and accelerator magnets are one of the major success stories of superconductivity and only possible by tailoring superconducting materials on various length scales. Besides the conventional low temperature superconductors, cuprate based High Temperature Superconductors (HTSC) and new superconducting materials will open completely new opportunities in modern magnet/power applications and are currently on the way into commercial products. In this talk I will discuss and review firstly the basics and current status of superconducting material and wire development as well as the realization of HTSC based applications like high power urban transmission lines, H₂-based electric aircrafts and high field magnets beyond 30T. Secondly I will address the main basic requirements for new superconducting materials with potential applicability and discuss the prospects of the new Fe-based superconductors for power and magnet applications based on single crystalline thin film electrical transport properties in magnetic fields.

Emergent phases in geometrically-frustrated lattices

Ming Yi

Rice University, United States of America

mingyi@rice.edu

Emergent phases often appear when the electronic kinetic energy is small compared to the Coulomb interactions. One approach to seek material systems as hosts of such emergent phases is to realize localization of electronic wavefunctions due to the geometric frustration inherent in the crystal structure, resulting in flat electronic bands. Recently, such efforts have found a wide range of exotic phases in the two-dimensional (2D) kagome lattice, including magnetic order, time-reversal symmetry breaking charge density wave (CDW), nematicity, and superconductivity. For the first part of the talk, I will present experimental evidence for the coexistence and intertwinement of magnetic order and charge density wave in the kagome FeGe system—the only kagome system so far found to exhibit both orders simultaneously. For the second part of the talk, I will present experimental realization of three-dimensional flat bands and Dirac cones found in a pyrochlore superconductor, where geometric frustration appears along all three crystal axes.

Magnetic features in nanocrystalline CoMnFeNiGa high entropy alloys: from bulk materials to nanoparticles

N.F. Shkodich¹, V. Nallathambi^{1,2}, S. Reichenberger¹, M. Farle¹

¹Faculty of Physics and Center of Nanointegration (CENIDE), University of Duisburg-Essen, 47057 Duisburg, Germany

²Max-Planck-Institut für Eisenforschung Max-Planck-Straße 1, 40237 Düsseldorf, Germany
natalia.shkodich@uni-due.de

The concept of high-entropy alloys (HEAs) introduces a fundamentally novel strategy for exploring unknown regions in multicomponent phase diagrams and opens ways to new materials [1, 2]. Most of research in HEAs is focused on a macroscale materials, and the studies on nanoscale properties have been limited. Exploiting features of nano-crystallinity may add another exciting aspect to the huge compositional space of HEAs for further development and improvement of their functional properties [3].

In our present study, we report the successful fabrication of three types of CoMnFeNiGa high entropy alloys: a) nanocrystalline metallic bulk, b) nanocrystalline micron-sized powder and c) nanoparticles.

Homogeneous micron-sized CoMnFeNiGa HEA powders with a nanocrystalline structure and compositional homogeneity were produced by high energy ball milling (HEBM) for 190 min in Ar at 900/1800 rpm. From these powders we synthesised (a) a homogeneous nanocrystalline bulk HEAs by Spark plasma sintering (SPS), and (b) HEA nanoparticles – by laser fragmentation (LF).

The XRD, SEM/EDX, and TEM results showed that the single *fcc* phase consisting of nanosized grains (~10 nm) obtained after 190 min of HEBM partially transforms into a *bcc* one after SPS at 973K. After laser fragmentation of the starting powder two morphologies, that is spheres and platelets (thickness 5.7 ± 1.4 nm, lengths $40 \div 80$ nm) with *fcc*, *bcc* and hexagonal structures, were observed in TEM.

Annealing up to 1000K of HEBM and LF HEA particles led to significant structural and composition changes and increased the saturation magnetization M_s (300K) by 171.5% (Fig. 1a) and by 44.3% (Fig. 1b) respectively.

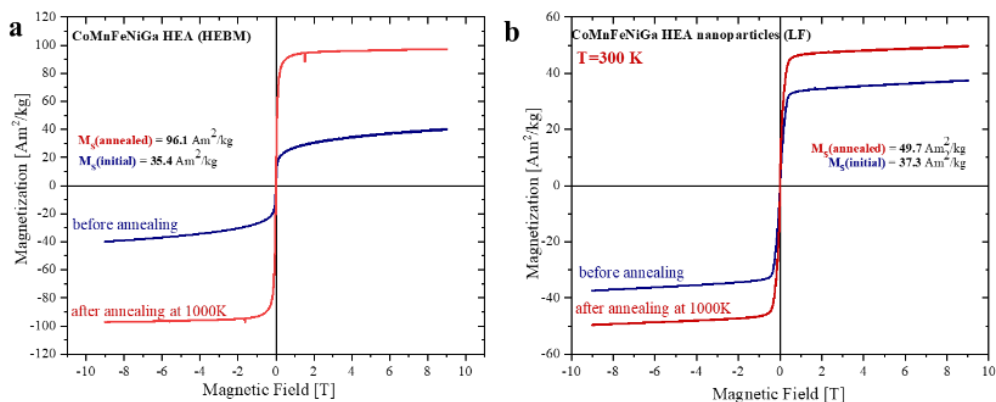


Figure 1. (a) Field dependence of magnetization recorded before annealing (blue) at 300 K and after annealing (red) at 300 K (a) for HEBM CoMnFeNiGa HEAs and (b) for LF CoMnFeNiGa HEA nanoparticles.

Two paramagnetic ordering temperatures in the temperature range of 800K–900K were observed for HEBM and LF HEA particles.



This work has been supported by the Deutsche Forschungsgemeinschaft (DFG) within CRC/TRR 270, project S01 (project ID 405553726).

- [1] Yeh, J.-W. et al., Adv. Eng. Mater., 6, 299 (2004).
- [2] Cantor et al., Mater. Sci. Eng. A 213 (2004).
- [3] D.B. Miracle et al., Acta Mater. 122, 448 (2017).

FCC-BCC phase transition and magnetism in MnFeCoNiCu_{20-x}A_x (A: Al, Ga) high-entropy alloys

Yaşar Orbay¹, Aslı Çakır¹, Tolga Tavşanoğlu¹, Mehmet Acet², Michael Farle²

¹Department of Metallurgical and Materials Engineering, Muğla University, 48000, Muğla, Turkey

²Fakultät für Physik and CENIDE, Universität Duisburg-Essen, Forsthausweg 2, 47057 Duisburg,
Germany

asli.cakir@uni-due.de

High entropy alloys (HEAs) containing five or more major elements with nearly equiatomic composition are receiving interest due to favorable mechanical and physical properties [1,2]. These alloys mostly form in solid solution FCC, BCC and HCP phases as a result of the high configurational entropy [3,4]. In this work, we investigate the FCC-BCC transition in MnFeCoNiCu_{20-x}A_x (A: Al, Ga) HEAs. X-ray diffraction, energy dispersive x-ray spectroscopy, magnetization, and microhardness measurements were performed on these systems. The equiatomic MnFeCoNiCu alloy is FCC and ferromagnetic with a Curie temperature, T_C , close to room temperature. However, the BCC structure emerges with increasing amount of Al (5 at%) and Ga (20 at%) with additional ferromagnetic interactions and associated T_C s.

- [1] B. Cantor et al., Mater. Sci. Eng. A. 375–377: 213–218 (2004).
- [2] J. W. Yeh et al., Adv. Eng. Mater., 6(5), 299-303 (2004).
- [3] Z. Lei et al., Nature 563, 546–550 (2018).
- [4] Y. Zhang. et al., Sci. Rep., 3:1455 (2013).

Emergence of magnetic moments in the high anisotropy antiferromagnets NiMn and PdMn

Nicolas Josten^{1,*}, Olga Miroshkina¹, Sakia Noorzayee¹, Benjamin Zingsem¹, Aslı Çakır², Mehmet Acet¹, Ulf Wiedwald¹, Markus Gruner¹, and Michael Farle¹

¹Faculty of Physics and Center for Nanointegration (CENIDE), University Duisburg Essen, Duisburg, 47057, Germany

²Department of Metallurgical and Materials Engineering, Mugla University, 48000 Mugla, Turkey
Nicolas.Josten@uni-due.de

Near-equiatomic L1₀ NiMn and PdMn are antiferromagnets with strong magnetic anisotropy. Annealing these compounds, with a slight excess of Ni or Pd (<5%), at around 650K in a magnetic field, results in the emergence of strongly pinned magnetic moments. This effect is observed as a vertical shift in the field-dependent magnetization, as shown in Fig. 1. The effect is caused by magnetically driven diffusional ordering of excess Ni (or Pd) atoms on Mn-sites [1]. Based on our experiments, we discuss a phenomenological model to explain the magnetically driven diffusion of excess atoms. The results are corroborated by *ab initio* calculations. The model accurately describes the effect of annealing-temperature, -duration and magnetic field strength.

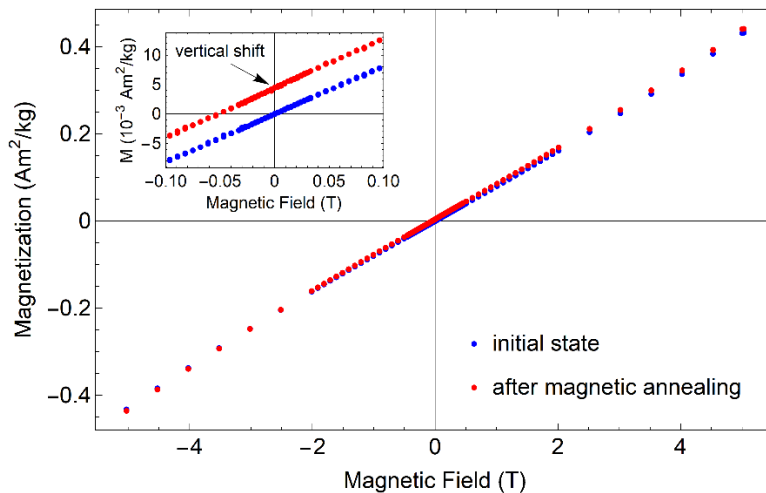


Figure 1. Magnetization vs magnetic field of Ni_{51.6}Mn_{48.4} at 300 K before and after magnetic annealing for 6h at 650K and 5T, leading to a vertical shift of the magnetization curve. The inset magnifies the data around zero field.

Funded by the Deutsche Forschungsgemeinschaft (DFG, German Research Foundation) – Project-ID 405553726 – TRR 270.

[1] L. Pál et al., Phys. Stat. Sol. 42, 49-59 (1970).

Magnetic-field-biased diffusion during temper-annealing in nearly equiatomic Ni-Mn alloys

Sakia Noorzayee^{1*}, Nicolas Josten¹, Aslı Çakır², Inci Nur Sahin¹, Mehmet Acet¹, Michael Farle¹

Sakia.Noorzayee@stud.uni-due.de

¹Faculty of Physics and Center for Nanointegration (CENIDE), Duisburg-Essen University, Duisburg, D-47057, Germany

²Department of Metallurgical and Materials Engineering, Muğla University, Muğla, 48000, Turkey

Ni₅₀Mn₅₀ is an intermetallic compound featuring a martensitic transformation from a low-temperature tetragonal L1₀ phase to a high-temperature cubic B2 phase at about 950 K [1]. Starting from the equiatomic composition and moving towards Ni-rich compositions, the *c/a* ratio of the L1₀ phase decreases and becomes 1 at about 56 at% Ni, at which the FCC phase is stabilized. In the L1₀ phase, Ni₅₀Mn₅₀ is a collinear antiferromagnet with strong magneto-crystalline anisotropy. Being so, it is widely used as the pinning layer-element in multilayer films constructed for exchange-bias purposes. Also, it has always attracted interest for its magnetic properties. A property of particular interest is the case when Ni₅₀Mn₅₀ is annealed for several hours in an external magnetic field *B* at about 700 K, a subsequent *M(B)*-measurement reveals a vertically shifted hysteresis loop. The vertical shift is only obtained with a magnetic field present during the heat treatment. This feature was first discovered by Pál et al. in 1970 [2]. They explained this phenomenon by considering the occurrence of strongly pinned excess Ni atoms in nearly-equiatomic Ni-Mn samples. In such a picture, the system should experience a bias in the diffusion process by the external magnetic-field during annealing. If this hypothesis holds true, no vertical shift would be expected for Ni-deficient Ni-Mn alloys, and the magnitude of the vertical shift would directly depend on the Ni-concentration. Here, we present an investigation on magnetic-field-biased diffusion in Ni-Mn with compositions varying between 44.7 and 57.2 at% Ni. We study this effect by examining the properties of the vertically shifted *M(B)*-loops and the compositional development of the lattice structures from the L1₀ to the FCC phase.

Funded by the Deutsche Forschungsgemeinschaft (DFG, German Research Foundation) – Project-ID 405553726 – TRR 270.

[1] L. Ding et al., Appl. Phys. Lett. 80, 1186 (2002).

[2] L. Pál et al., Phys. Stat. Sol. 42, 49-59 (1970).

Precise temperature control of exchange bias fields in graded ferromagnetic multilayers

Mikel Quintana, Adrián Meléndez, Carmen Martín Valderrama, Lorenzo Fallarino, Andreas Berger

CIC nanoGUNE BRTA, E-20018 Donostia, San Sebastián, Spain.

m.quintana@nanogune.eu

Thin films, in which the exchange energy is designed to be depth-dependent have arisen as an interesting tool to control properties of ferromagnets that are otherwise extremely difficult to modify [1,2]. It is known that such exchange-graded films behave at each depth as if their magnetic properties depend only on a ‘local’ Curie temperature T_C^{loc} , down to the 1-2 nm length-scale. This specific feature allows us to design structures exhibiting ferromagnetic exchange everywhere, but whose magnetic behavior can split into seemingly isolated ferromagnetic (FM) regions in certain T-ranges. This phenomenon can be particularly useful in magnetic multilayers, if such exchange-graded films are used as spacer layers.

In this work, we present a novel multilayer sequence composed of two CoRu thin films, separated by an exchange-graded $\text{Co}_{1-x(z)}\text{Ru}_{x(z)}$ spacer layer, in which the Ru concentration x is varied along the depth z of the film. Our particular design is such that the effective paramagnetic (PM) phase thickness in the spacer layer increases with T . This phenomenon results in a strong temperature-dependent interaction between the FM regions [3].

A detailed magnetometry analysis of our films allowed us to quantify the magnitude of the temperature-dependent bias fields, as well as the effective interlayer exchange coupling, which we managed to monitor over a temperature range of 75 K. We fabricate films with different thicknesses of the spacer layer and thus exchange gradients, and we observe that for thicker effective PM phases, the interaction between FM layers decreases monotonously.

Our particular design can be employed at any given temperature by means of $T_C^{\text{loc}}(z)$ design and it is generally applicable to any given FM material. Furthermore, the design of the temperature dependent bias fields could be interesting for technological applications. For example, we observed we can obtain temperature independent coercive fields over wide temperature ranges, which can be extremely useful for stable operation points as well.

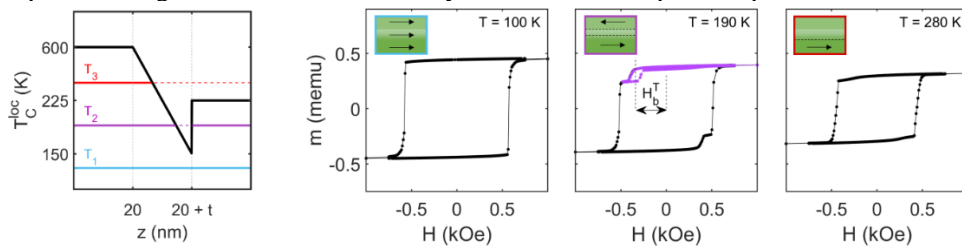


Figure 1. Schematic of the $T_C^{\text{loc}}(z)$ profile in our films and examples of three hysteresis loops at three different temperatures for a thin film with $t = 20$ nm.

Our work was supported by the Spanish Ministry of Science and Innovation under the Maria de Maeztu Units of Excellence Programme (Grant No. CEX2020-001038-M) and Project No. RTI2018-094881-B-100 (MCIU/Feder), and by Predoctoral Fellowship No. PRE2019-088428. C. M. V. acknowledges the Basque Government for fellowship No. PRE_2021_1_0056.

[1] L. Fallarino, E. López Rojo, M. Quintana, J. S. Salcedo Gallo, B. J. Kirby, & A. Berger, *Phys. Rev. Lett.* **127**, 147201 (2021).

[2] L. Fallarino, M. Quintana, E. López Rojo, & A. Berger, *Phys. Rev. Appl.* **16**, 034038 (2021).

[3] M. Quintana, A. Meléndez, C. Martín Valderrama, L. Fallarino, & A. Berger, submitted to *Phys. Rev. Appl.* (2022).

Atomic-scale insights to design of high-performing SmCo based sintered permanent magnets gained by atom probe tomography

Nikita Polin^{1,*}, Stefan Giron², Esmaeil Adabifiroozjaei², Yangyiwei Yang², Alaukik Saxena¹, Bai-Xiang Xu², Leopoldo Molina-Luna², Oliver Gutfleisch², Konstantin Skokov², Baptiste Gault^{1,3}

¹Max-Planck-Institut für Eisenforschung GmbH, Düsseldorf, Germany

n.polin@mpie.de

²Institute of Materials Science, Technische Universität Darmstadt, Germany

³Department of Materials, Royal School of Mines, Imperial College, Prince Consort Road, London SW7 2BP, United Kingdom

Hard disc drives, electric cars and wind turbines - in all these devices permanent magnets are key components to translate mechanical into electrical energy and vice versa. Enhancing performance of permanent magnets thus contributes to energy transition and sustainability. However, practically the performance of permanent magnets only reaches 20% of the possible maximum (called Brown's paradox). This is related to imperfect nanostructure and nanocomposition where atom probe tomography is a suitable tool to gain atomic-scale insights.

In this talk I will present a structural and magnetical investigation of high-end production-grade $\text{Sm}_2(\text{Co,Fe,Cu,Zr})_{17}$ permanent magnets which show unusual regions leading to suboptimal performance (Fig. 1, left). Local differences of nano-structure and nano-composition between both regions (Fig.1) are studied by atom probe tomography and transmission electron microscopy combined with micromagnetic simulations based on the experimental results. Based on these findings, design rules for higher performance of $\text{Sm}_2(\text{Co,Fe,Cu,Zr})_{17}$ magnets are proposed.

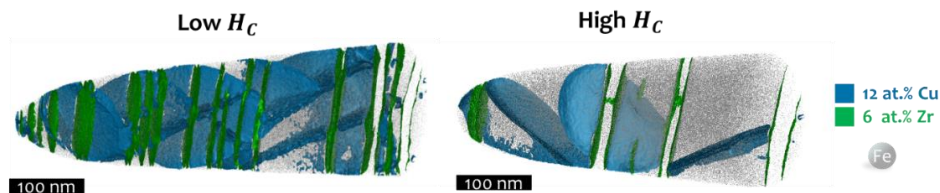


Figure 1. 3D reconstruction of APT data for the areas of low coercivity (left) and high coercivity observed in high-end production-grade $\text{Sm}_2(\text{Co,Fe,Cu,Zr})_{17}$.

The financial funding from IMPRS SusMet, DFG, CRC/TRR 270 and ERC is gratefully acknowledged.

Semisynthetic Magnetic Nanoparticles for Remote Actuation of Biological Processes

A. Neusch¹, D. Kuckla¹, I. Novoselova¹, C. Vicario², D. Lisse², J.-S. Brand¹,
M. Farle³, U. Wiedwald³, M. Dahan² and C. Monzel^{1,*}

¹Heinrich-Heine-Universität Düsseldorf, Düsseldorf, Germany

²Physico-Chimie, Institut Curie, Paris, France

³University of Duisburg-Essen, Duisburg, Germany

Cornelia.Monzel@hhu.de

Remote actuation of biological processes is of central interest for many biological, biotechnological or biomedical applications. However, only few tools are hitherto capable of providing a tunable stimulus with nano-scale precision. Superparamagnetic Nanoparticles demonstrated to meet this demand, as their magnetic properties allow for (i) their spatial displacement, (ii) to mediate mechanical forces, or (iii) to heat their environment in a contract-free manner while being positioned at distinct sites. Here, we introduce a semisynthetic magnetic nanoparticle (sMNP) based on the natural iron storage protein ferritin. We genetically modified the protein shell to provide biocompatibility as well as to target the sMNP to specific molecules. We further synthesize a magnetic core into the protein cage and characterize the sMNP properties with electron microscopy, magnetometry, dynamic light scattering and surface Zeta potential. We then show how sMNP in comparison to other superparamagnetic nanoparticles can be used to apply stimuli (i)-(iii) as well as to target and modify cell signal formation. This work is supported by Volkswagen Foundation (Grant Nr.: 94195).

[1] D. Lisse, et al. *Advanced Materials* (2017), 29, 1700189 DOI: 10.1002/adma.201700189

[2] L. Toraille, et al. *Nano Letters* (2018), 18, 7635-41 DOI: 10.1021/acs.nanolett.8b03222

[3] I. Novoselova, et al. *Nanomaterials* (2021) 11, 2267 DOI: 10.3390/nano11092267

Iron-biomineralizing encapsulin proteins as a new tool for the non-invasive tracking and manipulation of mammalian cells

Mariia Efremova^{1,2,3}, Anna N. Gavashvili^{4,5}, Felix Sigmund^{1,2}, Silviu-Vasile Bodea^{1,2}, Stepan S. Vodopyanov^{4,6}, Alevtina S. Semkina^{7,8}, Irina Beer⁹, Thomas Feggeler¹⁰, Hendrik Ohldag¹⁰, Ralf Meckenstock¹¹, Natalia P. Ivleva⁹, Maxim A. Abakumov^{4,7}, Ulf Wiedwald¹¹, Gil G. Westmeyer^{1,2}

¹Department of Chemistry & TUM School of Medicine, Technical University of Munich, Germany

²Institute for Synthetic Biomedicine, Helmholtz Zentrum München, Germany

³Department of Applied Physics, Eindhoven University of Technology, Netherlands

m.efremova@tue.nl

⁴Laboratory “Biomedical Nanomaterials”, National University of Science and Technology “MISIS”, Russia

⁵Biomedical Technology Department, National Medical Research Center for Hematology, Russia

⁶Biology Faculty, Lomonosov Moscow State University, 119234 Moscow, Russia

⁷Department of Medical Nanobiotechnology, Pirogov Russian National Research Medical University, Moscow, Russia

⁸Department of Basic and Applied Neurobiology, Serbsky National Medical Research Center for Psychiatry and Narcology, 119991 Moscow, Russia

⁹Institute of Hydrochemistry, Technical University of Munich, 85748 Garching, Germany

¹⁰Advanced Light Source, Lawrence Berkeley National Laboratory, Berkeley CA 94720, United States

¹¹Faculty of Physics and CENIDE, University of Duisburg-Essen, 47048 Duisburg, Germany

Proteinaceous nanoreactors called encapsulins naturally occurring in bacteria *Quasibacillus thermotolerans* can be expressed in human embryonic kidney HEK293T cells, as well as in human hepatocellular carcinoma HepG2 cells, and murine mammary carcinoma 4T1 cells [1,2,3,4,5]. These encapsulins represent a two-component system of a nanoshell and a ferroxidase cargo, enabling the biomineralization of up to 60000 iron atoms inside the nanocompartment. Encapsulin expression in the above-mentioned cells, together with their cultivation in a Fe-rich medium, did not affect cell viability and proliferation (in the case of carcinoma lines). *In vitro* MRI study showed a decrease in T2 relaxation time for all transfected cells compared to wild-type controls. We believe this to be an essential step towards the future *in vivo* MRI tracking of malignant cells. However, it should be better understood in terms of the physical properties of Fe-containing encapsulin nanoparticles, which we investigated in HEK293T cells isolated via magnet-assisted cell sorting. Transmission Electron Microscopy and Energy Dispersive X-Ray Spectroscopy revealed that each sorted cell contained thousands of 30±3 nm-sized iron oxide nanoparticles. Synchrotron radiation-assisted X-Ray Absorption Spectroscopy and Raman microspectroscopy pointed toward Fe₂O₃ stoichiometry of the nanoparticles. Vibrating Sample Magnetometry and Ferromagnetic Resonance measurement proved the ferrimagnetic response of the sorted cells at 5-250K, which corresponds to the ≈ 25% of maghemite-like (γ-Fe₂O₃) phase in the total Fe cell content. Finally, we demonstrated that the sorted HEK293T cells could be manipulated by magnetic gradient fields, making encapsulins a modern tool for the magnetism-driven actuation and imaging of mammalian cells.

We acknowledge the support of an Alexander von Humboldt Research Fellowship for Postdoctoral Researchers, an Add-on Fellowship for Interdisciplinary Life Science by the Joachim Herz Foundation (M.E.), as well as RSF grants number 19-45-06302/ 21-75-00096 and the Helmholtz-RSF Joint Research Group (HRSF0064).

[1] F. Sigmund, S. Pettinger, M. Kube et al., ACS Nano 13(7), 8114–8123 (2019).

[2] M.V. Efremova, S.-V. Bodea, F. Sigmund et al., Pharmaceutics 13(3), 397 (2021).

[3] A.N. Gavashvili, S.S. Vodopyanov, N.S. Chmelyuk et al., Int. J. Mol. Sci. 22(22), 12275 (2021).

[4] A.N. Gavashvili, M.V. Efremova, S.S. Vodopyanov et al., Nanomaterials 12(10), 1657 (2022).

[5] M.V. Efremova et al., in preparation.

Microwave-assisted large-scale synthesis approach for Fe₃O₄ nanoparticles

Konstantinos Simeonidis^{1,2}, Theopoula Asimakidou¹, Maria del Puerto Morales³, Sabino Veintemillas-Verdaguer³

¹Department of Chemical Engineering, Aristotle University of Thessaloniki, 54124 Thessaloniki, Greece

ksime@physics.auth.gr

²Ecoresources P.C., Giannitson-Santaroza Str. 15-17, 54627 Thessaloniki, Greece

³Instituto de Ciencia de Materiales de Madrid, CSIC, Sor Juana Inés de la Cruz 3, Cantoblanco, 28049 Madrid, Spain

In spite of the growing demand of magnetic nanoparticles for developing applications, not much effort has been devoted to transfer laboratory knowledge into large-scale production schemes. Continuous processes are always preferred over batch ones when reproducible and scalable industrial procedures are needed. For instance, the production of magnetite nanoparticles by oxidative precipitation of FeSO₄ in aqueous media has been demonstrated by a continuous approach that offers (i) the complete separation of the green rust's precipitation from Fe₃O₄ nucleation, (ii) constant concentrations in all ionic and solid forms, and (iii) the possibility to control critical parameters, through on-line regulation of synthesis parameters such as the reactor's pH [1]. However, this process requires a long ageing period of at least 4 h during which reaction mixture remains in a heated bath (90 °C). This step appears to have significant impact in the total energy consumption while the high residence time implies to the need for larger facilities. To overcome such issues, a different setup which introduces a microwave heating step was designed. Here, the ageing reactor (CSTR) was placed into a microwave oven and continuously fed with the green rust precursor. Following this scheme, Fe₃O₄ nanoparticles with diameter around 30 nm were successfully produced by applying a residence period of less than 10 min in a polyacetal tank. Surprisingly, by using a plug-flow reactor (PFR), a very high heating rate was succeeded and well-defined magnetic nanoparticles were received with a residence period of less than 30 s. The suggested setup provides an automatable solution for onsite nanoparticle synthesis in the biomedical sector by non-specialized staff.

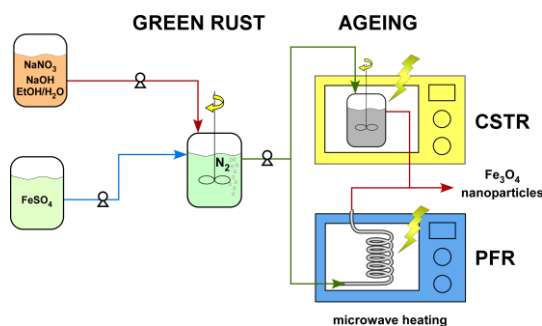


Figure 1. Microwave-assisted setup for continuous flow oxidative precipitation.

Research is funded by the IMAGINE: Implementing MAgnetic targeting of nano-Guided ImmuNE cells project funded by European Science Foundation Fight Kids Cancer 2020 programme. The research project was supported by the Hellenic Foundation for Research and Innovation (H.F.R.I.) under the “2nd Call for H.F.R.I. Research Projects to support Post-Doctoral Researchers” (Project Number: 00046 MagnoSorb).

[1] T. Asimakidou et al., Chemical Engineering Journal 393, 124593 (2020).

Versatile magnetic filament fabrication: A novel pathway for 3D printed biomagnetic scaffolds

A. Makridis¹, N. Okkalidis², M. Angelakeris¹

¹Magnetic Nanostructure Characterization: Technology and Applications (MagnaCharta) Center for Interdisciplinary Research and Innovation (CIRI-AUTH) 57001 Thessaloniki, Greece

anmakrid@physics.auth.gr

²Morphé, Praxitelous 1, Thessaloniki, 54641, Greece

3D printing technology has proven as a promising innovation for manufactured scaffolds with high accuracy and precision, revealing unique itemized biomimetic 3D designs. Fabricating magnetic scaffolds by using additive processes, such as 3D printing, opens a multitude of state-of-the-art areas of application like bone repair and regeneration, tissue engineering, drug delivery and magnetic hyperthermia. Developing polymeric composite magnetic materials is the crucial, innovative, first step that must be examined.

In this work, a 3D printed polymer-bonded magnets' fabrication protocol (Fig. 1), by using the Fused Deposition Modeling (FDM) method, is established. Composites with permanent-magnet powder embedded in a polymer binder matrix can be defined as Polymer-bonded magnets. A low-cost and ecological friendly mixing extruder (Fig. 1c) was used to mix commercial magnetite magnetic nanoparticles with PLA (PolyLactic Acid) powder (Fig. 1b), a typical thermoplastic material used as 3D printing filament. The powder mixture is compounded and extruded to fabricate the 3D printing filament (Fig. 1d) of different nanoparticle amounts (10 and 20 wt %) which is subsequently characterized structurally (Fig. 1e) and magnetically (Fig. 1f) before the printing process.

Finally, magnetic scaffolds are successfully printed and evaluated in magnetic hyperthermia. The promising heating results that this work presents, can be also compared with other studies [1], [2], where MNPs are mixed with types of PLA material to produce MBSS to use them as candidates for magnetic hyperthermia application.

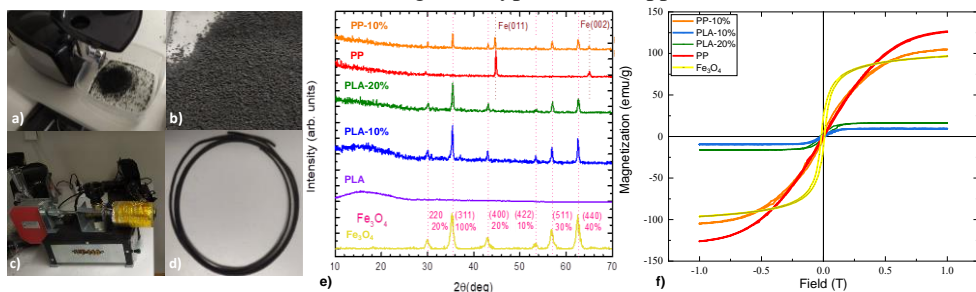


Figure 1. Main process for the filament extraction: a) After cutting PLA filament to pieces, a grinder is used to make PLA granules. The b) mixed material is used for feed stock of c) the single screw extruder to produce d) the resulted magnetic filament. (e) X-ray diffraction patterns of fabricated magnetic filaments. PLA and PP (ProtoPasta) filaments are also shown as reference. (f) 300 K hysteresis measurements of the fabricated magnetic filaments.

PP hysteresis loops is also given as reference.

[1] M. Bañobre-López et al., IEEE Transactions on Magnetics 50.11 (2014).

[2] A. Farzin et al., Materials Science and Engineering: C 70 (2017).

Magnetically driven therapies: Toxicity, Risks and Side-effects

Makis Angelakeris

School of Physics, Faculty of Sciences, Aristotle University, 54124 Thessaloniki, Greece
MagnaCharta, Center for Interdisciplinary Research and Innovation (CIRI-AUTH), 57001
Thessaloniki, Greece
angelaker@auth.gr

Magnetically driven therapies have a long and substantial history including diverse and combinatory aspects of diagnosis and therapy. Initially, magnetic field driven treatments involved, magnetic field application to deliver an energy form to tissues, resulting in a physiological change or stimulation, which can in turn be used to generate specific effects. Subsequently, magnetic materials came into play of magnetically driven therapies with to promote the therapy's efficiency. In modern theranostics, magnetic nanoparticles may act as multifunctional carriers delivering specific "cargo" under the guidance of an external magnetic field. For example, magnetic nanoparticles may play a contrast agent role in Magnetic Resonance Imaging while at the same time deliver either a heat load (hyperthermia agents) and/or mechanical stress at specific malignant sites. Thus, by adequate combination of magnetic particle features and magnetic field parameters, optimized performance may be achieved, while side-effects should also be considered and circumvented.

Although, magnetic fields are generally regarded as least invasive schemes when discussing side effects and potential risks, a field of controversy in scientific community is the role of Eddy currents. Eddy currents are a direct consequence of the link between magnetism and electricity and are in practice loops of electrical current induced by a time varying magnetic field according to Faraday's law of induction. Their magnitude is proportional to the strength of the magnetic field, the area of the loop, and the rate of change of flux, and inversely proportional to the resistivity of the material. Eddy currents are a cause of energy loss since their flow dissipates heat in their surroundings. Accordingly, typical parameters relating to magnetically driven treatments are a) the strength of the applied magnetic field needed to achieve the therapeutic benefit or adequate resolution, issues not yet fully resolved, hence making clinical decision remarkably problematic b) the treatment duration, ranging from a few minutes to some months providing very different energy 'doses' to the patient, certainly not comparable - even if the same energy is delivered. Eventually, the energy delivery must occur in such a way as to drop in the optimal window by fine tuning field strength (amplitude, intensity), pulsing (frequency) and treatment time, while attenuating potential field application side effects. The optimal bio and clinical effects may be achieved with this combined optimal dose combination with respect to the features of magnetic nanoparticles implemented, keeping in mind that the further one moves away from this optimal position, the less effective the intervention. I will examine case studies of Magnetic resonance imaging, Magnetic Particle Hyperthermia. I will unravel the parameters affecting treatment efficiency and what is hindering their performance. I will see alternative magnetic field application schemes and specific nanoparticle agents features that will ensure therapeutic efficiency together with mitigation of side effects and risk factors and toxicity.

This work was supported by European Union's Horizon 2020 research and innovation programme under grant agreement No 857502 (MaNaCa).

Development of Fe₃O₄-decorated Sn-hydroxide nanocomposites for advanced Cr(VI) capture in drinking water

Kyriaki Kalaitzidou, Christos Pantos, Theopoula Asimakidou, Nikolaos Maniotis, Fani Pinakidou, Konstantinos Simeonidis

Department of Chemical Engineering, Aristotle University of Thessaloniki, 54124 Thessaloniki, Greece

kalaitzidou@cheng.auth.gr

The objective of this work was to develop a novel class of water treatment adsorbents based on magnetically responding iron oxide (Fe₃O₄) nanoparticles and bivalent tin oxyhydroxides (abhurite) known for their potential to capture hexavalent forms of pollutants by a reducing/precipitation mechanism [1]. Such system was engineered in the nanoscale but realized in kilogram-scale production rates by the translation of nanoscale synthesis methods for nanoparticles into sequential continuous-flow reaction processes. Particularly, 30 nm magnetite nanoparticles synthesized by the oxidative precipitation process were combined with spherical layered formations of abhurite to obtain a homogeneous nanocomposite (Figure 1), featured with improved properties toward Cr(VI) uptake at concentrations complying with drinking water demands as well as with sufficient magnetization which enable the separation of the solid at the end of the purification procedure. The continuous flow production setup was optimized to allow the complete neutralization of the two phases before their mixture with a high-energy homogenizer.

Materials characterization and evaluation of nanocomposite's efficiency indicated a high reducing potential which established a good performance to capture aqueous Cr(VI) forms through their transformation into insoluble Cr(III) species deposited on the adsorbent's surface. Multiphysics analysis of the magnetic separation procedure supported by micromagnetic simulations of the nanocomposite assisted the design, construction and operation of a rotary separator with optimum placement of permanent magnets.

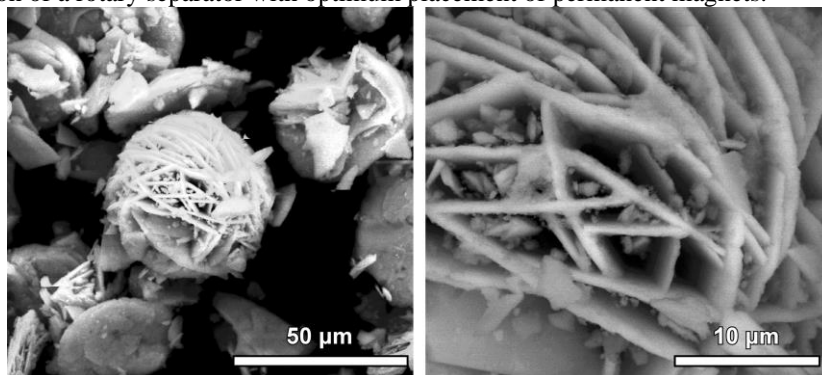


Figure 1. SEM images of Fe₃O₄-decorated Sn-hydroxide nanocomposites with magnetic nanoparticles placed in the layered structure of abhurite.

The research project was supported by the Hellenic Foundation for Research and Innovation (H.F.R.I.) under the “2nd Call for H.F.R.I. Research Projects to support Post-Doctoral Researchers” (Project Number: 00046 MagnoSorb).

[1] G. Papadopoulos et al., Water 11, 2477 (2019).

Hybrid Stents based on magnetic hydrogels for biomedical applications

Eirini Myrovali

School of Physics, Aristotle University of Thessaloniki, Thessaloniki, 54124, Greece

emiroval@physics.auth.gr

Magnetic Nanostructure Characterization: Technology and Applications, CIRI-AUTH, 57001 Thessaloniki, Greece

Hydrogels are crosslinked hydrophilic polymers with high-water content. Such formulation has received significant attention due to their mechanical and physical properties. Recently, magnetic hydrogels, i.e., hydrogels incorporating magnetic nanoparticles, have been proposed in biomedical applications due to facile and tunable response to externally applied magnetic fields. In this study, a prototype hybrid stent of magnetic hydrogel was fabricated, characterized, and evaluated for magnetic hyperthermia treatment. Firstly, magnetic hydrogel was produced by a solution of alginate with magnetic nanoparticles in a bath of calcium chloride (5 - 15 mg/mL) in order to achieve the external gelation and optimize the heating rate (Figure 1a). After that, magnetic hybrid stents were developed in a simple way using a plastic tube (Figure 1b-c) and were evaluated both in an agarose phantom model (Figure 1d) and in an ex-vivo tissue sample (Figure 1e) at 30 mT, 765 kHz magnetic hyperthermia conditions to examine the heating efficiency (Figure 1f). In both cases, hyperthermia results indicate excellent heat generation from the hybrid stent and facile temperature control via tuning magnetic nanoparticle concentration (2 – 8 mg/mL). Almost zero leakage of iron oxide nanoparticles was detected after hyperthermia treatment (0, 5 and 15 days) confirming the sustainability for biomedical applications. Thus, this study can be a promising method that promotes spatially thermal distribution in cancer treatment or restenosis treatment of hollow organs.

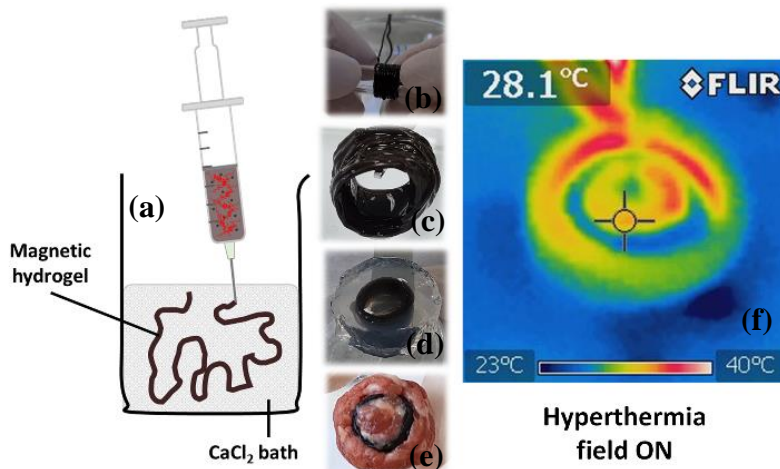


Figure 1: (a) Schematic illustration of the magnetic hydrogel using a syringe in a bath of calcium chloride. (b) Development of magnetic hybrid stent using a plastic tube. (c) Magnetic hybrid stent. (d) Agarose phantom model and (e) ex-vivo model using the hybrid magnetic stent. (f) Thermal distribution of the magnetic hybrid stent during the hyperthermia measurement. [1]

[1] E. Myrovali, ACS Appl. Bio Mater, (2022) DOI: 10.1021/acsabm.2c00088.

Magnetic heating properties of Fe-Fe₃C nanoparticles prepared by method of ferrocene pyrolysis

Narek Sisakyan^{1*}, Milan Tsompanoglou², Gayane Chilingaryan¹, Harutyun Gyulasaryan¹, Elisavet Papadopoulou³, Nicolaos Tetos³, Vardges Avagyan¹, Marina Spasova³, Michael Farle³, Makis Angelakeris², Aram Manukyan¹

¹Institute for Physical Research of National Academy of Sciences, Armenia

sisakyan@gmail.com

²Physics Department, Aristotle University of Thessaloniki, Greece

³Faculty of Physics and Center of Nanointegration (CENIDE), University of Duisburg-Essen, Germany

Magnetic nanomaterials have a great potential in the field of biomedicine due to their unique magnetic properties, which makes them a suitable candidate for diagnosis and therapeutic applications. Iron based magnetic nanoparticles with a core-shell architecture offers controllable and tunable magnetic properties and due to their low toxicity are efficient candidates in magnetic fluid hyperthermia of cancer cells. For advanced biomedical applications, it is important that the nanoparticles are also be coated with biocompatible functional ligands.

In this work, carbon coated Fe-Fe₃C magnetic nanoparticles were synthesized by a solid-phase pyrolysis of ferrocene (FeC₁₀H₁₀). The pyrolysis process was performed in a closed quartz tube at 5 min with temperatures 700-1000 °C. Obviously, by changing the pyrolysis temperature, it is possible to control the Fe:Fe₃C concentration ratio in metal nanoparticles and improve the magnetic and magnetic heating properties of the nanocomposites.

To study the dependence of the heating efficiency on the pyrolysis temperature of the synthesized samples, aqueous solutions were prepared with a 6.5 mg/ml concentration and subjected to an alternating magnetic field with parameters of 375 kHz/60 mT. The maximum SLP (Specific Loss Power) of 260 W / g was obtained in a sample prepared at 800 °C (Fig. 1).

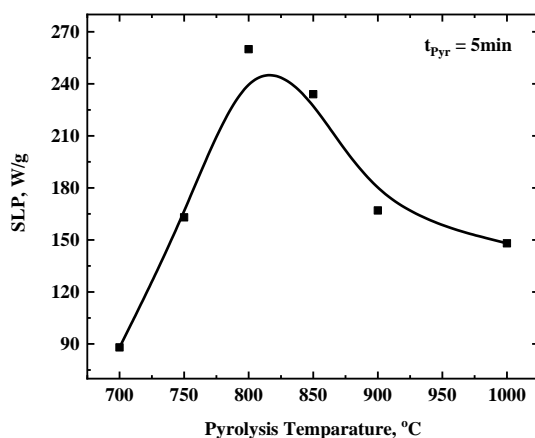


Figure 1. The values of SLP of synthesized (Fe-Fe₃C)/C nanocomposites dependence of pyrolysis temperature.

This work was supported by European Union's Horizon 2020 research and innovation programme under grant agreement No 857502 (MaNaCa).

Multiorbital perspective on correlated electrons in superconducting nickelates

Frank Lechermann

Institut für Theoretische Physik III, Ruhr-Universität Bochum, D-44801 Bochum, Germany

Frank.Lechermann@rub.de

The discovery of superconductivity in Sr-doped thin films of infinite-layer NdNiO₂ in summer 2019 [1] triggered an overwhelming research interest in these materials. Recently, similar superconductivity has also been detected in multi-layer systems of low-valence nickelates [2].

Because of their similarity to high-T_c cuprates concerning structure and formal 3d⁹ oxidation state, the long sought-after stable 'cuprate-akin' pairing in nickelates had apparently been found.

However, several striking differences to cuprate physics are revealed and already basic electronic structure features of superconducting nickelates are still a matter of intense debate.

In this talk I will show that latest developments in the first-principles approach to correlated materials are necessary to face the challenges of these fascinating systems. The case for manifest multiorbital Ni-eg physics to explain the various normal-state electronic regimes with doping will be made [3]. Additionally, the tight competition between different superconducting instabilities will be discussed [4].

[1] D. Li, et al., Nature 572, 624 (2019).

[2] G. A. Pan et al., Nat. Mater. 21, 160 (2022).

[3] F. Lechermann, PRX 10, 041002 (2020).

[4] A. Kreisel et al., arXiv:2202.11135 (2022).

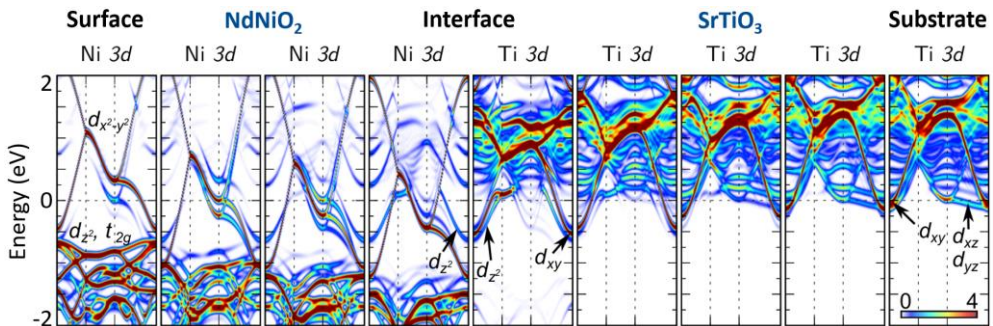
Role of the film geometry in the electronic reconstruction of infinite-layer nickelates on SrTiO₃(001)

Benjamin Geisler and Rossitza Pentcheva

Department of Physics and Center for Nanointegration (CENIDE), University of Duisburg-Essen, Lotharstraße 1, 47057 Duisburg, Germany
benjamin.geisler@uni-due.de

The recent discovery of superconductivity in infinite-layer NdNiO₂ films on SrTiO₃(001) has sparked significant interest [1]. However, details of the physical mechanism behind this observation remained so far elusive, since in contrast to the thin films [2] bulk NdNiO₂ shows neither superconductivity nor the antiferromagnetic interactions characteristic of high-*T_C* cuprates.

First-principles simulations unravel the key role of the interface: Polarity mismatch drives a surprising electronic reconstruction that results in the emergence of a correlated two-dimensional electron gas (2DEG) in the SrTiO₃(001) substrate. The concomitant depletion of the self-doping Nd 5*d* states renders infinite-layer nickelates close to cuprate superconductors [3,4]. Recent work identifies an unexpected interface composition that completely quenches the 2DEG, but preserves the electronic reconstruction in the nickelate film [5]. This supports the notion of nickelate superconductivity as novel quantum phase, induced in film geometry by electronic reconstruction.



This work was supported by the DFG within the SFB/TRR 80 (Projektnummer 107745057), Project No. G3. Computing time was granted by the Center for Computational Sciences and Simulation of the University of Duisburg-Essen (DFG Grants No. INST 20876/209-1 FUGG and No. INST20876/243-1 FUGG).

- [1] D. Li et al., Nature **572**, 624 (2019)
- [2] H. Lu et al., Science **373**, 213 (2021)
- [3] B. Geisler and R. Pentcheva, Phys. Rev. B **102**, 020502(R) (2020)
- [4] B. Geisler and R. Pentcheva, Phys. Rev. Research **3**, 013261 (2021)
- [5] B. H. Goodge, B. Geisler, K. Lee, M. Osada, B. Y. Wang, D. Li, H. Y. Hwang, R. Pentcheva, and L. F. Kourkoutis, arXiv:2201.03613 [cond-mat.supr-con]

Oxygen and Rare Earth Doping Effects on $\text{RE}_3\text{Ba}_5\text{Cu}_8\text{O}_{19-\delta}$ (RE=Y, Sm) Superconductors

Mohammad Sandoghchi¹, Mohammad Akhavan^{1,2,*}

¹Magnet Research Laboratory (MRL), Sharif University of Technology, Tehran, Iran

²Iran Academy of Sciences, Iran

m.akhavan1@gmail.com

There are two challenging issues with the physical properties of the recently reported cuprate $\text{Y}_3\text{Ba}_5\text{Cu}_8\text{O}_{19-\delta}$ (Y358) [1]: The value of its transition temperature (T_c), and its unknown crystal structure [2]. While some reports argue that T_c of Y358 and its crystal structure are completely different from those of the $\text{YBa}_2\text{Cu}_3\text{O}_{7-\delta'}$ (Y123) compound, some other reports indicate the similarity of both transition temperatures and XRD patterns (or crystal structure) of these materials. It has been suggested that these similarities are due to the oxygen deficiency (δ) of $\text{Y}_3\text{Ba}_5\text{Cu}_8\text{O}_{19-\delta}$ or the decomposition of Y358 to Y123.

Our results indicate that the oxygen deficiency ($\delta < 0.5$ or 2.6%) cannot explain the existence of the $\sim 10\text{K}$ difference in the reported T_c 's for the Y358 compound (prepared by the standard solid-state reaction or the sol-gel methods) in the literature. To investigate the similarities of the XRD patterns of Y358 and Y123 compounds, we have studied the analogous $\text{Sm}_3\text{Ba}_5\text{Cu}_8\text{O}_{19-\delta}$ (Sm358) compound. Since the difference in crystal radius of Ba and Sm are less than that of Ba and Y, it is possible to prepare $\text{Sm}_{1+x}\text{Ba}_{2-x}\text{Cu}_3\text{O}_{7+\delta}$ solid solutions which also includes the Sm358 compound. Therefore, the similarities of XRD patterns for Sm358 and Sm123 compounds can be understood on the basis of the $\text{Sm}_{1+x}\text{Ba}_{2-x}\text{Cu}_3\text{O}_{7+\delta}$ formula. Since the obtained transition temperatures for the Sm358 and Sm123 compounds are similar ($\sim 93\text{K}$), we have investigated the effects of doping on the transition temperature of the Sm358 compound by preparing the $\text{Sm}_{3+x}\text{Ba}_{5-x}\text{Cu}_8\text{O}_{19-\delta}$ and $\text{Sm}_{3-x-y}\text{Pr}_x\text{Ca}_y\text{Ba}_5\text{Cu}_8\text{O}_{19-\delta}$ compounds. The Sm substitution for Ba, or Pr and Ca substitution for Sm, indirectly changes the oxygen content and T_c of the Sm358 compound. The changes of T_c have been discussed based on the Abrikosov-Gorkov pair-breaking theory, hole-filling due to the extra valence of Pr ions, and the creation of holes by Ca ions. It seems that the behavior of T_c upon Pr and Ca doping is due to some collective mechanisms. Also, applying the Abrikosov-Gorkov pair-breaking and hole-filling theories, results a $T_c(x,y)$ equation for the $\text{Sm}_{3-x-y}\text{Pr}_x\text{Ca}_y\text{Ba}_5\text{Cu}_8\text{O}_{19-\delta}$ system for $x > 0.3$, which predicates the highest transition temperature of $\text{Sm}_{3-x-y}\text{Pr}_x\text{Ca}_y\text{Ba}_5\text{Cu}_8\text{O}_{19-\delta}$ compound to be $\sim 95\text{K}$.

[1] A. Aliabadi, Y. Akhavan Farshchi, M. Akhavan, Phys. C Supercond. 469 (2009) 2012–2014.

[2] H. Khosroabadi, M. Rasti, M. Akhavan, Phys. C Supercond. Its Appl. 497 (2014) 84–88.

Chiral interlayer coupling in magnetic multilayers

Can Onur Avci

Institute of Materials Science of Barcelona (ICMAB-CSIC), Spain

cavci@icmab.es

The ability to engineer the coupling between magnetic layers is central to revealing emergent magnetic and electronic interactions at interfaces as well as to improving the functionality of magnetic sensors, nonvolatile memories, and logic gates. Recently, increasing attention has been devoted to the exchange coupling mediated by the Dzyaloshinskii-Moriya interaction (DMI) that favors the orthogonal alignment of neighboring spins in materials with spatial inversion asymmetry. The DMI was originally investigated in bulk systems such as α -Fe₂O₃ and the B20 compounds. However, recent works have shown that a strong DMI emerges at ferromagnet/nonmagnet (FM/NM) interfaces with broken inversion symmetry and strong spin-orbit coupling stabilizing chiral spin textures such as Néel domain walls and skyrmions. More recently, Monte Carlo calculations and experiments have shown that the DMI can also couple two FM layers through a spacer layer where the DMI promotes nontrivial three-dimensional spin textures with both intralayer and interlayer chirality. The interlayer coupling mediated by the DMI thus offers novel opportunities to tune the magnetic texture and functionality of magnetic multilayers.

In this work, we report on the occurrence of strong interlayer DMI between an in-plane magnetized Co layer and a perpendicularly magnetized TbFe layer through a Pt spacer. The DMI causes a chiral coupling that favors one-handed orthogonal magnetic configurations of Co and TbFe, which we reveal through Hall effect and magnetoresistance measurements. The DMI coupling mediated by Pt causes effective magnetic fields on either layer of up to 10–15 mT, which decrease monotonically with increasing Pt thickness. Ru, Ta, and Ti spacers mediate a significantly smaller coupling compared to Pt, highlighting the essential role of Pt in inducing the interlayer DMI. These results are relevant to understand and maximize the interlayer coupling induced by the DMI as well as to design spintronic devices with chiral spin textures.

- [1] Yang et al., *Nat. Rev. Phys.* 3, 328–343 (2021)
- [2] Vedmedenko et al., *Phys. Rev. Lett.* 122, 257202 (2019)
- [3] Fernandez-Pacheco et al., *Nat. Mater.* 18, 679 (2019)
- [4] Han et al., *Nat. Mater.* 18, 703 (2019)
- [5] Avci et al., *Phys. Rev. Lett.* 127, 167202 (2021).

Laser pump induced hysteresis loop inversion on EuO/Co bilayers

David Mönkebüscher¹, Paul Rosenberger^{1,2}, Umut Parlak¹, Roman Adam³, Claus M. Schneider³, Martina Müller², Mirko Cinchetti¹

¹Department of Physics, TU Dortmund University, Otto-Hahn Straße 4, 44227 Dortmund, Germany
umut.parlak@tu-dortmund.de

²Department of Physics, University of Konstanz, 78457 Konstanz, Germany

³Peter Grünberg Institut, Research Centre Jülich, 42425 Jülich, Germany

Europium monoxide (EuO) is one of the rarely-found ferromagnetic oxides with dielectric properties. Due to the unpaired 4f electrons, it exhibits a saturation magnetic moment of $7 \mu_B$. Owing to these interesting magnetic properties, EuO is considered to be an excellent spin-filter for many spintronic heterostructures. However, its relatively low Curie temperature ($T_C = 69$ K) limits the usage in applications at non-cryogenic temperatures. The coupling between EuO and Co layers was proposed as a factor that could increase T_C by a proximity effect. Our experimental results indicate the existence of more complicated phenomena emerging at the EuO/Co interface.

We synthesized EuO/Co heterostructures in a well-established all *in situ* procedure using a state-of-the-art oxide-MBE system [1, 2]. EuO films were grown on yttria-stabilized zirconia (YSZ) substrates in the so-called adsorption limited growth mode. Following the confirmation of the quality of the EuO films by RHEED, LEED and XPS, the Co overlayer was deposited using e-beam evaporation. Subsequently, the samples were capped with a protective MgO layer against oxidation for *ex situ* handling.

We measured the hysteresis curves as a function of temperature using magneto optical Kerr effect (MOKE) magnetometry. Static hysteresis curves revealed the dominant magnetic component at each temperature, and indicated the antiferromagnetic-like coupling between EuO and Co. We obtained time-resolved hysteresis curves using a pump-probe technique. A series of femtosecond laser pulses ($\lambda_{\text{pump}} = 800$ nm) pumped the sample at 1 kHz repetition rate, and another synchronized series of pulses ($\lambda_{\text{probe}} = 400$ nm) probed sample magnetization after a certain time delay.

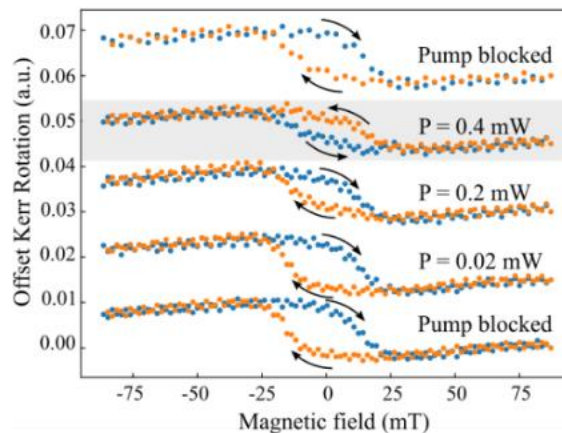


Figure 1. Magnetic hysteresis curves obtained using the longitudinal MOKE geometry at 5 K. The ground and final states (pump blocked) and pump induced magnetic states ($\Delta t = 6$ ps) are plotted from the bottom to the top.

The inverted hysteresis curves of EuO had already been reported in the literature about a decade ago [3]. In our experimental work, we studied the laser pump-induced hysteresis

curves below the Curie temperature of EuO. We report reversible and reproducible inversion of the hysteresis curves as a function of the laser pump power, which is attributed to the different demagnetization processes of Co and EuO layers.

The financial funding from TRR 160 project is gratefully acknowledged.

- [1] P. Rosenberger et al., Appl. Phys. Lett. 118, 192401 (2021).
- [2] P. Rosenberger and M. Müller, Phys. Rev. Materials 6, 044404 (2022).
- [3] P. Liu et al., J. Phys.: Condens. Matter 25, 125802 (2013).

Magnetic Spinel Ferrite Nanocomposites Engineered with MXene/Reduced Graphene Oxide for Electromagnetic Interference Shielding Application

Raghvendra Singh Yadav

Centre of Polymer Systems, University Institute, Tomas Bata University in Zlín, Trida Tomase Bati
5678, 760
yadav@utb.cz

A growth in electromagnetic radiation from the prompt developments of commercial electronic appliances has generated electromagnetic pollution [1]. The electromagnetic radiations emitted from numerous electronic appliances such as mobile phones, tablet PCs, wireless local area networks, scientific electronics, military, and defense equipment, home appliances, medical diagnostic equipment, etc. are responsible for malfunctions in electronic appliances and also raised human health concerns [2]. Electromagnetic interference (EMI) shielding is an important and proficient method to limit disruptive electromagnetic radiations [3]. Consequently, to overcome or diminish the impact of electromagnetic interference, good EMI shielding or microwave absorption materials are essential which have an effective ability to block the electromagnetic waves, as reported by me also in my authored book “Advanced Spinel Ferrite Nanocomposites for Electromagnetic Interference Shielding Applications”, published in Elsevier publishing [1]. The traditional electromagnetic shielding materials associated with single dielectric loss or magnetic loss features have delivered an insufficient electromagnetic shielding performance owing to the question of impedance mismatching [4]. One of the active methods to advance the performance of shielding material is to utilize spinel ferrite magnetic nanoparticles with reduced graphene oxide/MXene as impedance matching can be structured with the synergistic influence of magnetic and dielectric loss [5]. An ideal EMI shielding material should hold strong absorption features, low density, lightweight, design flexibility, thermal stability, etc. Thus, the development of nanocomposite consisting of polymer-magnetic and dielectric inorganic material with high magnetic and dielectric losses could be a better choice [6-8].

To attain this, the spinel ferrite magnetic nanoparticles were prepared by the sonochemical synthesis method /sol-gel auto-combustion method [9-15]. Further, these prepared magnetic spinel ferrite nanoparticles and reduced graphene oxide (rGO)/MXene were embedded in a polymer matrix by the melt-mixing method [2-8]. The coexistence of electric and magnetic dipoles in the prepared shielding nanocomposite can respond highly to electromagnetic waves and consequently, high electromagnetic loss. The highly efficient EMI shielding performance is attributed to the optimized impedance matching and attenuation constant, conductive, dielectric, and magnetic loss. The demonstrated nanocomposites accomplish significant key performance parameters including lightweight, flexibility, corrosion resistance, ease of processing, efficient utilization of energy, and low cost, which are requested in several important fields such as aerospace, aircraft, electronics, radars, flexible portable, and wearable electronic devices, military applications or stealth technology, and automotive, and so forth.

We thank the financial support of the Ministry of Education, Youth, and Sports of the Czech Republic - DKRVO (RP/CPS/2022/007).

- [1] R. S. Yadav, I. Kuritka, and J. Vilčáková, *Advanced Spinel Ferrite Nanocomposites for Electromagnetic Interference Shielding Applications*, Elsevier, Cambridge, MA, USA, 2020; ISBN 978-0-12-821291-2.
- [2] Anju, R. S. Yadav, P. Pötschke, et.al., *ACS Omega*, 6 (42) (2021) 28098-28118.
- [3] Anju, R. S. Yadav, P. Pötschke, et.al., *Int. J. Mol. Sci.* 23 (2022) 2610.

- [4] R. S. Yadav, Anju, T. Jamatia, et.al., *Nanomaterials*, 11 (2021) 1112.
- [5] R. S. Yadav, Anju, T. Jamatia, et.al., *Nanomaterials* 10 (2020) 2481.
- [6] R. S. Yadav, I. Kuřitka, J. Vilcakova, et.al., *ACS Omega*, 4 (26) (2019) 22069-22081.
- [7] R. S. Yadav, I. Kuřitka, J. Vilcakova, et.al., *Composites Part B* 166 (2019) 95-111.
- [8] R. S. Yadav, I. Kuritka, J. Vilcáková, et.al., *Nanomaterials* 9 (2019) 621.
- [9] R. S. Yadav, I. Kuřitka, J. Vilcakova, et.al., *Ultrasonics - Sonochemistry* 61 (2020) 104839.
- [10] R. S. Yadav, I. Kuřitka, J. Vilcakova, et.al., *Ultrasonics - Sonochemistry* 40 (2018) 773-783.
- [11] R. S. Yadav, I. Kuřitka, J. Vilcakova, et.al., *Journal of Magnetism and Magnetic Materials* 447 (2018) 48-57.
- [12] R. S. Yadav, J. Havlica, J. Masilko, et.al., *Journal of Magnetism and Magnetic Materials* 399 (2016) 109-117.
- [13] R. S. Yadav, J. Havlica, J. Masilko, et.al., *Journal of Magnetism and Magnetic Materials* 394 (2015) 439-447.
- [14] R. S. Yadav, J. Havlica, M. Hnatko, et.al., *Journal of Magnetism and Magnetic Materials* 378 (2015) 190-199.
- [15] R. S. Yadav, I. Kuřitka, J. Vilcakova, et.al., *Journal of Physics and Chemistry of Solids* 107 (2017) 150-161.

Magneto-optical Kerr effect (MOKE) measurements on magnetic nanofiber mats

Andrea Ehrmann¹, Tomasz Blachowicz^{2,3}

¹Faculty of Engineering and Mathematics, Bielefeld University of Applied Sciences, Bielefeld, Germany

andrea.ehrmann@fh-bielefeld.de

² Institute of Physics, Silesian University of Technology, Gliwice, Poland

The magneto-optical Kerr effect (MOKE) can be used to measure the magnetic hysteresis loop of a specimen optically. MOKE measurements are usually performed on highly even samples, such as thin-film samples, or regular nanostructure arrays. Only few approaches were reported yet to measure MOKE also on uneven surfaces [1].

Recently, we showed for the first time that MOKE measurements are also possible on electrospun nanofiber mats (Fig. 1) which were coated with a Co thin film [2]. A single MOKE measurement on a Co-coated nanofiber mat is depicted in Fig. 2.

Averaging over 10 or more hysteresis loop, it is possible to distinguish between different shapes of hysteresis loops on different spots of the sample [2]. These shapes can be interpreted as diffractive MOKE (D-MOKE) signals [3].

Here we give an overview of different MOKE signals, measured on magnetically coated nanofiber mats, in comparison with perfectly flat thin-film samples and slightly uneven magnetically coated polymer films. We present interpretations of the measured signals in correlation with simulated D-MOKE signals and show which conclusions can be drawn from the measured hysteresis loops on the sample topography.

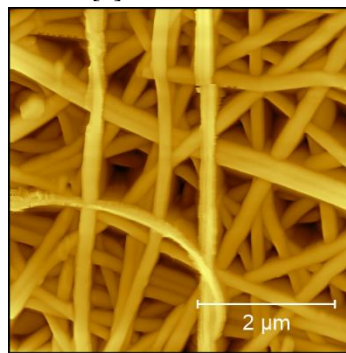


Figure 1. Atomic force microscopy (AFM) images of electrospun nanofiber mat.

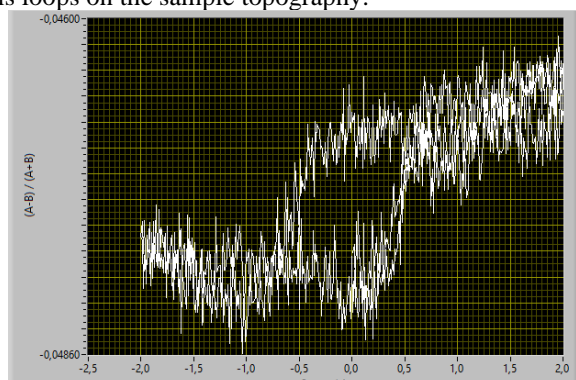


Figure 2. Single MOKE measurement on magnetic nanofiber mat.

This research was partly funded by the German Federal Ministry for Economic Affairs and Energy (grant no. KK5129710KT1).

[1] T. Blachowicz et al., AIP Adv. 7, 045306 (2017).

[2] O. Brocks et al., Appl. Phys. Lett., submitted (2022).

[3] T. Blachowicz and A. Ehrmann, Spintronics – Theory, Modelling, Devices, De Gruyter 2019

Switchable Wettability of Micro-structured Magnetoactive Elastomers

Raphael Kriegl^{1,*}, Gaia Kravanja², Luka Hribar², Lucija Čoga³, Mitjan Kalin³, Irena Drevenšek-Olenik⁴, Matija Jezeršek², Mikhail Shamonin¹

¹East Bavarian Centre for Intelligent Materials (EBACIM), Ostbayerische Technische Hochschule Regensburg

²Laboratory for Laser Techniques, Faculty of Mechanical Engineering, University of Ljubljana

³Laboratory of Tribology and Interface Nanotechnology, Faculty of Mechanical Engineering, University of Ljubljana

⁴Faculty of Mathematics and Physics, University of Ljubljana, and J. Stefan Institute, Ljubljana
raphael.kriegl@oth-regensburg.de

The control of wettability of magnetoactive elastomer (MAE) surfaces by magnetic fields is investigated. Newly developed fabrication methods allow one to fabricate two types of MAE surfaces: i) MAE films are cast on substrates with different roughness, which is transferred to the resulting surface. When a maximum magnetic field of ≈ 0.4 T is applied perpendicular to the MAE surface, an increase in the static contact angle (SCA) by $\approx 40^\circ$ is observed. Switching of wettability is probably caused by the transition from the Wenzel to the Cassie-Baxter regime. Higher initial roughness does not result in a significant increase in the SCA in the absence of magnetic field. In the highest field, differences between smooth and rough surfaces are observed. ii) Micro-lamellar and micro-pillared structures are fabricated on MAE surfaces by laser micromachining (Fig. 1).

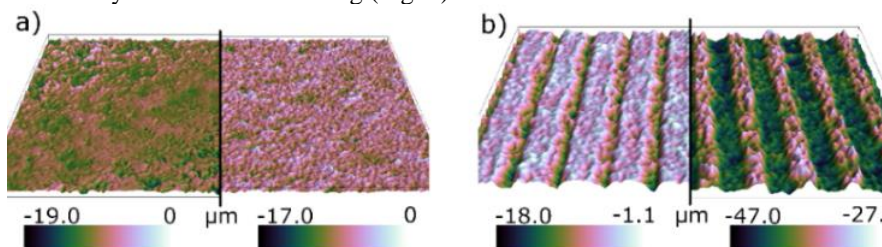


Figure 1. 3D optical profilometry of the cast (a) and structured (b) MAE surfaces in the absence (left image) and in the presence (right image, groove depth ≈ 15 μm , width = 50 μm , separation distance = 50 μm) of magnetic field ($B \approx 0.23$ T).

Above the critical magnetic field of ≈ 0.1 T, the SCA is significantly increased (Fig. 2). The field dependence of the SCA is dependent on the dimensions of structures and material stiffness.

The effects of magnetic field are investigated in detail using classical goniometry, 3D optical profilometry and rheological measurements. In general, the magnetic field causes significant changes in surface topography (Fig. 1), which are observable for both cast and laser-structured MAE surfaces.

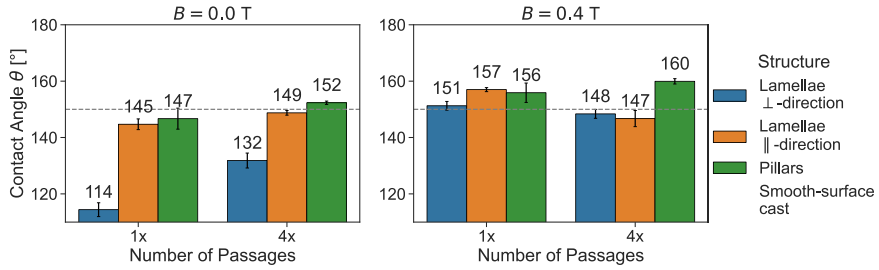
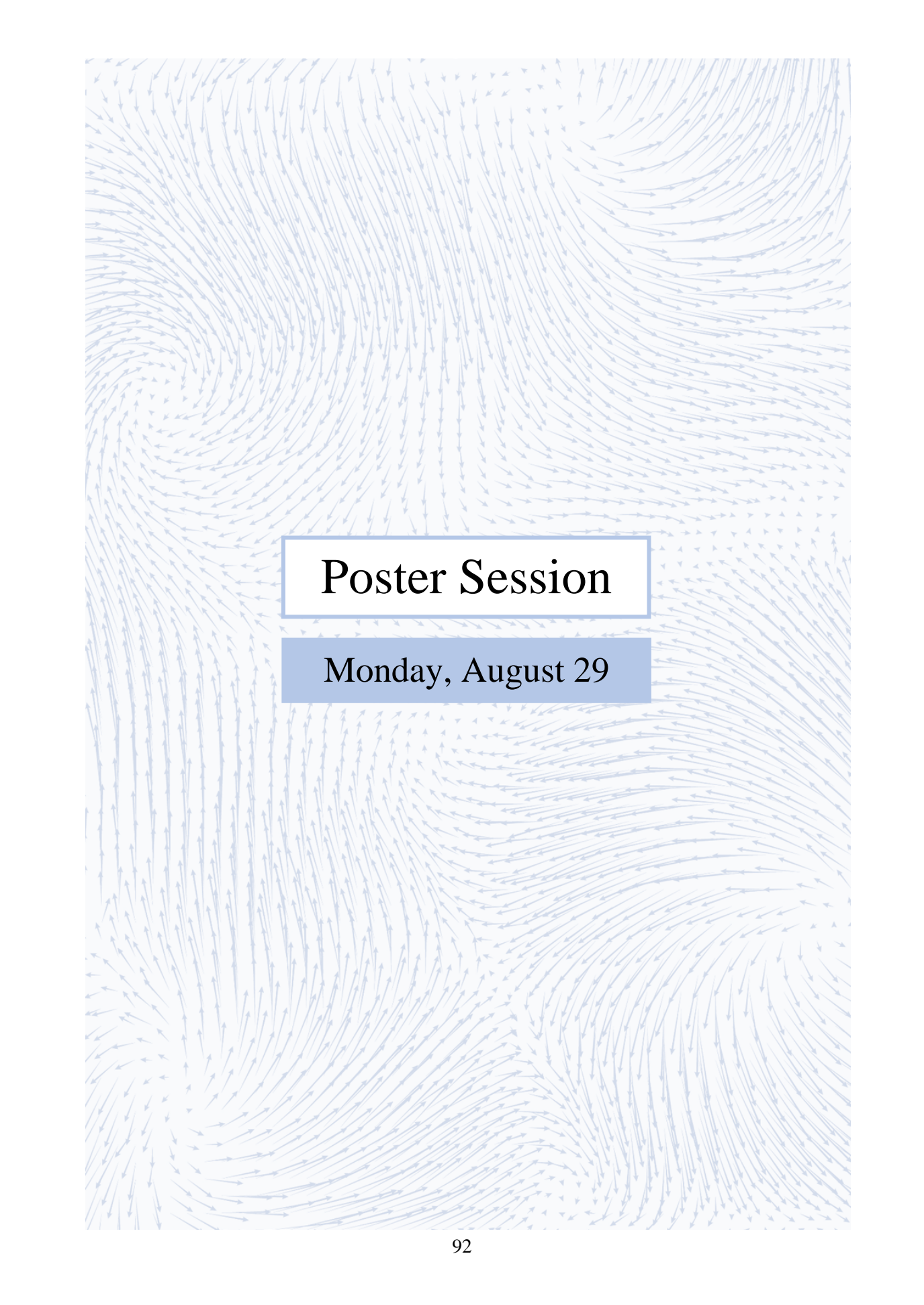


Figure 2. Measurements of SCA for laser-structured MAE surfaces with varying depth in the absence and in the presence of a magnetic field. A single structuring passage results into $\approx 15 \mu\text{m}$ of depth.

The financial funding from DFG (project no. 437391117) and ARRS (project no. J1-3006) is gratefully acknowledged.



Poster Session

Monday, August 29

Anomalous Hall Effect and Magnetoresistance in Ferromagnetic Topological Crystalline Insulator (111) $\text{Sn}_{1-x}\text{Mn}_x\text{Te}$ Epilayers

A. Kazakov¹, V.V. Volobuev¹, M. Zięba², B. Turowski¹, W. Zaleszczyk^{1,2}, T. Wojciechowski^{1,2}, K. Gas², M. Sawicki², T. Story^{1,2}, T. Dietl¹, T. Wojtowicz¹

¹International Research Centre MagTop, Institute of Physics, Polish Academy of Sciences, al. Lotników 32/46, 02-668 Warsaw, Poland

kazakov@magtop.ifpan.edu.pl

²Institute of Physics, Polish Academy of Sciences, al. Lotników 32/46, 02-668 Warsaw, Poland

The combination of long-range ferromagnetic (FM) ordering and topological insulator can lead to the dissipationless surface transport, i.e., quantum anomalous Hall effect. It has been previously shown that ferromagnetism can be induced in the prototypical topological crystalline insulator (TCI) SnTe by the hole-mediated RKKY interaction between Mn ions introduced into the lattice. An additional contribution to the Hall effect and magnetoresistance, the so-called anomalous Hall effect (AHE) and negative magnetoresistance (NMR) respectively, are commonly observed in many classes of magnetic materials. Both AHE and NMR are unique experimental tools in that they allow magnetic properties of a material to be characterized by transport technique. In the present work, a systematic study of the anomalous magnetic properties of $\text{Sn}_{1-x}\text{Mn}_x\text{Te}$ TCI epilayers as a function of Mn content x was performed using electronic transport method.

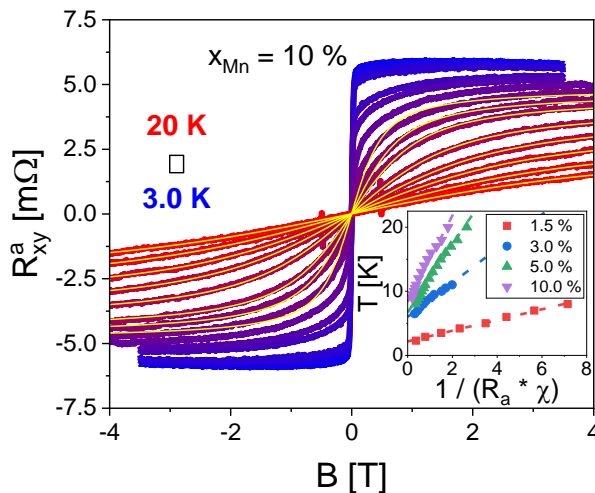


Figure 1. Anomalous Hall resistance R_{xy}^a in $\text{Sn}_{0.9}\text{Mn}_{0.1}\text{Te}$ as a function of the magnetic field B depicted with variable temperature (yellow lines are paramagnet magnetization fits). Inset depicts determination of the Curie temperature from plots of the inverse susceptibility (χ) multiplied by anomalous Hall constant (R_a).

High-quality $\text{Sn}_{1-x}\text{Mn}_x\text{Te}$ epilayers of 1 μm thickness, with x varying from 0 to 0.1, were grown on (111)-oriented BaF_2 substrates by molecular beam epitaxy. It is shown that an increase in Mn content causes an increase in both the longitudinal resistance R and in residual scattering, resulting in a weaker temperature dependence. This is confirmed by the determination of the residual resistivity ratio for the measured films, which decreases for films with higher Mn content. The ferromagnetic phase transition is well defined by the magnetotransport behavior at low temperatures (see Figure 1). Magnetotransport

characteristics systematically evolve with increasing Mn content, e.g., the negative magnetoresistance becomes more pronounced for higher Mn concentrations. Possible scenarios leading to such behavior will be discussed. An anomalous Hall effect was observed in all the Mn-containing layers studied. The high temperature Hall curves in the paramagnetic region were used to determine the Curie temperature (T_C) from plots of the inverse susceptibility (χ) multiplied by the anomalous Hall constant (R_a). Both T_C and AHE contribution to Hall resistance increase with increasing Mn content. It is also shown that T_C determined from magnetotransport measurements agrees well with the results of SQUID measurements. The obtained results can be further used for experimental verification of the magnetically induced time-reversal breaking in TCIs.

This research was partially supported by the Foundation for Polish Science through the IRA Programme co-financed by EU within SG OP (Grant No. MAB/2017/1) and by the NCN Grant: UMO 2017/27/B/ST3/02470

Feedback of non-local d_{xy} nematicity on the magnetic anisotropy in FeSe

Steffen Bötzel¹, Ilya M. Eremin¹

¹Institut für theoretische Physik III, Ruhr-Universität Bochum, Bochum, Germany
Steffen.Boetzel@ruhr-uni-bochum.de

Details of the nematic state in FeSe and its connection to superconductivity are still a matter of debate. There is a general believe about the existence of a xz/yz splitting in the nematic state, that can be represented by an order parameter $\Phi^{xz/yz} = \langle d_{xz}^\dagger d_{xz} - d_{yz}^\dagger d_{yz} \rangle$, which is positive near the Γ point and negative around the M point of the 1-Fe Brillouin Zone. The resulting electronic bandstructure is expected to display a large electron pocket with mixed xz and xy character additional to a small peanut shaped pocket with yz and xy character. However, only the latter is seen in the recent ARPES measurements, which has been tried to explain by including orbital-selective quasiparticle weights. Recently, an alternative scenario with additional non-local xy nematicity has been considered [1]. The inclusion of an order parameter $\Phi^{xy} = \langle d_{xy}^{X\dagger} d_{xy}^X - d_{xy}^{Y\dagger} d_{xy}^Y \rangle$ can shift the unwanted band away from the Fermi surface.

In our contribution we discuss the consequences of the non-local xy nematic scenario for the magnetic susceptibility considering spin and orbital contributions. In particular, the temperature dependence for the bulk susceptibility is calculated and compared to experiment [2], which is shown in Fig. 1. We find that within this scenario the spin susceptibility displays a drop below the nematic transition temperature $T_N = 90$ K and flattens towards a plateau below 60 K before decreasing again below the superconducting transition at about $T_C = 8$ K. The orbital susceptibility yields the correct in-plane anisotropy. [3]

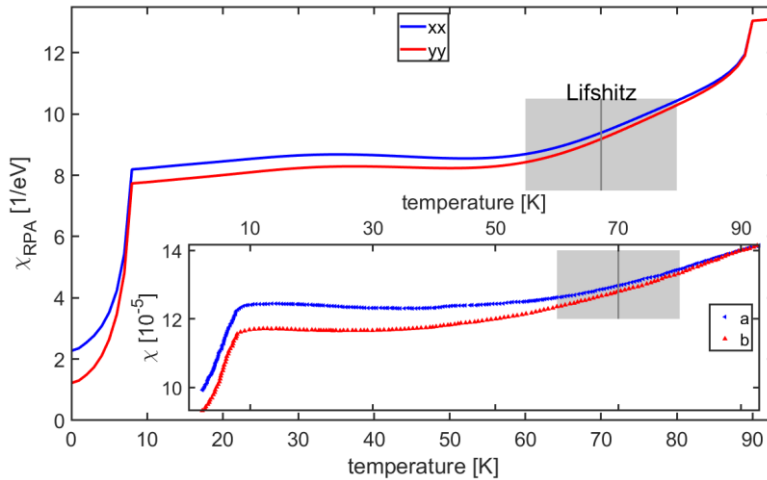


Figure 2. Calculated temperature dependence of the in-plane components of magnetic susceptibility $\chi(q \rightarrow 0)$. The experimental data extracted from [2] are shown for comparison in the inset.

- [1] L.C. Rhodes et al., npj Quantum Materials 6,45 (2021).
- [2] M. He et al., Phys. Rev. B 97,104107 (2018).
- [3] S. Bötzel, I.M. Eremin, arXiv:2205.07718v1 (2022).

Weak-Links on the MOD-prepared YBa₂Cu₃O₇ Thin Films

Mohammad Sandoghchi, Mahdi Torkashvand, Mohammad Reza Mohammadizadeh
 Superconductivity Research Laboratory (SRL), Department of Physics, University of Tehran, North Kargar Ave., P O Box 14395-547, Tehran, Iran
Msandoghchi64@gmail.com

Thin films of superconductors can be used in electronic devices such as microwave-filters, the Josephson Junctions (JJ), or superconducting quantum interference devices (SQUID). For these applications, the quality of the films is of great importance. High-quality epitaxial YBa₂Cu₃O₇ (YBCO) thin film can be prepared by the metal-organic chemical solution deposition (MOCSD or MOD) process [1]. In particular, the requisite high superconducting critical current density for weak links or Josephson junction is achievable in the MOD-prepared YBCO thin film. In the current study, we deposited the YBCO thin films on the SrTiO₃ (STO) substrate using the MOD process. Typically, the superconducting transition temperatures (T_c) of these films were higher than 90 K whereas their transition widths were less than 3 K (Fig. 1). Figure 2 presents a typical AFM image of these films. The average roughness and root mean square roughness of these films were about 40 nm and 50 nm, respectively.

Overall, these results indicated that the MOD-prepared films had good quality for the fabrication of weak links [2]. To fabricate a bridge-like weak link from these films, we exploit the standard wet photolithography processes. By optimizing these processes, several micro-constrictions of YBCO were fabricated. Although, the electrical resistances of these constrictions were higher than the pristine YBCO films, their transition temperatures changed slightly. Finally, the bridge-like weak links of YBCO were made by AFM lithography. It has been shown that when the width of these bridges become less than 1 μm , the current-voltage characteristic of them behave like a Josephson Junction.

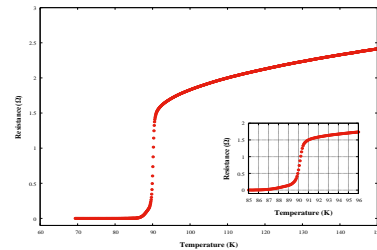


Figure 1. Typical Resistance vs. Temperature of the MOD-prepared YBa₂Cu₃O₇ thin film.

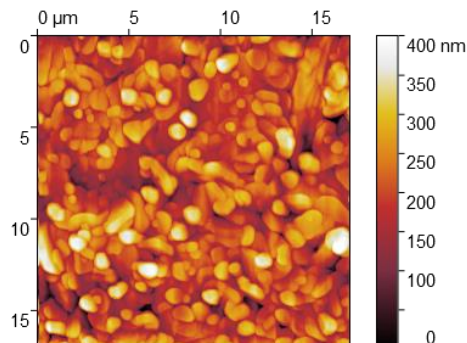


Figure 2. Typical AFM image of the MOD-prepared YBa₂Cu₃O₇ thin film.

[1] M. Rasti, M.R. Mohammadizadeh, IEEE Trans. Appl. Supercond. 30, 1 (2020).

[2] F. Tafuri, ed., Fundamentals and Frontiers of the Josephson Effect, Springer International Publishing, Cham, 2019.

The expected simulation on the structural phase of high- T_c superconductor compound $YBa_2Cu_{3-y}Pb_yO_{6.5+\delta}$

Emad K. Al-Shakarchi¹, Salwan K.J. Al-Ani², and Wedad M. Faysal³

¹Al-Nahrain University, College of Science, Physics Department, P.O. Box 64055, Baghdad, IRAQ

eks2000@hotmail.com

²Al-Mustansiriya University, College of Science, Physics Department, Baghdad, Iraq

salwan_kamal@yahoo.com

³Baghdad University, College of Science, Physics Department, Baghdad, Iraq

wmaha2004@yahoo.com

The aim of this work is to make a simulation on the possible change in a structural phase of superconducting compound $YBa_2Cu_{3-y}Pb_yO_{6.5+\delta}$ prepared by a solid-state reaction. The simulation had been taken into account by the XRD patterns for all phases represented by ($y=0-0.5$). Theoretically, the possible structural phase was derived from a pure phase $YBa_2Cu_3O_{6.5+\delta}$, which was an orthorhombic phase with lattice constants ($a=3.8203$, $b=3.8855$, and $c=11.6835$ Å) and space group Pmmm. The substitution ratio of Pb-ions in a structure made a partial variation in the orthorhombic unit cell of pure phase. The results showed the phase transition from orthorhombic to tetragonal phase at ($y=0.2, 0.3$). There is a limited variation in the lattice constant around the theoretical values with the orthorhombic phase. Principally, the Pb-atom has valency (+2), so the insertion of Pb-ions in the structure took the position of Cu^{+2} -ion as a substituted ion in the composition $YBa_2Cu_{3-y}Pb_yO_{6.5+\delta}$. There is a sharp increase in the lattice constants (b, c) at $y=0.4$ with the remaining of orthorhombic phase and space group Pmmm. This study is dealing with structure simulation and expected the position of atoms within the unit cell. This expectation gives us more details on the bonds nature between atoms and their effect on the conductivity behavior of 123-phases that appeared with and without Pb substitution. The results showed a linear relationship between the amount of substitution that was affected on the c -axis and oxygen excess (δ), it was organized by a certain equation.

Au-Fe₃O₄ nanohybrids: synthesis and characterization

Tatiana Smoliarova, Marina Spasova, Ulf Wiedwald and Michael Farle

Faculty of Physics, University of Duisburg-Essen, Duisburg, 47057, Germany

tatiana.smoliarova@uni-due.de

Over the years, magnetic nanoparticles have raised significant interest in many fields such as biological separation and protein purification [1], target delivery [2], therapy [3], biosensors [4], and catalysis [5]. Herein, we report on the facile room-temperature synthesis for Au-Fe₃O₄ nanohybrids preparation and their optical and magnetic properties investigation.

Au-Fe₃O₄ nanohybrids were synthesized by chemical precipitation and a chemisorption process of Au nanoparticles (NPs) on the Fe₃O₄ surface using polyvinylpyrrolidone (PVP) interface. Octahedral Fe₃O₄ NPs were prepared by mixing water solution of NaNO₃ and NaOH with 150 ml of 1:1 DI water and ethanol solution. Then, the water solution of Fe₃SO₄·7H₂O was mixed with 0.01 M H₂SO₄ solution, and the resulting mixture was added to the total solution. The resulting solution was left for 2 h at T = 90-95 °C and cooled to room temperature. The resulting NPs were separated from the solution by magnetic decantation and washed by centrifugation for 5 min (3000 rpm). Au NPs were prepared according to the procedure described in [6] and finally were attached to the PVP-covered Fe₃O₄ surface. Some results of transmission electron microscopy (TEM) and size distribution analysis are presented in Fig. 1 (a, b, c, d, e). Absorbance spectra of Au, Fe₃O₄, and Au-Fe₃O₄ NPs are shown in Fig. 1 (f). Au NPs (red line) have the typical behavior with the plasmon peak at 520 nm. In comparison with the absorbance spectrum of Fe₃O₄ NPs (black line), the spectrum for Au-Fe₃O₄ NPs (green line) demonstrates the presence of the light plasmon peak at 536 nm, which is an impact of attached Au NPs.

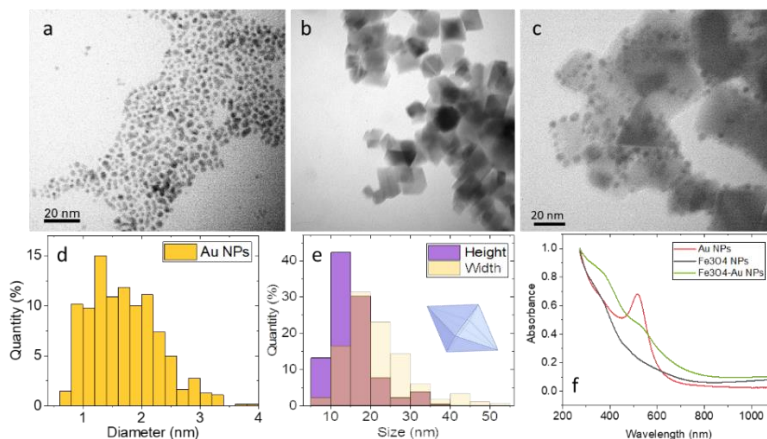


Figure 1. TEM images of synthesized (a) Au and (b) Fe₃O₄ NPs and (c) Au-Fe₃O₄ nanohybrids; size distributions of (d) and (e) Fe₃O₄ NPs; (f) absorbance spectra of the synthesized NPs.

We acknowledge AG Lorke, Faculty of Physics, University of Duisburg-Essen for kindly provided access to UV-vis spectrometer for absorbance spectra measurements. This work was supported by European Union's Horizon 2020 research and innovation program under grant agreement No 857502 (MaNaCa).

- [1] Bao J. et al., ACS nano 1, 14 (2007).
- [2] Xu C. et al., Journal of the American Chemical Society 131, 12 (2009).
- [3] Li C. et al., Advanced functional materials 24, 12 (2014).
- [4] Zhang W. et al., Scientific reports 5, 1 (2019)
- [5] Cui X. et al., Separation and Purification Technology 5, 1 (2021).
- [6] Brown K. R. et al., Chemistry of Materials 12, 2 (2000).

Tuning synthesis of Fe₃O₄ nanoparticles for maximum Cr(VI) uptake from polluted water

Theopoula Asimakidou, Kyriaki Kalaitzidou, Nikolaos Maniotis, Zografina Tsiggenopoulou, Evangelia Chioti, Konstantinos Simeonidis, Manassis Mitrakas

Department of Chemical Engineering, Aristotle University of Thessaloniki, 54124 Thessaloniki, Greece

tasimaki@physics.auth.gr

Water treatment research has justified the potential of Fe₃O₄ nanoparticles to function as a promising hexavalent chromium removal adsorbent initiating a reduction mechanism into insoluble species. This study evaluates the Cr(VI) uptake efficiency of Fe₃O₄ nanoparticles when prepared via the oxidative precipitation of FeSO₄ by nitrates in a water/ethanol solution, focusing on the role of synthesis pH in the surface configuration and the adsorption mechanism. The impact of hydroxyl excess as defined by the Fe(II)/hydroxide ratio during synthesis was found to be a critical parameter able to determine the chemistry, the crystal structure, the aggregation extent and the magnetic response of the nanoparticles.

Batch adsorption tests were carried out under similar conditions with drinking water purification to evaluate Cr(VI) removal. Results indicate that near the zero-excess point for hydroxyl balance, the uptake capacity for residual Cr(VI) concentration equal to regulation limit (25 µg/L) remains at very low levels (Figure 1). However, a small increase above +0.02 M features synthesized nanoparticles with an uptake capacity of 2.5 mg/g owed to the decrease in particles size (28 nm) and enhancement of the reducing potential (Fe²⁺/Fe³⁺=0.42). In addition, utilizing negative excess values below -0.05 M triggers a similar efficiency rise, although the morphology of the obtained aggregates is rather different. Such finding is attributed to a possible exchange mechanism between adsorbed sulfates and chromate anions that assist approach of Cr(VI) to the materials surface. Importantly, the high magnetic response of the samples appears as another significant advantage toward the facile post-use magnetic separation of nanoparticles which supports the implementation in drinking water purification.

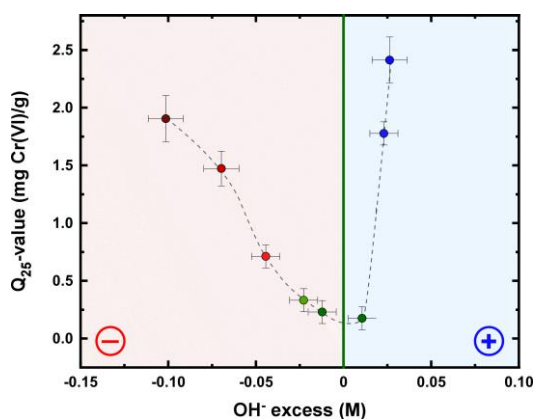


Figure 1. Correlation of uptake capacity for residual Cr(VI) concentration 25 µg/L with the hydroxyl excess used in the Fe₃O₄ nanoparticle synthesis.

The research project was supported by the Hellenic Foundation for Research and Innovation (H.F.R.I.) under the “2nd Call for H.F.R.I. Research Projects to support Post-Doctoral Researchers” (Project Number: 00046 MagnoSorb).

[1] K. Kalaitzidou et al., Water 14, 1335 (2022).

Correlation of magnetism with magnetic particle hyperthermia efficiency in iron/cementite nanohybrids

Milan Tsompanoglou^{1,2}, Harutyun Gyulasaryan³, Gayane Chilingaryan³, Narek Sisakyan³, Haris Sarafidis^{1,2}, Makis Angelakeris^{1,2} and Aram Manukyan³

¹School of Physics, Faculty of Sciences, Aristotle University, 54124 Thessaloniki, Greece
mtsompan@physics.auth.gr

²MagnaCharta, Center for Interdisciplinary Research and Innovation (CIRI-AUTH), 57001 Thessaloniki, Greece

³Institute for Physical Research of National Academy of Sciences, Ashtarak, Armenia

Cementite (Fe₃C) is a hard and brittle iron/carbon compound with well-established, wide range of applications due to its properties, abundance, and low cost. Fe₃C structure has a primitive lattice type crystallizing in an orthorhombic system. At stoichiometric state, cementite is ferromagnetic with a Curie temperature of ~186 °C. In the recent decades, research is conducted for the development of magnetic compounds in the nanoscale and their potential exploitation in biomedical applications such as magnetic particle hyperthermia [1]. This is an alternative anticancer technique effectively stressing malignant cells through a heating protocol, thus achieving cellular apoptosis or a higher susceptibility to other treatments i.e., chemotherapy or radiotherapy minimizing side effects.

In this work, magnetic nanohybrids composed of iron, cementite and amorphous carbon phases are evaluated as potential magnetic particle hyperthermia agents. Synthesis occurred with a single step, solid phase pyrolysis of iron based organometallic compound [2] obtaining magnetic nanohybrids with a speculated formation of carbon-encapsulated iron-cementite structure. Control over the synthesis parameters of pyrolysis temperature and time interval provides a series of samples of distinct structural and magnetic properties. Namely, the range of pyrolysis parameters were 700-1100 °C and 5-120 min respectively. A variable degree of crystallinity was observed for each sample by implementing X-ray diffraction structural characterization technique. The magnetic characterization was carried out with Vibrating Sample Magnetometry by magnetic hysteresis loops outlining the magnetic profile of the samples.

The eligibility of such particles is tested by introducing them in an alternating current magnetic field inducing heat generated by hysteresis losses. 1 mL aqueous solutions with a 2mg_{Fe}/mL concentration were formed and brought under the influence of a 375 kHz/60 mT AC magnetic field in a metal coil. Heating curves of temperature vs time were measured showcasing the heating efficiency of the samples. For an effective hyperthermia treatment, the temperature of the samples is optatively required to be elevated in a 41-45 °C thermal range. The heating duration for each measurement was 200 seconds with a 0.4 s step followed with 200 seconds of cooling with the absence of the magnetic field. Heating efficiency is estimated alternatively from minor magnetic hysteresis loops and is found in good agreement with calorimetric derivation showing tunable heating efficiency in the range of 200-600 W/g with respect to structural and collective magnetic features.

This work was supported by European Union's Horizon 2020 research and innovation programme under grant agreement No 857502 (MaNaCa).

[1] Angelakeris, M. Magnetic nanoparticles: A multifunctional vehicle for modern theranostics. *Biochim Biophys Acta Gen Subj* **2017**, *1861*, 1642-1651.

[2] Avakyan, L.; Manukyan, A.; Bogdan, A. et al. Synthesis and structural characterization of iron-cementite nanoparticles encapsulated in carbon matrix. *J. Nanoparticle Res.* **2020**, *22*, 30.

Heating properties of Fe₃O₄ magnetite nanoparticles dispersed in agarose

Inci Nur Sahin*, Leon Josua Daniel, Marina Spasova, Ulf Wiedwald and Michael Farle
Faculty of Physics and Center of Nanointegration (CENIDE), University of Duisburg-Essen, Duisburg,
47057 Germany
inci.sahin@stud.uni-due.de

Magnetic hyperthermia has emerged as a promising method for the local treatment of cancer: The main goal is to heat the malignant tissue with biocompatible magnetic iron oxide nanoparticles in an external alternating magnetic field in such a way that lethal temperatures for the tumor cell of at least 42-45°C are reached [1].

Within the scope of this research, Fe₃O₄ nanoparticles with an average diameter of 114 nm dispersed in agarose have been analyzed. The concentration of the agarose gel and therefore the viscosity, to mimic human tissue, was varied from 5 to 15 mg agarose per ml water. The nanoparticle concentration ranges from 5 to 20 mg NP per ml agarose gel. The samples were then exposed to an external alternating magnetic field to determine their heating capabilities by the specific loss power (SLP). Magnetic flux densities of 20 mT to 55 mT were used at frequencies ranging from 103 kHz to 247 kHz, which are in the tolerable range for rf-exposure of humans.

The particles are mainly in the multidomain state, and the hysteresis losses dominate the particle heating instead of the well-known Néel and Brown relaxation in superparamagnets. From the literature it is known that the SLP behaves directly proportional to the frequency and has a constant exponent of $\alpha \leq 3$ for the magnetic field H^{α} [2]. In fact, the measured values show a linear frequency dependence, but a constant exponent was not determined, since α saturates with increasing magnetic field by reaching the irreversibility point. Moreover, the specific loss power does not show any dependence on the viscosity of the agarose. Overall, temperature of up to 60°C were successfully achieved and an average SLP value of 139 W/g was obtained.

Funding by the European Union within the Horizon 2020 MaNaCa Project (No.857502) is gratefully acknowledged.

- [1] B. Mehdaoui et al., Adv. Funct. Mater., 21: 4573-4581 (2011)
[2] S. Dutz, & R. Hergt, Nanotechnology, 25,45: 452001 (2014)

The role of the magnetocrystalline anisotropy on the frequency-dependent hyperthermia performance of magnetite nanoparticles

N. Maniotis^{1,2}, D. Serantes³, O. Iglesias^{4,5}

¹School of Physics, Faculty of Sciences, Aristotle University, Thessaloniki, 54124 Greece

²MagnaCharta, Center for Interdisciplinary Research and Innovation (CIRI-AUTH), Thessaloniki, 57001 Greece

nimaniot@physics.auth.gr

³Applied Physics Department and iMATUS, Universidade de Santiago de Compostela, Santiago de Compostela, 15782 Spain

⁴Departament de Física de la Matèria Condensada, Universitat de Barcelona, Martí i Franquès 1, 08028 Barcelona, Spain

⁵Institut de Nanociència i Nanotecnologia (IN2UB), Universitat de Barcelona, 08028 Barcelona, Spain

Magnetic particle hyperthermia (MPH) is a novel, minimally invasive, therapeutic modality, used as a cancer treatment, that employs magnetic nanoparticles (MNPs) as the heating source [1]. Once accumulated to the tumor area, nanoparticles are exposed to an external alternating magnetic field (AMF) that causes reversal of their magnetic moments, activating mechanisms of energy deposition in the form of heat. The key measure used for characterizing the heating efficiency of nanoparticles in MPH is the specific loss power (SLP), which is often estimated from quasi-static hysteresis loops [2].

The aim of this work is to present the impact of MNPs anisotropy K and AMF frequency f on the rate-dependent hysteresis loop. The area of the later is also used to estimate the SLP magnitude. The system under study is an assembly of non-interacting magnetite nanoparticles, focusing on a large particle size of 30 nm for which the direct comparison of SLP from quasistatic hysteresis loops should work well [3]. Dynamical simulations based on the Landau-Lifshitz-Gilbert equation were performed by using the OOMMF software package [4] to obtain the hysteresis loops under a 24 kA/m alternating magnetic field amplitude and for various frequencies (50-765 kHz) typically used in MPH. The shape of nanoparticles is also considered by taking into account different anisotropy contributions: perfectly spherical particles should possess only the cubic magnetocrystalline anisotropy term (K_c), whereas a deviation from this ideal case will bring into play other anisotropy terms, here introduced as a first approximation through a uniaxial anisotropy K_u . Its presence will give rise to the presence of other easy magnetization pathways, and thus will affect the corresponding SLP value. We will discuss how this more realistic situation compares with the only- K_u approach that is usually utilized in literature. Thus, we performed a systematic study of SLP vs. f trends in the quasistatic regime $T=0$, for different K_u values (0, 5, 10, and 15 kJ/m³) with and without $K_c = -11$ kJ/m³ and compared the results to those obtained by dynamic simulations at 300 K. In the latter case, the influence of damping on the SLP dependence on f was also studied by performing hysteresis loops at different values of the damping coefficient ($\alpha=1.0, 0.1$ and 0.01).

Our simulation results show that the origin of the marked change in the frequency dependence of SLP at intermediate frequencies observed in some experiments might be related to the uniaxial shape anisotropy contributions due to small departures from perfect sphere shape of the particles.

[1] M. Angelakeris, Biochim. Biophys. Acta Gen. Subj., 1861 1642-1651 (2017).

[2] K. Simeonidis, et al. J. Appl. Phys. 114, 103909 (2013).

[3] I. Conde-Leboran, et al. J. Phys. Chem. C 119, 15698 (2015).

[4] M. Donahue, OOMMF User's Guide, Version 1.0. (1999).

Synthesis and magnetic heating properties of Fe-Fe₃C nanoparticles in a carbon matrix

Harutyun Gyulasaryan^{1*}, Eirini Myrovali², Gayane Chilingaryan¹, Elisavet Papadopoulou³, Nicolaos Tetos³, Armine Ginoyan¹, Antonis Makridis², Narek Sisakyan¹, Marina Spasova³, Michael Farle³, Makis Angelakeris², Aram Manukyan¹

¹Institute for Physical Research of National Academy of Sciences, Armenia

gharut1989@gmail.com

²Physics Department, Aristotle University of Thessaloniki, Greece

³Faculty of Physics and Center of Nanointegration (CENIDE), University of Duisburg-Essen, Germany

Magnetic fluid hyperthermia of tumor tissue has evolved into an approved therapy for cancer competing with the chemotoxic and radiological approaches. Hyperthermia is generally understood as a local (cellular) temperature increase up to 45 °C in malignant cells based on the heating effect of localized magnetic nanoparticles (MNPs) in cancerous tissue under alternating magnetic fields (AMF) to achieve selective damage of tumor tissue. The heat generation efficiency of MNPs depends on the intrinsic characteristics of particles, such as the particle size, composition and magnetic anisotropy, and parameters of external AMF (amplitude, frequency).

In this work, iron-cementite (Fe-Fe₃C) magnetic nanoparticles in a carbon matrix were synthesized by a solid-phase pyrolysis of ferrocene (FeC₁₀H₁₀). The pyrolysis process was carried out in a closed quartz tube at 750°C with the duration of 5-120 minutes. By varying the pyrolysis time, one can change the concentration of Fe and Fe₃C in metal nanoparticles, which leads to a change in the magnetic characteristics and magnetic heating properties of the nanoparticles.

The heating efficiency of synthesized samples was evaluated by preparing aqueous solutions of 6.5 mg/mL concentration and exposing them in AC magnetic field with parameters 375 kHz/60 mT. The maximum SLP (Specific Loss Power) of 350 W / g, which is attractive for the application in magnetic hyperthermia, was obtained in a sample prepared in 45 minutes (Fig. 1).

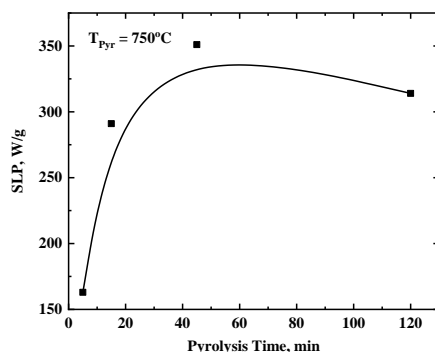


Figure 1. The values of SLP of synthesized (Fe-Fe₃C)/C nanocomposites dependence of pyrolysis time.

This work was supported by European Union's Horizon 2020 research and innovation programme under grant agreement No 857502 (MaNaCa).

Magneto-mechanical stress on MDA-MB-231 cancer cells

Aikaterini-Rafailia Tsiapla^{1,2}, Veselina Uzunova³, Rumiana Tzoneva³, Theodoros Samaras¹,
Orestis Kalogirou^{1,2}, Makis Angelakeris^{1,2}

¹School of Physics, Aristotle University of Thessaloniki, 54124 Thessaloniki, Greece

aitsiapl@physics.auth.gr

²MagnaCharta, Center for Interdisciplinary Research and Innovation (CIRI-AUTH), 57001 Thessaloniki, Greece

³Laboratory of Transmembrane Signaling, Institute of Biophysics and Biomedical Engineering, Bulgarian Academy of Sciences, Acad. G. Bonchev Street, Block 21, 1113 Sofia, Bulgaria

Magneto-mechanical stress is a new research field for cancer therapy, in which magnetic field exerts magnetic forces on the magnetic nanoparticle, which in turn exerts mechanical forces on malignant and non-malignant cell membranes, causing damage only to cancerous tissues.

In this work, the proliferation rate of treated and untreated MDA-MB-231¹ breast cancer cells with and without the presence of magnetic nanoparticles (MNPs) was investigated in three different types of low-frequency magnetic fields: static, pulsed, and rotating field mode with intensity of 200 mT and frequency of 2 Hz. Figure 1 shows the internalization of MNPs within the MDA-MB-231 cells using Prussian blue staining, prior the magneto-mechanical activation, and was visualized by optical microscopy.

MTT colorimetric assay² for assessing cell metabolic activity before and after magneto-mechanical treatment was also evaluated. It was observed that the highest reduction in cell viability was detected for the applied pulsed field mode with MNPs (about 70%). A significant reduction in the rotating field mode with MNPs after 120 h of incubation (more than 50%) was noticed too. In all other treatments (static field mode with and without MNPs and rotating field mode without MNPs), the cell viability was maintained at high levels (70–100%). Therefore, pulsed field mode was chosen as the optimum one. After MTT test, F-actin staining³ was used to observe the changes in the cytoskeleton and DAPI staining⁴ was performed to reveal the apoptotic alterations in cells' nuclei after magneto-mechanical stress with pulsed field mode only. Indeed, after this field mode actin stress fiber loss and apoptotic nuclear changes were perceived and compared with those without magneto-mechanical treatment.

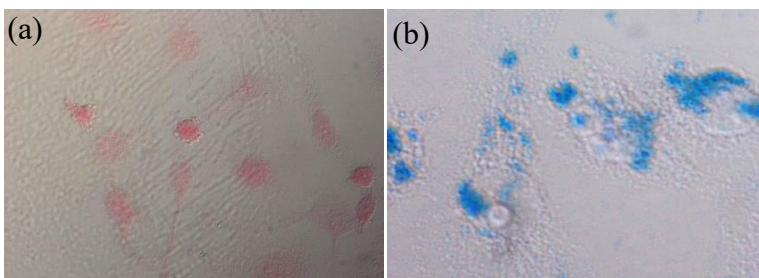


Figure 1. Prussian blue staining results of MDA-MB-231 cells: (a) control cells, which correspond to the cells that were not treated with MNPs; and (b) cells after 24 h incubation with MNPs, which were stained with Prussian blue reaction and visualized by

optical microscopy imaging at 20× magnification. Blue: MNPs; Red: nucleus of cells.

The financial funding from the Bulgarian Ministry of Education and Science under the National Research Programme “Young scientists and postdoctoral students” approved by DCM#577/17.08.2018 and by Joint Research Project BAS-AUTH, 2018-2020 is gratefully acknowledged.

¹ MDA-MB-231 cells: an epithelial, human breast cancer cell line that was established from a pleural effusion of a 51-year-old caucasian female with a metastatic mammary adenocarcinoma.

² MTT colorimetric assay: dimethylthiazol-diphenyltetrazolium bromide, which determines the functional state of mitochondria, indicating cell viability.

³ F-actin staining: phalloidin-tric, a red-orange fluorescent cytoskeleton stain, which binds and labels F-actin.

⁴ DAPI staining: 4,6-diamidino-2-phenylindole, a blue-fluorescent stain, that binds to AT-rich regions of double-stranded DNA.

Deciphering magnetization dynamics on the micro- and nanoscale by time-resolved Scanning Transmission X-ray Microscopy

Thomas Feggeler^{1*}, Ralf Meckenstock², Detlef Spoddig², Benjamin Zingsem^{2,3}, Santa Pile⁴, Taddäus Schaffers⁴, Johanna Lill², Damian Günzing², Sebastian Wintz⁵, Markus Weigand⁶, Andreas Ney⁴, Michael Winklhofer⁷, Michael Farle², Heiko Wende², Katharina Ollefs², and Hendrik Ohldag^{1,8,9}

¹Advanced Light Source, Lawrence Berkeley National Laboratory, Berkeley CA 94720, United States

²Faculty of Physics and CENIDE, University of Duisburg-Essen, 47048 Duisburg, Germany

³Ernst Ruska Centre and Peter Grünberg Institute, Forschungszentrum Jülich GmbH, Jülich, Germany

⁴Institute of Semiconductor and Solid-State Physics, Johannes Kepler University, 4040 Linz, Austria

⁵Max Planck Institute for Intelligent Systems, 70569 Stuttgart, Germany

⁶Helmholtz Center Berlin, Albert Einstein Straße 15, 12489 Berlin, Germany

⁷School of Mathematics and Science, University of Oldenburg, 26129 Oldenburg, Germany

⁸Department of Material Sciences and Engineering, Stanford University, Stanford CA 94305, United States

⁹Department of Physics, University of California Santa Cruz, Santa Cruz CA 95064, United States
tfeggeler@lbl.gov

State-of-the-art applications of micro- and nanoscaled magnetic materials, e.g. cancer research and spintronic and magnonic solutions for modern information technology [1-3] require a comprehensive element-specific understanding of dynamic magnetic properties. Scanning Transmission X-ray Microscopy (STXM) offers the element-specific and spatially resolved chemical and magnetic characterization of such materials in a wide range of X-ray absorption energies incorporating X-ray Magnetic Circular Dichroism (XMCD) effect as contrast mechanism. By means of XMCD information on orientation and size of magnetic moments can be determined probing the sample at an X-ray absorption edge of the investigated element [4]. With time-resolved STXM (TR-STXM) dynamic excitations of the magnetization up to 10th of GHz with < 30 ps sampling can be monitored [5]. Here we show the spatially resolved sampling of magnetization dynamics of uniform and non-uniform resonant responses in Py/Co microstructures, Py stripe ensembles [6] and magnetite nanoparticle chains inside magnetotactic bacteria *Magnetospirillum Magnetotacticum* [7].

This work is funded by the Deutsche Forschungsgemeinschaft (DFG, German Research Foundation) - Project No. OL513/1-1, 321560838, and in part by the DFG Project-ID 405553726 TRR 270, and the Austrian Science Fund (FWF project: I 3050-N36). Lawrence Berkeley National Laboratory is acknowledged for funding through LDRD Award: Development of a Continuous Photon Counting Scheme for Time Resolved Studies. The use of the Stanford Synchrotron Radiation Lightsource, SLAC National Accelerator Laboratory, is supported by the US Department of Energy, Office of Science, Office of Basic Energy Sciences under Contract No. DE-AC02-76SF00515. We thank HZB for the allocation of synchrotron radiation beamtime.

- [1] V.V. Kruglyak, S.O. Demokritov, et al. *Journal of Physics D: Applied Physics*, 2010. **43**(26).
- [2] A. Hoffmann and S.D. Bader. *Physical Review Applied*, 2015. **4**(4): p. 047001-1-047001-18.
- [3] B. Zingsem, T. Feggeler, et al. *Nature Communications*, 2019. **10**: p. 4345.
- [4] J. Stöhr and H.C. Siegmann, *Magnetism From Fundamentals to Nanoscale Dynamics*. Springer, ed. M. Cardona, et al. 2006, Berlin, Heidelberg: Springer.
- [5] S. Bonetti, R. Kukreja, et al. *Review of Scientific Instruments*, 2015. **86**(9): p. 093703-1-093703-9.
- [6] S. Pile, T. Feggeler, et al. *Applied Physics Letters*, 2020. **116**(7): p. 072401-1-072401-5.
- [7] T. Feggeler, R. Meckenstock, et al. *Physical Review Research*, 2021. **3**(3)

Solvent Influence on the Magnetization and Phase of Fe-Ni Alloy Nanoparticles generated by Pulsed Laser Ablation in Liquids

I. Y. Khairani¹, Q. Lin², C. Doñate-Buendía¹, J. Landers³, S. Salamon³, E. Karapetrova², H. Wende³, G. Zangari², B. Gökce¹

¹Materials Science and Additive Manufacturing, University of Wuppertal, Germany

goekce@uni-wuppertal.de

²Department of Materials Science and Engineering, University of Virginia, United States

³Faculty of Physics, University of Duisburg-Essen, Germany

The interesting combination of properties produced from core-shell nanoparticles (NPs) has increased the popularity of this type of nanoalloy [1]. The encapsulation of a cytotoxic yet functional magnetic core with a biocompatible shell, for example, increases the biocompatibility of the core-shell NPs and unlocks their potential usage in living organisms. Unfortunately, the synthesis methods to produce core-shell NPs usually overlook the green chemistry principle due to the multi-step processes required to remove the chemical byproducts generated in the process. Pulsed laser ablation in liquid (PLAL) provides a one-step method to produce NPs in the desired solvent, such as acetone, ethanol, or even water, depending on the required application. By tuning the liquid employed for PLAL [2], the core-shell structure of the generated NPs can be modified, hence, tuning the properties [3] of the resulting NPs.

This study showed that the magnetization, oxidation level, NPs size, core-shell structure, and the crystallographic phases of Fe₅₀Ni₅₀ (FeNi) NPs produced by PLAL are influenced by the water content of the solvent (acetone). Molecular sieves (3 Å) are used to capture water impurities in acetone and produce ‘dried acetone’. The FeNi target was ablated in three liquids, i.e., dried acetone, acetone, and water. XRD synchrotron analysis was performed to determine the FeNi phases. The high-pressure HCP FeNi phase was found in the sample produced in acetone and dried acetone but not in water. Mössbauer spectroscopy revealed that the oxidation of FeNi in dried acetone is reduced by 8% compared to acetone, while the EDX-TEM shows a reduction of the oxygen atomic % of 15%. The saturation magnetization value of FeNi ablated in water is the highest, 75 Am²/kg. The core-shell structures formed in these three liquids are also distinctive (Fig. 1), revealing potential possibilities of various core-shell formations by changing the water content in the organic solvent.

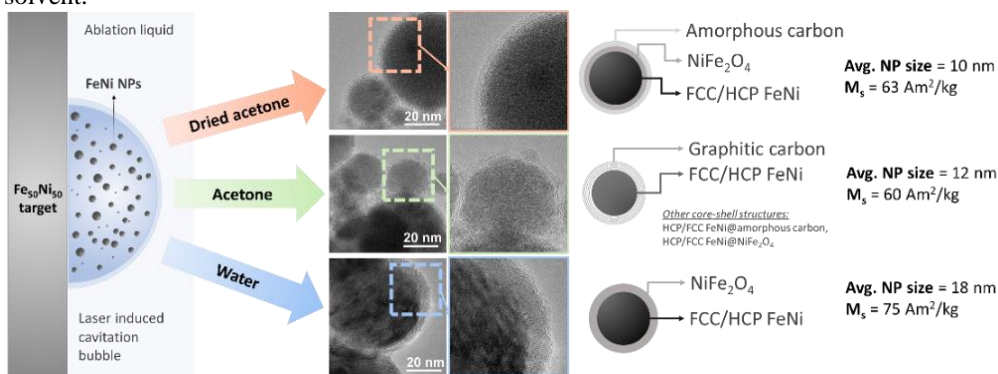


Figure 4. Schematic illustration of FeNi ablation in various liquids.

Financial funding from the European Union's Horizon 2020 research and innovation program under the grant agreement No 952068 (project LESGO) and funding from the DFG (CRC/TRR) 270 (Project-ID 405553726) is gratefully acknowledged.

- [1] R. G. Chaudhuri and S. Paria, *Chem. Rev.*, vol. 112, no. 4, pp. 2373–2433, (2012).
- [2] D. Zhang, B. Gökce, and S. Barcikowski, *Chem. Rev.*, vol. 117, no. 5, pp. 3990–4103, Mar. (2017).
- [3] A. Tymoczko et al., *Nanoscale Horizons*, vol. 4, no. 6, pp. 1326–1332, (2019).

Direct laser writing of Fe₅₀Rh₅₀ magnetocaloric structures

Shabbir Tahir, Carlos Doñate-Buendía and Bilal Gökce

Materials Science and Additive Manufacturing, School of Mechanical Engineering and Safety Engineering, University of Wuppertal, Germany

tahir@uni-wuppertal.de

Magnetocaloric refrigeration has proven to be a potential replacement for compress gas-based refrigeration systems due to its energy efficiency and contamination reduction. Most of the magnetocaloric materials currently studied for room temperature refrigeration consist of rare-earth metals, limiting their use in bulk due to availability and cost for commercial use. An alternative use of these materials that reduces the material required are miniaturized applications such as cooling of portable microelectronics, thermal switching, hyperthermia, drug delivery and many micro electro-mechanical based applications. Different approaches have been tested to print the required geometries for miniaturized devices. Among them, laser printing has proved to have low production cost, easy integration of industrial facilities, and its capability to achieve complex micro/nanometric structures.

Among magnetocaloric materials, the FeRh alloy system demonstrates the largest magnetocaloric effect at first order antiferromagnetic-ferromagnetic (AFM-FM) phase transition at near-to-equimolar composition. Here, we demonstrate the laser printing of FeRh nanoparticles which were synthesized using picosecond pulsed laser ablation in ethanol (Fig 1a). The nanoparticles generated consist of near to equimolar solid solution FeRh nanoparticles initially paramagnetic [1]. The nanoparticles were employed to formulate an ink (up to 1 wt.%) in ethanol, dispersed on PVP-coated glass substrates and patterned using a 532 nm continuous wave laser (Fig 1b and 1c) [2]. The laser parameters were optimized to achieve the best sintering characteristics (Fig 1d and 1e), thereby decreasing the electrical sheet resistance to 20 ohms/sq and inducing the phase transition up to 65% from paramagnetic to the desired antiferromagnetic structure.

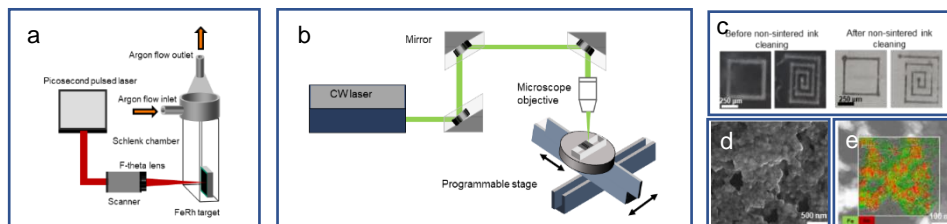


Figure 5: Laser ablation of FeRh in ethanol inside a Schlenk chamber b) Laser sintering of FeRh nanoparticle ink dispersed on glass substrate patterned using X-Y stage c) Micropattern formation procedure d) SEM image of sintered FeRh nanoparticles e) EDX mapping of sintered FeRh nanoparticles.

The authors gratefully acknowledge funding by the German Research Foundation (DFG) within the Collaborative Research Centre / Transregio (CRC/TRR) 270 (Project-ID 405553726)

[1] R. Nadarajah et al., *Nanomaterials* 10(12), 2362 (2020)

[2] R. Nadarajah et al., *Scientific Reports*, 11 (1), 13719 (2021)

Magnetolectric properties of $0,7(0,5\text{BaZr}_{0,2}\text{Ti}_{0,8}\text{O}_3 - 0,5\text{Ba}_{0,7}\text{Ca}_{0,3}\text{TiO}_3) - 0,3\text{NiFe}_{1,9}\text{Co}_{0,02}\text{O}_4$ ceramics

Natallia Poddubnaya, Vladimir Laletin

Institute of Technical Acoustics of the National Academy of Sciences of Belarus, Vitebsk, Belarus

laletin57@rambler.ru

The paper presents the study on the magnetolectric (ME) effect in $0,7(0,5\text{BaZr}_{0,2}\text{Ti}_{0,8}\text{O}_3 - 0,5\text{Ba}_{0,7}\text{Ca}_{0,3}\text{TiO}_3) - 0,3\text{NiFe}_{1,9}\text{Co}_{0,02}\text{O}_4$ composite ceramics.

The linear ME coefficient was determined by measuring the electric field generated in the sample when an alternating (1 Oe) and slowly varying (0 – 2500 Oe) magnetizing field was applied to it. The measurements were performed at a frequency of 1 kHz. The nonlinear ME coefficient was determined by measuring the electric field generated in the sample when a variable (0 – 2500 Oe) was applied to it. The measurements were performed at a frequency of 50 Hz. The experiment had two variants. In the first case, the electric polarization was parallel to the magnetic fields (longitudinal ME effect). In the second, the electric polarization was perpendicular to the magnetic fields (transverse ME effect).

The figure shows the field dependences of the linear (a) and nonlinear (b) ME coefficient for the longitudinal and transverse effects. In both cases, the dependencies have a classical form. For a linear effect, the magnitude of the signal at first increases reaching a maximum, and then decreases tending to zero. For a longitudinal ME effect, the coefficient reaches 39 mV/(cm Oe) in a field of 500 Oe, and for a transverse effect it reaches 24 mV/(cm Oe) in a field of 200 Oe. In the case of a nonlinear ME effect, the signal grows, reaching saturation in magnetic fields above 2.5 kOe for the longitudinal effect and 1.5 kOe for the transverse effect. The electric field strength in saturation mode is 5 V/mm and 2 V/mm, respectively.

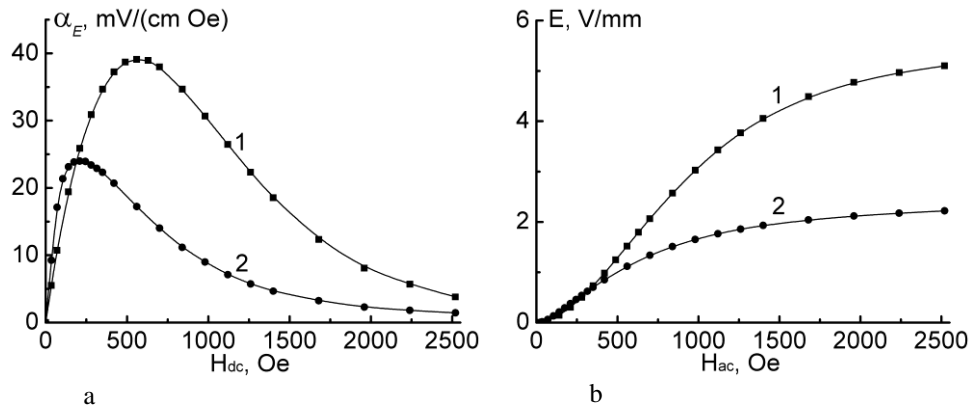


Figure 1. Field dependence of linear (a) and nonlinear (b) ME signal for longitudinal (1) and transverse (2) ME effect.

Bulk ME composites with an ME coefficient of 39 mV/(cm Oe) for the linear effect and electric field strength in saturation mode 5 V/mm for a non-linear effect were obtained. This confirms the possibility of obtaining new highly efficient ME materials based on lead-free piezoceramics.

This work was supported by the Belarusian Republican Foundation for Fundamental Research (Grant № F21VA-006).

Synthesis and characterization of novel multifunctional magnetic bioceramic nanocomposites

Konstantina Kazeli^{1,2,3}, Antonis Makridis^{1,2}, Eleana Kontonasaki⁴, Evgenia Lymperaki³,
Makis Angelakeris^{1,2}

¹School of Physics, Faculty of Sciences, Aristotle University of Thessaloniki, 54124 Thessaloniki, Greece

²Center for Interdisciplinary Research and Innovation (CIRI-AUTH), Thessaloniki-Thermi Rd, P.O.

³Department of Biomedical sciences, National Hellenic University, Thessaloniki, Greece,

⁴Department of Prosthodontics, School of Dentistry, Faculty of Health Sciences, Aristotle University of Thessaloniki, Thessaloniki, Greece, GR-54124

kkazeli@physics.auth.gr

Bone is the second most transplanted tissue worldwide, with over four million operations using bone grafts or bone substitute materials annually to treat bone defects. However, significant limitations affect current treatment options and clinical demand for bone grafts continues to rise due to conditions such as trauma, cancer, infection, and arthritis. Developing bioactive three-dimensional (3D) scaffolds to support bone regeneration has therefore become a key area of focus within bone tissue engineering [1,2].

Due to the plethora of physicochemical and biological properties demonstrated by magnetic bioceramic scaffolds, they are considered very attractive for bone tissue regenerative techniques, opening a whole lot of possibilities in the field of bone regeneration through a synergistic action of *in situ* apatite formation derived from bioceramics and stem cell stimulation and differentiation towards the osteogenic lineage from targeted magnetic fields application, hyperthermia-based therapy and localized drug delivery [3,4].

As perspective, the aim of the work is to design and synthesize a novel magnetic nanocomposite followed by fabrication of a multifunctional 3D scaffold via polymer sponge technique. Firstly, the synthesis of CoFe_2O_4 nanoparticles was carried out by sol-gel method, secondly, the synthesis and characterization of novel magnetic $\text{Mg}_2\text{SiO}_4\text{-CoFe}_2\text{O}_4$ nanocomposite follows, implementing a two-pot sol-gel synthesis strategy and finally, 3D scaffold fabrication through polymer sponge technique.

For the accurate definition of their structure and morphology all synthesized materials were characterized with Fourier-transform infrared Spectroscopy (FTIR) and X-ray Diffractometer (XRD) for phase identification. For both CoFe_2O_4 nanoparticles and the final composite, the peaks relate to both forsterite and cobalt ferrite were identified, which is evidence of a successful synthesis. Magnetic characterization of the CoFe_2O_4 nanoparticles and the nanocomposite was carried out to determine the magnetic response of samples, using a vibrating sample magnetometer (VSM) and the results exhibited that M_s appears suppressed in nanocomposite-coated indicating that the nanocomposite was coated successfully with a non-magnetic biocompatible layer. Also, Thermogravimetric Analysis (TGA) performed, to analyze their thermal profile in conjunction with Magnetic Particle Hyperthermia (MPH) to outline the heating efficiency potential and perspectives for biomedical applications. Cobalt ferrite nanoparticles presented the highest SLP values whereas the composite material and scaffold samples presented, as expected, lower SLP values. Higher SLP values may enhance effectiveness with lower treatment agents resulting in a reduction in cytotoxicity and hyperthermia improvement.

[1] H. Ma et al., Acta Biomaterials 79, 37–59 (2018)

[2] A. Bigam et al., Mater. Sci. Eng. C, 99, 83–95 (2019)

[3] F.M. Martín-Saavedra et al., Acta Biomater. 6, 12 (2010)

[4] Y. Wang et al., Adv. Mater 27, 3, 576–585 (2015)

Synthesis, structural and magnetic properties of multiferroic BiFeO₃ nanoparticles

Kyrillos Papadopoulos^{1,2}, Eirini Myrovali^{1,2}, Marina Spasova³, Michael Farle³, Ulf Wiedwald³, Makis Angelakeris^{1,2}

¹School of Physics, Aristotle University of Thessaloniki, Thessaloniki, 54124, Greece

²Magnetic Nanostructure Characterization: Technology and Applications, CIRI-AUTH, 57001 Thessaloniki, Greece

³Faculty of Physics and Center for Nanointegration Duisburg-Essen (CENIDE), University of Duisburg-Essen, Duisburg 47048, Germany

kyrilpap@physics.auth.gr

Multiferroic materials exhibit strong coupling of electric, magnetic and structural order parameters, resulting in the coexistence of ferroelectricity, ferromagnetism and/or ferroelasticity in the same phase. Among them, BiFeO₃ (BFO) receives noticeable attention due to its potential applications in spintronics, data storage or microelectronics. BFO has a rhombohedrally distorted perovskite structure with the *R3c* space group symmetry. In bulk form, it is an antiferromagnetic, ferroelectric and ferroelastic multiferroic material with electrical, magnetic and structural ordering temperatures well above room temperature. The combined action of exchange and spin-orbit interactions produces spin canting lifting the perfect antiferromagnetic order. The direction of the resulting small magnetic moments rotates, superimposing the spiral spin arrangement, with a modulation period of ~62 nm. Such a spin structure would cancel its net magnetization in bulk form and inhibit the observation of linear magnetoelectric (ME) effect. In addition, the existence of Fe²⁺ ions and the volatilization of Bi element during the calcination process would always create some oxygen vacancies in BFO and thereby result in a large leakage current, limiting its practical applications. Moreover, the emergence of impurity phases such as Bi₂Fe₄O₉, Bi₂O₃ and Bi₂₅FeO₄₀ is difficult to be avoided due to the volatilization of some reactants and decomposition of BFO at high temperatures.

In this study, a simple chemical coprecipitation method is proposed for the synthesis of highly crystalline BFO nanoparticles in different nominal Bi/Fe molar ratios (0.9, 1.0, 1.1) with average particle sizes of 55 ± 36 nm, 78 ± 53 nm and 101 ± 65 nm, respectively. It is shown that the mean particle size diminishes with decreasing the Bi concentration in the chemical composition (BFO 0.9), giving rise to an enhanced magnetization due to size effects and strain-induced structural modulations. Conversely, by rising the Bi-content (BFO 1.0, BFO 1.1), the symmetry-lowering impurity phase appearing in BFO 0.9 is vanished, as the surplus Bi compensates the volatile nature of Bi at high temperatures, thus, giving rise to the stabilization of the highly polar *R3c* rhombohedral structure and the enhancement of the dielectric properties of the corresponding samples at room temperature. Moreover, BFO 1.0 shows strong visible light absorption, making it a promising candidate for photovoltaics, solar cells, photocatalysis or optoelectronics. The correlation of structure and morphology with collective magnetic and dielectric response are investigated by X-Ray diffraction (XRD), transmission electron microscopy (TEM), thermogravimetric analysis (TGA), Fourier transform infrared spectroscopy (FT-IR), UV-Vis spectrophotometry, vibrating-sample magnetometry (VSM) and impedance spectroscopy. Consequently, parameters affecting structural characteristics and phase constitution for all chemical compositions, crystallization temperature of the initial amorphous powder, ferroelectric to paraelectric phase transition at the Curie temperature and energy band gap are derived and their tuning, with respects to synthetic controls, is discussed.

Magnetic ground state of potential giant dielectric constant material $\text{Ba}(\text{Fe}_{1/2}\text{Sn}_{1/2})\text{O}_{3-\delta}$

Arun Kumar , Sunil Nair

Department of Physics, Indian Institute of Science Education and Research Pune-411008, India

arun.kumar@acads.iiserpune.ac.in

The lead (*Pb*-) free complex perovskite barium ferrostannate $\text{Ba}(\text{Fe}_{1/2}\text{Sn}_{1/2})\text{O}_{3-\delta}$ (BFSO) is considered as a potential candidate for technological applications owing to its giant dielectric constant at room temperature similar to the well-known $\text{CaCu}_3\text{Ti}_4\text{O}_{12}$ (CCTO) compound [1-2]. In CCTO, the giant dielectric phenomena has been linked with its low temperature antiferromagnetic (AFM) ground state with $T_N \sim 25$ K [3]. Since BFSO also shows a low-temperature magnetic transition ~ 16 K with negative Curie-Weiss temperature θ_{CW} , it is of interest to understand the nature of this magnetic transition. Based on the bifurcation of zero-field cooled (ZFC) and field cooled (FC) magnetization ($M(T)$) curves, a spin-glass like transition has been reported in the literature [4] but such a bifurcation could also arise from superparamagnetic blocking or even large magnetocrystalline anisotropy in long-range ordered systems. It remains therefore to be confirmed whether the low-temperature magnetic transition is indeed a spin-glass transition using multiple criteria.

We present here comprehensive investigation of BFSO using x-ray diffraction, dielectric, dc and ac magnetizations and specific heat measurements. BFSO is seen to crystallize in a cubic $Pm\bar{3}m$ symmetry. It shows a cluster glass freezing at $T_f \sim 16$ K, which is characterized by (1) the observation of irreversibility between ZFC and FC $M(T)$ curves, (2) frequency dispersion across $T_f(\omega)$ in ac susceptibility and analysis follows power-law type critical dynamics with glass transition temperature $T_G \sim 15.7$ K and characteristic relaxation time $\tau_0 \sim 10^{-7}$ s, (3) appearance of non-zero remanent magnetization and coercivity below T_f , (4) existence of de Almeida-Thouless line in the T-H plane with mean-field exponent $m \sim 0.63$, (5) presence of aging effect and time-dependent magnetic relaxation following stretched exponential function dependence below T_f , and (6) a linear temperature dependence of magnetic contribution to specific heat C_m below T_f . All these observations, for the first time, unambiguously confirm the cluster glass magnetic ground state of BFSO. We believe that the present study would provide the key ingredients for future theoretical studies directed towards understanding the $\text{CaCu}_3\text{Ti}_4\text{O}_{12}$ type giant dielectric constant behaviour of BFSO.

- [1] M. A. Subramanian, D. Li, N. Duan, B.A. Reisner, A.W. Sleight, Journal of Solid State Chemistry 151, 323 (2000).
- [2] C.C. Homes, T. Vogt, S.M. Shapiro, S. Wakimoto, A.P. Ramirez, Science 293, 673 (2001).
- [3] Y.J. Kim, S. Wakimoto, S.M. Shapiro, P.M. Gehring, A.P. Ramirez, Solid State Communications 121, 625 (2002).
- [4] K.S. Roh, M.G. Kim, K.S. Ryu, C. H. Yo, Solid State Communications 100, 565 (1996).

Electric field control of Snell's law for spin waves

Vladimir Krivoruchko¹, Andrii Savchenko^{1,2} and Stefan Blügel²

¹Donetsk Institute for Physics and Engineering, National Academy of Sciences of Ukraine, 03028 Kyiv, Ukraine

²Peter Grünberg Institut and Institute for Advanced Simulation, Forschungszentrum Jülich, D-52425 Jülich, Germany
a.savchenko@fz-juelich.de

The spin waveguides are key cells in magnonics. In recent years, immense experimental progress has been made in the generation, detection, and manipulation of spin waves (SWs) for data processing and information transmission. Direct observations of the dispersion relations for quantized coherent spin waves excited by a microwave antenna have provided a basic understanding of the properties of spin-waves in nanoscale ferromagnetic films [1-3]. Several methods have also been proposed to use an artificially induced Dzyaloshinskii-Moriya (DM) interaction that leads to a nontrivial asymmetric dispersion relation of SWs, enabling manipulation of the phase and propagation direction of SWs.

SWs propagating in an external static electric field acquire a topological phase, the so-called Aharonov-Casher (AC) phase. This is equivalent to a selective shift in the dispersion and power flow direction of the SW by an electric field. To linear order on the electric field, the AC effect can be considered by adding a DM-like interaction between neighboring spins. In our study, we apply these findings to examine a possibility of the electric field control on the refraction of coherently propagating SWs. Using analytical calculations and micromagnetic simulations, we demonstrate the possibility of an electric field controlling the refraction and reflection of SWs at the interface formed by regions under the action of different electric fields in a homogeneous magnetic film.

In particular, the critical angles for Snell's law, the type of positive or negative spin-wave refraction, and their nonreciprocity with respect to the incident angle can be controlled by the electric field. Such results have been obtained for both dipole-exchange and exchange spin waves. Examples of the negative and positive refraction of dipole-exchange SW at different directions of the electric field \mathbf{E} along the normal to the yttrium iron garnet film are shown in Fig. 1a and Fig. 1b, respectively.

Authors are grateful to the European Research Council for financial support under the European Union's Horizon 2020 research and innovation program (Grant No. 856538, project "3D MAGiC") and the Helmholtz Association for support under the HGF-RSF joint research programme (project: TOPOMANN).

- [1] C. Song et al., Prog. Mater. Sci. 87, 33 (2017).
- [2] B. Rana and Y. Otani, Commun. Phys. 2, 90 (2019).
- [3] X. Zhang et al, Phys. Rev. Lett. 113, 037202 (2014).

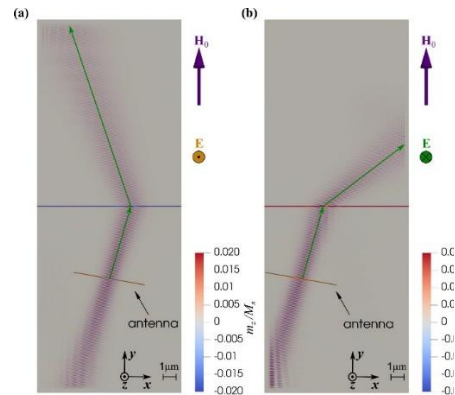


Figure 1. Refraction of dipole-exchange SW at the frequency $f = 7.9$ GHz under the effect of the electric field in the upper part of the YIG film. Static magnetization \mathbf{M}_s is along normal to the boundary between areas with $|\mathbf{E}| = 0.35 \text{ V/nm}$ and $E_z = 0$; \mathbf{m} is dynamic magnetization. (a) $E_z > 0$; (b) $E_z < 0$.

Curie temperature in the GdFe_{1-x}M_xSi and GdRu_{1-x}M_xSi systems

A. Lukoyanov^{1,2}, A. Kuchin¹, S. Platonov¹, R. Mukhachev^{1,2}, A. Volegov^{1,2}, V. Gaviko^{1,2} and M. Yakovleva¹

¹Institute of Metal Physics UB RAS, 620108, 18 S. Kovalevskaya Str., Ekaterinburg, Russia

²Ural Federal University, 620002, 19 Mira Str., Ekaterinburg, Russia

lukoyanov@imp.uran.ru

The GdT₂Si (T = Fe, Ru) intermetallic compounds crystallize in the tetragonal CeFeSi-type structure (*P4/nmm*) [1]. The hybridization between Si *p* and Fe 3*d* states causes the absence of the magnetic moment of Fe in the GdFeSi compound. It is of interest to study the magnetic and magnetocaloric properties of the GdT_{1-x}M_xSi substitutional alloys with T = Fe, Ru, M = Cr, V, Ni, Mo with different atomic radii and the number of 3*d* or 4*d* electrons.

It was found that the Curie temperature T_C sharply increases from 130 K to 255 K and 250 K for GdFe_{1-x}Cr_xSi and GdFe_{1-x}V_xSi and decreases to 98 K for GdFe_{1-x}Ni_xSi when x changes from 0 to 0.5, 0.3, and 0.3, respectively. Calculations of the electronic structure indicated that the Fermi level E_F for GdFeSi is localized on the right slope of the total density of states $N(E)$ peak. In the rigid band shift method, when Fe is replaced by V, Cr or Ni in GdFeSi, E_F shifts to the left or to the right along the slope due to the smaller or larger number of 3*d* electrons in the V (3), Cr (5) or Ni (8) atoms compared to the Fe (6) atom, respectively. As a result, the density of states at the Fermi level $N(E_F)$ and, therefore, T_C in the GdFe_{1-x}T_xSi systems increases with T = V, Cr or decreases with T = Ni, within the framework of the model of effective *d-f* exchange interaction in R-3*d* metal intermetallics, in which $T_C \sim N(E_F)$. The Curie temperature in the GdRu_{1-x}Cr_xSi and GdRu_{1-x}Mo_xSi systems practically does not change, as can be seen in Fig. 1. In the $N(E)$ calculated by us for the GdRuSi alloy, the Fermi level E_F is localized on the right slope of the $N(E)$ peak for spin-up electrons and at the maximum of the $N(E)$ peak for spin-down electrons. In the rigid band shift method, when Ru is replaced by Mo in GdRuSi, E_F shifts to the left due to the smaller number of 4*d* electrons in the Mo atom (5) compared to the Ru atom (7). In this case, $N(E_F)$ increases for spin-up electrons and decreases for spin-down electrons; as a result, their total $N(E_F)$ and $T_C \sim N(E_F)$ practically do not change. Assuming hybridization of 4*d* electrons of Ru and 3*d* electrons of Cr, similar reasoning is also suitable for explaining the practical invariance of $T_C(x)$ in the GdRu_{1-x}Cr_xSi system, since the Cr atom (5) has fewer 3*d* electrons than the Ru atom (7) has 4*d* electrons.

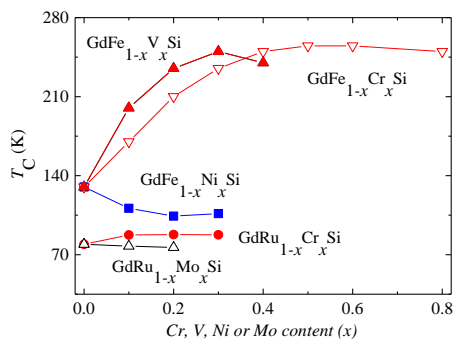


Figure 1. Concentration dependences of the Curie temperature $T_C(x)$ for the GdFe_{1-x}M_xSi and GdRu_{1-x}M_xSi, M = Cr, V, Ni or Mo compounds

The study was supported by Russian Science Foundation No **18-72-10098**, <https://rscf.ru/en/project/18-72-10098/>.

[1] A.G. Kuchin et al., *Intermetallics* 133, 107183 (2021).

Ferromagnetic resonance of a $\text{Ni}_{37}\text{Co}_{13}\text{Mn}_{33}\text{Ti}_{17}$ -Heusler single crystal

M. Vanselow¹, N. Josten¹, D. Koch², R. Meckenstock¹, B. Beckmann², O. Gutfleisch², W. Donner², M. Farle¹

¹Faculty of Physics and Center for Nanointegration (CENIDE), University Duisburg Essen, Duisburg, 47057, Germany

²Institute of Material science, Alarich-Weiß-Straße 2,64287 Darmstadt
moritz.vanselow@stud.uni-due.de

Magnetocaloric research has focused Heusler-alloys for many years. There are many NiMn-based Heusler alloys which undergo a martensitic phase transition. The phase transition can be used for magnetic cooling and is well investigated from theoretical and experimental side. The magnetic behavior of the technique to use Ti in place of p-elements within Heusler [1] has not yet been fully investigated.

Here we investigate a novel Ti based Heusler alloy [2] with the chemical formula $\text{Ni}_{37}\text{Co}_{13}\text{Mn}_{33}\text{Ti}_{17}$.

At 200K, the material undergoes a phase transition. Incommensurate modulated monoclinic 6M(IC) is the material's lower temperature state, and it is in a B2 austenitic phase above 200K.

Using temperature- and angle-dependent ferromagnetic resonance, the magnetic characteristics were studied.

To do this, the material was gradually cooled in 20 K steps from room temperature to 140 K, and the measurement steps were taken in 4 degree steps from in-plane to out-of-plane. Around 200 K, the phase transition was confirmed; the high-temperature phase displayed ferromagnetic characteristics, and the low-temperature phase displayed antiferromagnetic behavior with traces of ferromagnetic domains.

This work has been supported by the Deutsche Forschungsgemeinschaft (Project 405553726-CRC/TRR 270)

[1] Z. Y. Wie et al. Appl. Phys. Lett. 107, 022406 (2015)

[2] D. Koch et al., J. Appl. Phys. 131, 073903 (2022)

Magnetocaloric effect in nanocrystalline MnFeNiGeSi high entropy alloys prepared by High energy ball milling and Spark plasma sintering

M. Sünnner, N.F. Shkodich, M. Farle

Faculty of Physics and Center for Nanointegration (CENIDE), University Duisburg Essen, Duisburg,
47057, Germany
natalia.shkodich@uni-due.de

To date, the magnetocaloric properties of various materials such as Heusler alloys, perovskites and others have been widely studied [1]. In turn, high-entropy alloys (HEAs) developed based on the new alloying strategy [2,3] can exhibit unexpected functional properties due to chemical and topological disorder that are interesting from both fundamental and applied points of view for magnetic cooling.

Recently, MnFeNiGeSi rare earth free HEA prepared by arc melting with a high isothermal entropy change of $13.1 \text{ J kg}^{-1}\text{K}^{-1}$ (for 2.5 T) have been reported [4].

In present study, the structural, magnetic and magnetocaloric properties of equiatomic and non-equiatomic MnFeNiGeSi HEAs have been investigated.

The nanocrystalline MnFeNiGeSi powder particles with good structural and compositional homogeneity were successfully produced by short-term high energy ball milling (HEBM), and then SPS-consolidated at 1073 K for 10 min.

The XRD results showed that single *bcc* structure for MnFeNiGe and MnFeNi(GeSi)_{12.5} HEA powders could be obtained after 30 min of HEBM, while for Mn_{22.3}Fe_{22.2}Ni_{22.2}Ge_{16.65}Si_{16.65} and MnFeNiGeSi – a mixture of *bcc*+*fcc* solid solutions were observed.

The largest value of an isothermal entropy change ΔS_{iso} of $0.9 \text{ J kg}^{-1}\text{K}^{-1}$ (for 2.5 T) at 190K was observed in nanocrystalline Mn_{22.3}Fe_{22.2}Ni_{22.2}Ge_{16.65}Si_{16.65} HEA powder obtained after 120 min of HEBM at 700 rpm.

The SPS consolidation at 1073K led to an increase in ΔS_{iso} by ~30% for Mn_{22.3}Fe_{22.2}Ni_{22.2}Ge_{16.65}Si_{16.65} HEA powder obtained after 150+20 min of HEBM at 700 rpm.

As shown above, different processing parameters (for example HEBM time) and a slight change in elemental concentration of HEAs play a crucial role in microstructure and magnetism. Consequently, further investigations are needed to enhance and tune the magnetic parameters.

This work has been supported by the Deutsche Forschungsgemeinschaft (DFG) within CRC/TRR 270, project S01 (project ID 405553726).

[1] Ram, N.R., Prakash, M., Naresh, U. et al. J Supercond Nov Magn., 31, 1971 (2018).

[2] Yeh, J.-W. et al., Adv. Eng. Mater., 6, 299 (2004).

[3] Cantor et al., Mater. Sci. Eng. A 213 (2004).

[4] J.Y. Law, Acta Mater. 212 (2021).

Setup of a UHV chamber for growing ultra-thin epitaxial MAX phase films and in situ characterization

Tim Salzmann, Ali Can Aktas, Ulf Wiedwald, Michael Farle

AG Farle, Faculty of Physics, University of Duisburg-Essen, 47057 Duisburg, Germany

tim.salzmann@uni-due.de

MAX phases combine the properties of metals and ceramics and are promising materials for a wide range of applications in industry and research. The structure and composition of MAX phases are well understood by numerous studies, whereas the magnetic properties are mostly unknown. [1],[2]

As an approach to decipher the magnetic behavior further, ultra-thin epitaxial single-phase $(\text{Cr}_x, \text{Mn}_{1-x})_2\text{GaC}$ MAX phase films are prepared and analyzed in situ in a purpose-built ultrahigh vacuum (UHV) chamber.

The UHV chamber has 3 thermal evaporators with which it is possible to evaporate up to 6 elements simultaneously. Furthermore, the samples can be heated up to 1600K or cooled down to 10K. For structural analysis an AES, LEED and REED are available. For magnetic characterization, the chamber allows one in situ FMR, MOKE and AC susceptibility measurements.

[1] A S Ingason *et al* 2016 *J. Phys.: Condens. Matter* **28** 433003.

[2] P. Eklund *et al.* / *Thin Solid Films* 518 (2010) 1851–1878

Metallic Lithium thin films: UHV deposition and CESR studies

Ali Can Aktas, Jonas Wiemeler, Tim Salzmann, Anna Semisalova, Michael Farle
AG Farle, Faculty of Physics and CENIDE, University of Duisburg-Essen, 47057 Duisburg, Germany
alican.aktas@uni-due.de

In this study, we investigate the best deposition parameters for the growth of thin films of metallic Li to study the conduction electron spin resonance (CESR) for spintronic applications. As being the lightest among all other bulk elements, the Li atom is in an S state in its both ionic and neutral electronic configurations. That is, the spin-orbit coupling in its ground state is zero, allowing for the conducting electron to carry its own spin at a significantly long distance before losing its spin memory. In other words, the contributions of the spin-orbit coupling to the spin relaxation can be expected to be negligibly small. This property can make Li metal one of the best candidates to transfer and exchange magnetic information between magnetic materials in nano-structured multilayers. Since the lithium is quite reactive to form chemical compounds with other elements, especially with oxygen. It must not be left open against the ambient conditions. Especially for ultra-thin film deposition, the film growth time must be kept as short as possible in order to get sufficiently pure ultra-thin Li film.

In this study, we have used an ultra-high vacuum chamber which is equipped with an e-beam evaporator, LEED, Auger electron spectroscopy (AES), and in-situ electron spin resonance spectrometer. A special and suitable crucible was designed and manufactured to keep the bulk Li source material to be usable for a long time in an ultra-high vacuum chamber and collimate the lithium vapor in the desired way. To improve and guarantee the purity and the quality of the Li film, the conventional surface-sensitive AES technique was applied in every step of the film growth to see and control the chemical structure.

A charging effect, affecting the position of Auger peaks of elements in the structure (Li, O, C, Ga, As), was observed when the film is deposited on a very clean single crystalline GaAs substrate. The relative shift of AES peaks was found to depend on the Li film thickness and reached up to 198 eV for 10 nm Li thickness -an effect open for discussion. In order to verify the origin of the shift of the Auger peaks in the energy axis, we have also deposited the Li film on clean Cu metal, which is also electrically grounded. In this case, the peak position of all elements, found on the sample holder, including Li, was found at positions corresponding to the literature values [1].

An initial CESR study was made on both the bulk and thin film form of Li. A noise-free CESR signal is observed in bulk Li and fitted with the Dysonian line shape to deduce ESR parameters (g – factor $g = 2.004 \pm 0.001$). In the case of a thin film, the CESR signal [2] is very weak but still observable depending on the film thickness.

[1] Handbook of Auger Electron Spectroscopy, “Lawrence E. Davis, Noel C. Macdonald, Paul W. Palmberg, Gerald E. Riach, Roland E. Weber” Physical Electronic Division Perkin-Elmer Corp. (1976)

[2] Measurement of Conduction-Electron Spin Relaxation Due to Rare Gases Physisorbed on a Lithium Surface,”D.M. Eigler and S. Schultz (1985)

Correlation of growth modes and magnetic properties of $(\text{Cr}_{1-x}\text{Mn}_x)_2\text{GaC}$ MAX phase epitaxial films on rigid and flexible substrates

I. Tarasov, M. Farle and U. Wiedwald

Faculty of Physics and Center for Nanointegration (CENIDE), University of Duisburg-Essen, 47057
 Duisburg, Germany
ivan.tarasov@uni-due.de

Due to their nanolaminated structure, tunable chemistry, and high oxidation resistance, MAX phases (where M is an early transition metal, A is a main group element, and X is carbon or nitrogen) are interesting materials for a wide variety of applications. The partial substitution of M atoms is one of the ways to tailor their properties to specific applications. In this study, we grow $(\text{Cr}_{1-x}\text{Mn}_x)_2\text{GaC}$ MAX phase films to fine-tune their magnetic response by stoichiometry variations for $x = 0-1$. High-quality epitaxial $(\text{Cr}_{1-x}\text{Mn}_x)_2\text{GaC}$ MAX phase films (thickness 50 – 70 nm) are synthesized by pulsed laser deposition on rigid MgO(111), $\text{Al}_2\text{O}_3(0001)$ and flexible muscovite $\text{KAl}_3\text{Si}_3\text{O}_{10}(\text{OH})_2(001)$ substrates using $(\text{Mn}_{0.5}\text{Cr}_{0.5})_{66}\text{Ga}_{34}$, $\text{Mn}_{66}\text{Ga}_{34}$, $\text{Cr}_{66}\text{Ga}_{34}$ and C targets. Structural and morphological characterization reveals a strong competition between the $(\text{Cr}_{1-x}\text{Mn}_x)_2\text{GaC}$ MAX phase and $(\text{Cr}_{1-x}\text{Mn}_x)_3\text{GaC}$, $(\text{Cr}_{1-x}\text{Mn}_x)_3\text{Ga}$ phases. We suppress the formation of side phases by variation of the growth temperature and the growth on seed layers. Using different N_2 background gas pressure the orientation of the MAX phase is shown to change from the (0001) plane to the (10-13) plane. Background gas pressure regulates the kinetic energy of incoming species and subsequently changes adatom mobilities facilitating basal-plane or tilted grain growth.

Vibrating sample magnetometry of the MAX phase reveals increasing magnetization and ordering temperature with increasing Mn content. The flexibility of substrates allows tuning the magnetic properties via different external strains applied. The $(\text{Cr}_{0.55}\text{Mn}_{0.45})_2\text{GaC}$ films under a strain show a higher magnetization and a noticeable change in shape and remanent magnetization of the hysteresis loops. A delaminated $(\text{Cr}_{0.55}\text{Mn}_{0.45})_2\text{GaC}(0001)$ film transferred on a tape reveals a complex magnetic behavior likely caused by a superposition of different local strain configurations of the flexible tape.

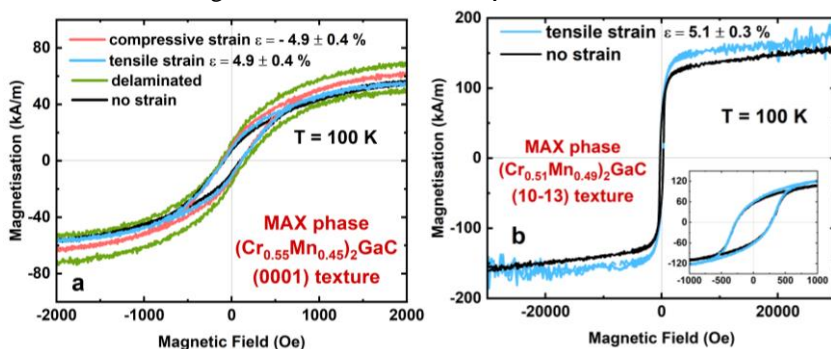


Figure 1. (a) Hysteresis loops of a $(\text{Cr}_{0.55}\text{Mn}_{0.45})_2\text{GaC}(0001)$ film in in-plane orientation at $T = 100$ K under different types of strain (b) Hysteresis loops of a $(\text{Cr}_{0.51}\text{Mn}_{0.49})_2\text{GaC}(10-13)$ film in in-plane orientation with and without an applied tensile strain at $T = 100$ K.

Funding by the Deutsche Forschungsgemeinschaft (DFG) within CRC/TRR 270, project B02 (Project-ID 405553726) is gratefully acknowledged. The authors thank Detlef Spoddig for assistance with SEM and EDX imaging. We thank Merlin Schmuck and Doru Lupascu for assistance and providing access to the XRD with Eulerian cradle. We also thank Ulrich von Hörsten for their support in the optimization of the deposition chamber.

Band structure and local energy gaps in $(\text{Cr}_{1-x}\text{Mn}_x)_2\text{GaC}$ MAX phases studied by ellipsometry in epitaxial films

I. Tarasov, M. Farle and U. Wiedwald

Faculty of Physics and Center for Nanointegration (CENIDE), University of Duisburg-Essen, 47057
 Duisburg, Germany
ivan.tarasov@uni-due.de

MAX-phase materials ($\text{M}_{n+1}\text{AX}_n$, $n = 1, 2$ or 3) are a family of nano-layered hexagonal compounds. In these materials, M is an early transition metal, A is an element of the main group, and X is C or N ($n = 1-3$). These systems have an atomic-layered structure consisting of M_2X layers alternating with the atomic layers of the A-element. The atomic layers are stacked along the c axis. MAX phases combine both ceramic and metal characteristics. Here, we examine the electronic structure of $(\text{Cr}_{1-x}\text{Mn}_x)_2\text{GaC}$ MAX phase epitaxial films via analysis of the complex dielectric function $\epsilon(\omega) = \epsilon_1 + i\epsilon_2$ derived from ellipsometry at room temperature (Fig. 1). The local energy gaps produced by the periodic static potential in $(\text{Cr}_{1-x}\text{Mn}_x)_2\text{GaC}$ compounds, for $x = 0-1$, are determined by examination of interband transitions, which is the result of the number of bands with maxima for $\epsilon_2(\omega)$. The experimental study is correlated with density functional theory calculations for detailed analysis of the band structure (Fig. 1a). A given example of the dielectric function of a $(\text{Cr}_{0.5}\text{Mn}_{0.5})_2\text{GaC}$ thin film reveals its anisotropic behaviour (Fig. 1a, b). A pronounced band with maxima at 2.16 eV corresponds well to theoretically calculated $\epsilon_2(\omega)$ of the Cr_2GaC , whereas the Mn_2GaC compound shows a broader interband transition at this value. With help of the experimental function of $\epsilon_2 - \gamma(\delta\epsilon_1/\delta E)$, which allows one a better distinguishability of absorption maxima, two different sets of distinguishable maxima at 0.64 (0.78), 1.48 (1.85), 1.78 (2.16), 2.58(-), -(2.86) eV are resolved in the infrared and visible regions of the spectra which agrees with energies in the Cr_2GaC at 0.83 (0.92), 1.95 (2.09), 2.5(2.5), 3.16(3.16) eV and the Mn_2GaC at 1.43 eV. The ultraviolet range is characterized by the presence of maxima common for in-plane and out-of-plane directions. Thus, the behaviour of the dielectric function of the $(\text{Cr}_{0.5}\text{Mn}_{0.5})_2\text{GaC}$ thin films resembles in general features characteristic of the Cr_2GaC MAX phase. It is also worth noting that the DFT Drude term fails to describe the experiments (Fig. 1a), which may be caused by chemical disorder at M-site or structural defects and short-range chemical order.

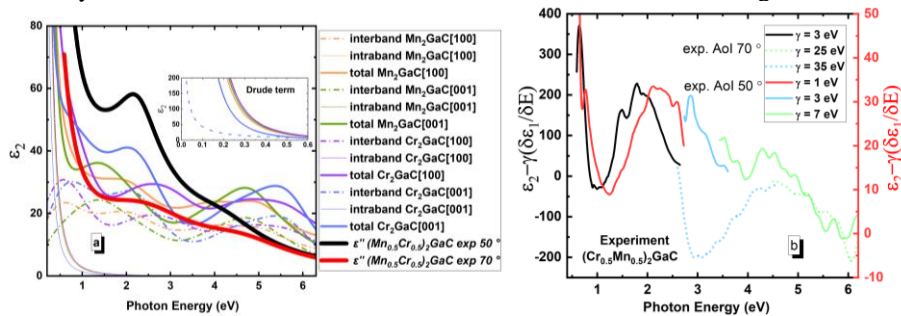


Figure 1. (a) Imaginary part of dielectric function ϵ_2 of Mn_2GaC and Cr_2GaC MAX phases calculated by DFT and experimental ϵ_2 spectrum for an epitaxial $(\text{Cr}_{0.5}\text{Mn}_{0.5})_2\text{GaC}$ film (b) Separation of the interband-conduction band of $(\text{Cr}_{0.5}\text{Mn}_{0.5})_2\text{GaC}$ with the experimental spectrum plotted as function of $\epsilon_2 - \gamma(\delta\epsilon_1/\delta E)$, where γ is an adjustment constant. AoI stands for angle of incidence.

Funding by the Deutsche Forschungsgemeinschaft (DFG) within CRC/TRR 270, project B02 (Project-ID 405553726) is gratefully acknowledged. We thank Klaus Pärschke and Martina Schmid for assistance and providing access to the ellipsometer.

Magneto-electronic and optical properties of full Heusler alloy, Y_2FeSi : Theoretical investigation using density functional theory with and without spin orbit coupling effect

Arvind Kumar

Materials Science Research Lab (Theory and Experimental), Department of Physics, ARSD College,
University of Delhi-110021 (India)

arvindkumar@arsd.du.ac.in

Recently, Heusler alloy (HA) materials have created noteworthy commercial applications in spintronic devices due to significant magneto-electronic properties. In this study, a first principle calculation has been performed to investigate the structural, opto-electronic and magnetic properties of the Yttrium (Y) based, Y_2FeSi Heusler alloy (HA) using the Wien2K code. To estimate the physical properties of the HA, PBE-GGA and mBJ exchange correlation functional were applied. Compound has been optimized for non-magnetic (NM), ferromagnetic (FM) and antiferromagnetic (AFM) phases. Structural optimization curves and phonon spectra shows the dynamical stability of the compound in FM phase. Electronic charge density contour plot represents the dominant ionic character among the atomic configurations of Y_2FeSi compound. Density of states (DOS) plots reveals the major role of Fe-3d electronic states along with Y-4d and Si-2p electronic states. Estimated spin polarization for the compound found to be ~ 75 % which is near to half metallic character. DOS and band structure curves suggest the metallic nature with magnetic (ferromagnetic having magnetic moment ~ 1.65 μ_B /cell for the HA) ordering of the compound. Consequence of spin orbit coupling (SOC) on materials physical properties was also analyzed. Band structure (BS) with SOC effect shows additional energy levels across the Fermi level, due of splitting of energy levels of Y-atoms. Dielectric function has also been estimated with and without SOC to study the optical properties in detail for the compound. Study reveals the interesting electronic, magnetic and optical properties of the Y_2FeSi HA which have potential for optical and spintronic devices.

Autor Index

A

Abakumov M. A.	73
Abbasnejad M.	33
Abd-Shukor R.	35
Acet M.	67, 68, 69
Adabifiroozjaei E.	71
Adam R.	84
Ahrens V.	57
Akhavan M.	82
Aktas A. C.	25, 116, 117
Al-Ani S. K. J.	96
Albertini F.	38
Alizadeh Z.	33
Allodi G.	38
Al-Shakarchi E. K.	30, 96
Amirabbasi M.	17
Angelakeris M.	75, 76, 79, 99, 102, 103, 109, 110
Arab H.	33
Asimakidou T.	74, 77, 98
Aubert A.	39
Avagyan V.	79
Avci C. O.	83

B

Baigutlin D.	37, 42
Balashov T.	59
Becherer M.	57
Beckmann B.	114
Beer I.	73
Berger A.	70
Berndt R.	60
Blachowicz T.	88
Black-Schaffer A.	50
Blügel S.	45, 46, 112
Bodea S.-V.	73
Bogdanoff N.	52
Böhmer A.	51
Bonfà P.	38
Bötzel S.	94
Bourianoff G.	56
Brand J.-S.	72
Bruckhoff M. J.	41

Buchelnikov V.	36, 37, 42
---------------------	------------

Ç

Çakir A.	67, 68, 69
---------------	------------

C

Cavazzini G.	38
Chen H.	59
Chen J.	4
Chicco S.	38
Chilingaryan G.	79, 99, 102
Chioti E.	98
Choi H.-C.	54
Cinchetti M.	84
Čoga L.	89
Cugini F.	38

D

Dahan M.	72
Dahir S.	8
Daniel L. J.	100
De Renzi R.	38
Derenbach G.	59
Díaz S. A.	48
Dietl T.	92
Dilmieva E.	39
Doñate-Buendía C.	105, 107
Donner W.	114
Drevenšek-Olenik I.	89
Du H.	45
Dunin-Borkowski R. E.	45
Dzhumanov S.	34

E

Edathumkandy Y. K.	18
Efremova M.	58, 73
Ehrmann A.	88
Eremin I. M.	8
Eremin I. M.	94
Everschor-Sitte K.	22, 44, 48, 56

F

Fallarino L.	70
-------------------	----

Farle M.	25, 58, 65, 67, 68, 69, 72, 79, 97, 100, 102, 104, 110, 114, 115, 116, 117, 118, 119
Faysal W. M.	96
Feggeler T.	58, 73, 104
Fernández-Pacheco A.	43
Flatté M. E.	7
Franke K. J.	27, 28, 52
Frauhammer T.	59

G

Gabashvili A. N.	73
Gas K.	92
Gati E.	31
Gault B.	71
Gaviko V.	113
Geisler B.	81
Ginoyan A.	102
Giron S.	71
Gökce B.	105, 107
Gozlinski T.	62
Greene L. H.	10
Gruber M.	60
Gruner M.	36, 38, 41, 68
Günzing D.	58, 104
Gupta A. K.	53
Gupta S.	53
Gutfleisch O.	3
Gutfleisch O.	71, 114
Gyulasaryan H.	79, 99, 102

H

Hals K. M. D.	22, 23, 48
Heid R.	62
Holzappel B.	63
Homberg J.	60
Hribar L.	89
Hung T. V.	40
Hwang H. Y.	11

I

Iglesias O.	101
Ivleva N. P.	73

J

Jana S. P.	53
Jang H.	15

Jezeršek M.	89
Josten N.	68, 69, 114

K

Kalaïtzidou K.	77, 98
Kalin M.	89
Kalogirou O.	103
Kappler J.-P. J.	39
Karapetrova E.	105
Kazakov A.	92
Kazeli K.	109
Kenzelmann M.	15
Kessler S.	48
Khairani I. Y.	105
Kiselev N. S.	45, 46
Klyatskaya S.	59
Koch D.	114
Koeksal O.	16
Kontonasaki E.	109
Kovács A.	45
Kratzer P.	17
Kravanja G.	89
Kriegl R.	89
Krivoruchko V.	112
Ku W.	55
Kuchin A.	113
Kuchkin V. M.	45, 46
Kuckla D.	72
Kumar A.	111, 120

L

Laletin V.	61, 108
Landers J.	105
Lechermann F.	80
Lee S.-H.	54
Leliaert J.	56
Li Q.	62
Liebhaber E.	27, 28
Lill J.	58, 104
Lin Q.	105
Lisse D.	72
Löthman T.	50
Love J.	56
Lukoyanov A.	113
Lund M. A.	23
Lymperaki E.	109

M

Maekawa S.	5
Mahendru B.	52
Makridis A.	75, 102, 109
Malkemper E. P.	9
Manchon A.	6
Maniotis N.	77, 98, 101
Manukyan A.	79, 99, 102
Meckenstock R.	58, 73, 104, 114
Medarde M.	15
Meléndez A.	70
Melischek L.	52
Meng T.	48
Miroshkina O.	36, 37, 38, 42, 68
Mitrakas M.	98
Mohammadizadeh M. R.	95
Mohammadizadeh M.R.	33
Mohsin A.	30
Molina-Luna L.	71
Mönkebüscher D.	84
Montañez L.	57
Monzel C.	72
Moreno- Pineda E.	59
Msiska R.	56
Mukhachev R.	113
Mulkers J.	56
Müller M.	84
Myrovali E.	78, 102, 110

N

Nair S.	111
Nallathambi V.	65
Neusch A.	72
Ney A.	104
Noorzayee S.	68, 69
Nothhelfer J.	48
Novoselova I.	72
Núñez L. A.	49
Nur-Akasyah J.	35

O

Ohldag H.	58, 73, 104
Okkalidis N.	75
Ollefs K.	58, 104
Oppen F.	27, 28, 52
Orbay Y.	67
Orlandi F.	38

P

Pantos C.	77
Papadopoulos K.	110
Papadopoulou E.	79, 102
Parhizgar F.	50
Park J.-H.	15
Park T.	15
Parlak U.	84
Pentcheva R.	16, 41, 81
Pervin R.	53
Peters O.	52
Petrovic C.	32
Pickett W.	29
Pile S.	104
Pinakidou F.	77
Platonov S.	113
Poddubnaya N.	61, 108
Polin N.	71
Pomjakushina E.	15
Puerto Morales M.	74
Pujol P.	49
Pütter S.	57

Q

Quan Y.	29
Quintana M.	70

R

Ramos-Salamanca D.	49
Razdolski I.	21
Reecht G.	27, 28, 52
Reichenberger S.	65
Richter M.	40
Rizzi M.	48
Rodrigues D. R.	22
Rogalev A.	12, 39
Rohlf S.	27
Rosenberger P.	84
Rosnagel K.	27, 28
Ruben M.	59
Rütten L.	27, 28
Rybakov F. N.	45, 46

S

Sahakyan M.	40
Sahin I. N.	69, 100

Salamon S.	105
Salimath A.	22, 23
Salzmann T.	116, 117
Samaras T.	103
Sandoghchi M.	82, 95
Sarafidis H.	99
Savchenko A.	46, 112
Sawicki M.	92
Saxena A.	71
Schaffers T.	104
Schmalian J.	62
Schmid H.	27
Schmidt J.	50
Schneider C. M.	84
Sedighei M.	33
Semisalova A.	25, 117
Semkina A. S.	73
Serantes D.	101
Shamonin M.	89
Shin S.	15
Shkodich N.F.	65, 115
Sibille R.	15
Sigmund F.	73
Simeonidis K.	74, 77, 98
Sisakyan N.	79, 99, 102
Skokov K.	39, 71
Smoliarova T.	97
Sochnikov I.	14
Sokolovskiy V.	36, 37, 42
Solzi M.	38
Song D.	45
Spasova M.	79, 97, 100, 102, 110
Spoddig D.	58, 104
Srikanth H.	19
Staab M.	29
Steiner J. F.	27, 52
Story T.	92
Stupakiewicz A.	21
Sünner M.	115
Sztenkiel D.	18

T

Tahir S.	107
Tamir I.	52
Tarasov I.	118, 119
Taufour V.	29
Tavşanoğlu T.	67
Temnov V.	20
Tetos N.	79, 102

Torkashvand M.	95
Trahms M.	52
Tsiapla A.-R.	103
Tsiggenopoulou Z.	98
Tsompanoglou M.	79, 99
Turowski B.	92
Tzoneva R.	103

U

Uzunova V.	103
-----------------	-----

V

Vahid Hosseini S.	33
Valderrama C. M.	70
Vanselow M.	114
Veintemillas-Verdaguer S.	74
Vezzoni V.	38
Vicario C.	72
Vishik I.	29
Vodopyanov S. S.	73
Volegov A.	113
Volkov A. F.	8
Volobuev V.V.	92

W

Weigand M.	58, 104
Weismann A.	60
Wende H.	58, 104, 105
Westmeyer G. G.	73
Wiedwald U.	68, 72, 73, 97, 100, 110, 116, 118, 119
Wiemeler J.	25, 117
Wilhelm F.	12, 39
Winkelmann C. B.	52
Winklhofer M.	104
Wintz S.	58, 104
Wojciechowski T.	92
Wojtowicz T.	92
Wulfhekel W.	59, 62

X

Xu B.-X.	71
---------------	----

Y

Yadav R. S.	86
------------------	----

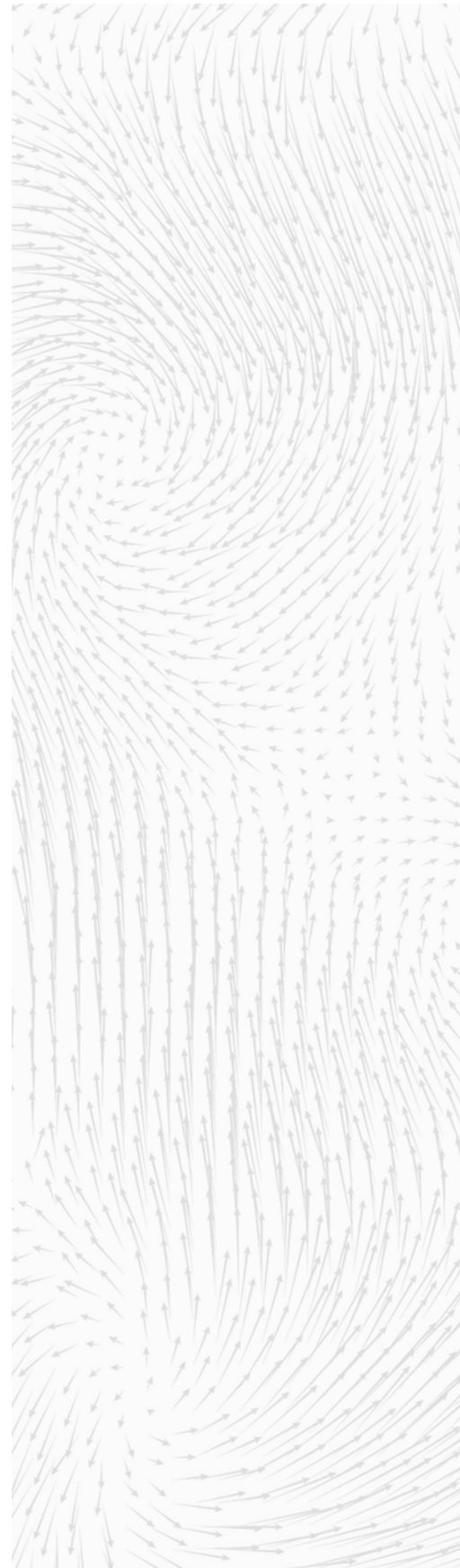
Yakovleva M.113
Yang B.-J.54
Yang L.45
Yang Y.71
Yi M.64

Z

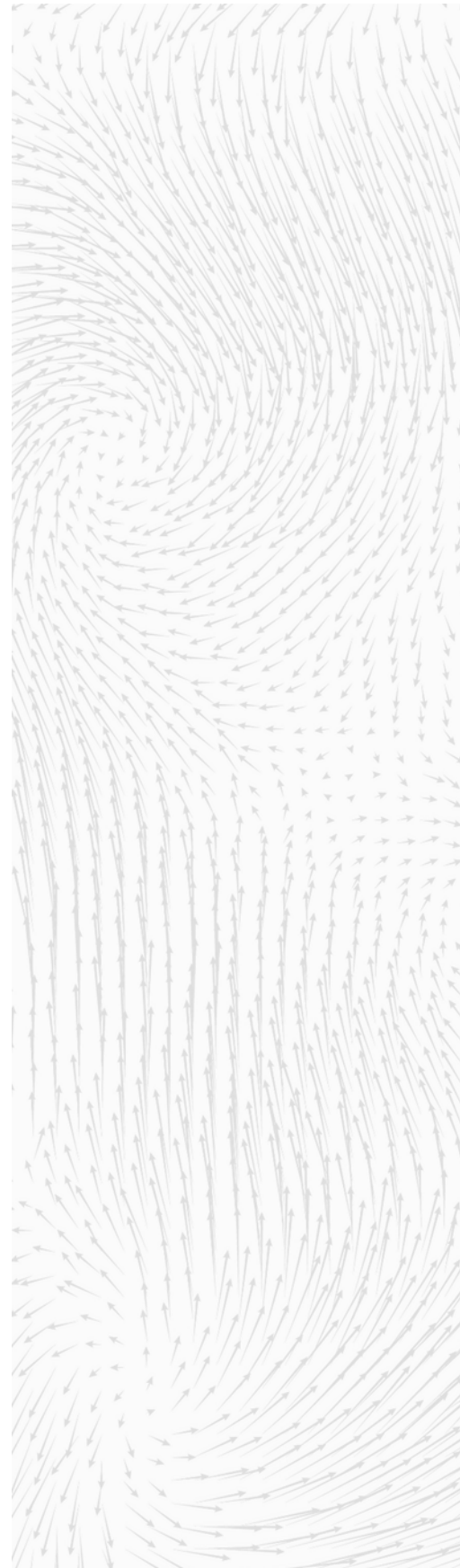
Zaharko O.15
Zaleszczyk W.92
Zangari G.105
Zheng F.45
Zięba M.92
Zingsem B.58, 68, 104

List of author e-mails

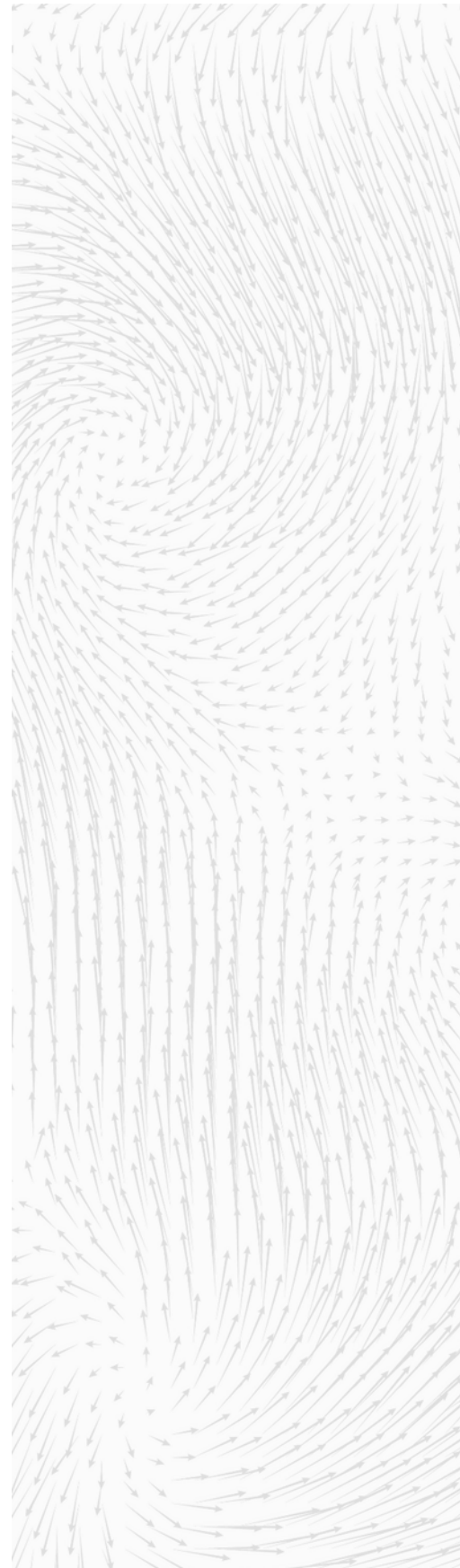
Akhavan Mohammad	m.akhavan1@Gmail.com
Ali Can Aktas	alican.aktas@uni-due.de
Al-Shakarchi Emad K.	eks2000@hotmail.com
Asimakidou Theopoula	tasimaki@physics.auth.gr
Avci Can Onur	cavci@icmab.es
Baigutlin Danil	d0nik1996@mail.ru
Black-Schaffer Annica	annica.black-schaffer@physics.uu.se
Böhmer Anna	boehmer@physik.rub.de
Bötzel Steffen Lennart	Steffen.Boetzel@rub.de
Bruckhoff Mike Jos	mike.bruckhoff@uni-due.de
Buchelnikov Vasily	buche@csu.ru
Çakır Aslı	cakir@mu.edu.tr
Chen Hongyan	hongyan.chen@kit.edu
Chilingaryan Gayane	gayane.chilingaryan.93@gmail.com
Díaz Santiago Sebastián Alejandro	sebastian.diaz@uni-due.de
Dilmieva Elvina	elvina.dilmieva@esrf.fr
Dzhumanov Safarali	dzhumanov@inp.uz
Edathumkandy Yadhu Krishnan	yadhu@ifpan.edu.pl
Efremova Mariia	m.efremova@tue.nl
Ehrmann Andrea	andrea.ehrmann@fh-bielefeld.de
Eremin Ilya	Ilya.Eremin@rub.de
Everschor-Sitte Karin	karin.everschor-sitte@uni-due.de
Feggeler Thomas	tfeggeler@lbl.gov
Fernandez-Pacheco Amalio	amaliofp@unizar.es
Franke Katharina	franke@physik.fu-berlin.de
Gati Elena	elena.gati@cpfs.mpg.de
Geisler Benjamin	benjamin.geisler@uni-due.de
Greene Laura	lhgreene@magnet.fsu.edu
Gruber Manuel	manuel.gruber@uni-due.de
Gupta Suraina	suraina@iitk.ac.in
Hals Kjetil M. D.	kjetil.hals@uia.no
Holzapfel Bernhard	bernhard.holzapfel@kit.edu
Hwang Harold	hyhwang@stanford.edu
Josten Nicolas	Nicolas.Josten@uni-due.de
Kalaitzidou Kyriaki	kalaitzidou@cheng.auth.gr
Kazakov Aleksandr	kazakov@magtop.ifpan.edu.pl



Kazeli Konstantina	kkazeli@physics.auth.gr
Khairani Inna Yusnila	khairani@uni-wuppertal.de
Koeksal Okan	okan.koeksal@uni-due.de
Kratzer Peter	Peter.Kratzer@uni-due.de
Kriegl Raphael	raphael.kriegl@oth-regensburg.de
Ku Wei	weiku@sjtu.edu.cn
Lechermann Frank	Frank.Lechermann@rub.de
Lukoyanov Alexey	lukoyanov@imp.uran.ru
Lund Mike Alexander	mikeal@uia.no
Maekawa Sadamichi	sadamichi.maekawa@riken.jp
Makridis Antonios	anmakrid@physics.auth.gr
Malkemper Erich Pascal	pascal.malkemper@mpinb.mpg.de
Manchon Aurélien	aurelien.manchon@univ-amu.fr
Maniotis Nikolaos	nimaniot@physics.auth.gr
Miroshkina Olga	olga.miroshkina@uni-due.de
Mohammadizadeh Mohammad Reza	zadeh@ut.ac.ir
Montañez Huamán Liz Margarita	l.montanez.huaman@fz-juelich.de
Msiska Robin	robin.msiska@uni-due.de
Myrovali Eirini	emiroval@physics.auth.gr
Noorzayee Sakia Sophia	sakia.noorzayee@stud.uni-due.de
Papadopoulos Kyrillos	kyrilpap@physics.auth.gr
Petrovic Cedomir	petrovic@bnl.gov
Pickett Warren	wepickett@ucdavis.edu
Poddubnaya Natallia	poddubnaya.n@rambler.ru
Polin Nikita	n.polin@mpie.de
Quintana Mikel	m.quintana@nanogune.eu
Ramos Salamanca David Leonardo	david.ramos.salamanca@outlook.com
Razdolski Ilya	i.razdolskiy@uwb.edu.pl
Rogalev Andrei	rogalev@esrf.fr
Rütten Lisa Marie	l.ruetten@fu-berlin.de
Sahakyan Mane	m.sahakyan@intibs.pl
Sahin Inci Nur	inci.sahin@stud.uni-due.de
Salzmann Tim	tim.salzmann@uni-due.de
Savchenko Andrii	a.savchenko@fz-juelich.de
Shin Soohyeon	soohyeon.shin@psi.ch
Shkodich Natalia	natalia.shkodich@uni-due.de
Simeonidis Konstantinos	ksime@physics.auth.gr
Sisakyan Narek	sisakyan@gmail.com



Smoliarova Tatiana	tatiana.smoliarova@uni-due.de
Sokolovskiy Vladimir	vsokolovsky84@mail.ru
Srikanth Hari	sharihar@usf.edu
Sünner Moritz	moritz.suenner@stud.uni-due.de
Tarasov Ivan	ivan.tarasov@uni-due.de
Trahms Martina	martina.trahms@fu-berlin.de
Tsompanoglou Milan	mtsompan@physics.auth.gr
Vanselow Moritz	moritz.vanselow@stud.uni-due.de
Wulfhekel Wulf	wulf.wulfhekel@kit.edu
Yadav Raghvendra Singh	yadav@utb.cz
Yang Bohm Jung	bjyang@snu.ac.kr
Yi Ming	mingyi@rice.edu



**12th International Conference on Magnetic
and Superconducting Materials**



**University of Duisburg-Essen, Faculty of Physics
August 28 – September 2, 2022**